Semiconductor and Integrated Optoelectronics

SIOE 2019

Semiconductor & Integrated Optoelectronics Conference

Cardiff, Wales

16th – 18th April 2019

Programme and Abstracts

Conference Locations (see map opposite)

Tues 16th April
Location: Queens Buildings site CF24 3AA (North and South Buildings)
Address: Queen's Buildings, 5 The Parade, Newport Road, CF24 3AA

Parking: NCP parking is available in the Knox Road car park (we cannot reimburse costs)

Registration location: North Building foyer.
Session 1 location: room N3-28 (third floor – 3 flights of stairs, turn left)
Poster session & Reception location: WX3.07 & 3.14

Wed 17th and Thurs 18th April
Sessions location: Law Building CF10 3AT, Room 0.22
Refreshments location: Aberdare Hall CF10 3UP

Address: Law Building, Museum Avenue (entrance on either side of building - Park Place) CF10 3AT. Room 0.22 closest room to the entrance.

Parking: On-street pay and display on Museum Avenue (we cannot reimburse costs)

Banquet location: National Museum Cardiff, Cardiff CF10 3NP

See map opposite – arrows indicate approximate position of entrances

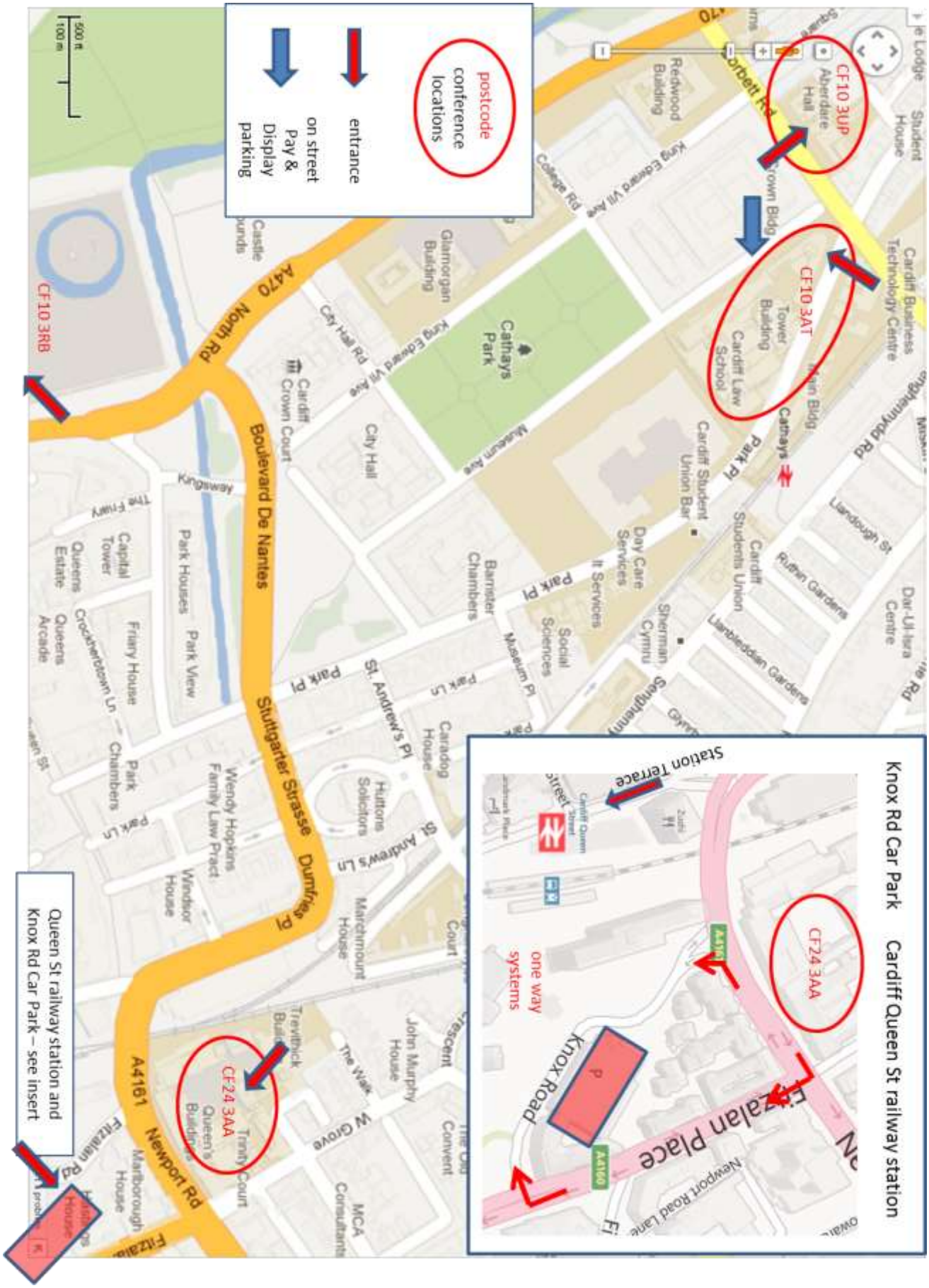
postcode conference locations
entrance
on street Pay & Display parking
CF10 3UP
CF10 3AT
CF10 3RB
CF24 3AA
Knox Rd Car Park Cardiff Queen St railway station
one way systems
Knox Road
Fitzalan Place
Station Terrace
Queen St railway station and Knox Rd Car Park – see insert
A470 North Rd
Boulevard De Nantes
Stuttgarter Strasse
Dumfries Pl
A4161 Newport Rd
Corbett Rd
Cathays Park
Park Pl
Kingsway
St. Andrew's Pl
St Andrew's Ln
Museum Ave
King Edward VII Ave
College Rd
Llandough St
Llanbleddian Gardens
Senghennydd Rd
Cardiff Business Technology Centre
Redwood Building
Crown Bldg
Tower Building
Cardiff Law School
Main Bldg
Cardiff Student Union Bar
Cardiff Students Union
Ruthin Gardens
Dar-Ul-Isra Centre
Glamorgan Building
City Hall
Cardiff Crown Court
Barrister Chambers
Day Care Services
IT Services
Social Sciences
Sherman Cymru
Park Houses
Park View
Capital Tower
Queens Estate
Queens Arcade
Friary House
Crockherbtown Ln
Park Chambers
Wendy Hopkins Family Law Pract
Windsor House
Caradog House
Hutton's Solicitors
Marchmount House
John Murphy House
Trevithick Building
Trinity Court
Queen's Building
The Old Convent
MCA Consultants
Marlborough House
Fitzalan Rd
W Grove
The Walk
Newport Road Lane
Cardiff Queen Street
500 ft
100 m

Welcome Message

SIOE '19

Croeso i Gaerdydd a chroeso unwaith eto i SIOE

It gives me great pleasure to welcome you to the 33rd SIOE conference in Cardiff.

We have an exciting programme that demonstrates the continuing evolution of Semiconductor Integrated OptoElectronics. On Tuesday afternoon we begin with three guest speakers. We welcome internationally renowned experts, Ian Sandall from the University of Liverpool, Lianping Hou of the University of Glasgow, and Bernardette Kunert of IMEC, to deliver invited talks in their areas of expertise. The invited talks will then be complemented by a subsequent session on "Photodetectors", which highlights some of the new developments in this area. We finish Tuesday with a reception and Poster session allowing you to interact and socialise with your colleagues and make new connections. IET Publishing have sponsored the poster session, and will be facilitating a special issue associated with the conference. The guest editors' role will be taken this year by **Dr Sang Soon Oh** and **Dr Qiang Li**, who will be available to discuss potential papers with authors that want to expand their conference presentation for this special issue.

On Wednesday morning **we relocate to the Law Building, Park Place** and begin with two sessions focussed on "Lasers & Light Sources", with a focus on optical elements and modelling, optical effects in lasers, temperature, and quantum dots. In the afternoon we change focus to a short but informative session on "Integration Strategies & Approaches", covering areas including passives, PICs, SiP as well as theory and numerical simulation, before concluding in good time for our conference banquet. After a full day we can relax in the galleries of the National Museum Cardiff with some music and refreshments, followed by a three course conference dinner.

Following the conference banquet, our sessions on Thursday focus on "Materials Development and Devices" with topics spanning a range of novel materials. We conclude the conference with lunch in Aberdare Hall, a final opportunity to network and connect with new colleagues after taking in all the conference presentations.

The SIOE 2019 Organisation Committee have been instrumental in assessing abstracts, putting together the programme and booklet, as well as in making the necessary arrangements for the conference. Committee members are (alphabetical by surname) Dr Nicolás Abadía, Dr Daryl Beggs, Dr Sara-Jayne Gillgrass (associate member), Dr Manoj Kesaria, Dr Qiang Li, Dr Sang Soon Oh, Dr Sam Shutts, Dr Juan Pereiro Viterbo (associate member). The committee were assisted by Sarah Taylor and Kate James.

The Organisation Committee wish to thank the following sponsors: Cardiff University, IET Publishing (for sponsoring the Poster Reception), the IOP Semiconductor Physics Group and IOP Quantum Electronics and Photonics Group, and IOP Wales (for contributing to the musical introduction to the banquet).

I am also pleased to be able to remind you to pick up our souvenir glass as a memento of the meeting during the poster session on Tuesday evening.

Prof. Peter Smowton, School of Physics and Astronomy, Cardiff University

Contents

Tuesday 16th April

Registration North Building Foyer; 13:00 onwards
Welcome address North Building N3.28; 13:40 – 13:45
Session 1: Guest Speakers North Building N3.28; 13:45 – 16:00
16:00 Refreshment Break Room N3.23 (Opposite N3.28)
Session 2: Photodetectors North Building N3.28; 16:30 – 18.00
Session 3: Posters & IET Publishing Reception (including drinks and buffet)
West Extension Building WX3.07/WX3.14; 18:00 – 20:00

Wednesday 17th April

Session 4: Lasers & Light Sources I Law Building 0.22; 08:45 – 10:30
10:30 Refreshment Break, Aberdare Hall
Session 5: Lasers & Light Sources II Law Building 0.22; 11:15 – 13:00
13:00 Lunch, Aberdare Hall
Session 6: Integration Strategies and Approaches I Law Building 0.22; 14:00 – 15:00
15:00 Refreshment Break, Aberdare Hall
Session 7: Integration Strategies and Approaches II Law Building 0.22; 15:45 – 16:30
Session 7b: Discussion - Integration Strategies Law Building 0.22; 16:30 – 17:30
Conference Banquet, National Museum Cardiff; 18:00 onwards

Thursday 18th April

Session 8: Materials Development & Devices I Room 0.22, Law Building; 08:45 - 10:45
10:45 Refreshment Break, Aberdare Hall
Session 9: Materials Development & Devices II Room 0.22, Law Building; 11:15 - 12:45
12:45 Lunch, Aberdare Hall
Conference Close

Programme, Tuesday 16th April

Registration
North Building Foyer; 13:00 onwards

Welcome address
North Building N3.28; 13:40 – 13:45

Session 1: Guest Speakers
North Building N3.28 13.45 – 16.00

13.45 *INVITED* **Utilization of Dielectrophoresis positioning and selection for Nanowire based Bio-Sensors**

S. Laumier[1], N. Sedghi[1], A. Marshall[2], A. Krier[2], M. Bosi[3], I. Sandall[1]*

[1]Department of Electrical Engineering and Electronics, The University of Liverpool, Brownlow Hill, Liverpool, L69 3GJ, UK; [2]Physics Department, Lancaster University, Lancaster, LA1 4YB, UK; [3]IMEM-CNR, Institute, Parma, Italy.

14.30 *INVITED* **Photonic Integrated Circuits for Terahertz Photonics**

Lianping Hou, JH Marsh

School of Engineering, University of Glasgow, Glasgow, G12 8QQ, U.K

15:15 *INVITED* **III/V Nano-ridge Engineering for novel Device Integration on (001) Si**

Bernardette Kunert

Imec, Kapeldreef 75, B-3001 Leuven, Belgium

16:00 to 16:30 Refreshment Break Room N3.23 (Opposite N3.28)

Session 2: Photodetectors
North Building N3.28; 16.30 – 18.00

16.30 A19_08 **Growth and characterization of long-wavelength Type-II InAs/GaSb superlattice infrared detectors**

DCM Kwan[1], M Delmas[1], B Liang[2], D Huffaker[1,].

[1]School of Physics and Astronomy, Cardiff University, The Parade, Cardiff, CF24 3AA, UK; [2]California NanoSystem Institute, University of California, Loa Angeles, CA90095, USA

16.45 A19_02 **InGaAs-InP PIN-HBT Optoelectronic Integrated Circuit with Extended Bandwidth and High Optical Power Capability**

SG Muttlak, OS Abdulwahid, J Sexton and M Missous.

School of Electrical and Electronic Engineering, University of Manchester, UK

17.00 A19_23 **$AlAs_{0.56}Sb_{0.44}$ avalanche photodiodes with high gain-bandwidth product over 300 GHz**

S Xie[1], X Yi [2], BL Liang[3], CH Tan[2], JPR David[2] and DL Huffaker[1].
[1]School of Physics and Astronomy, Cardiff University, Cardiff; [2]Department of Electronic and Electrical Engineering, University of Sheffield; [3]California NanoSystems Institute, University of California-Los Angeles

17.15 A19_07 Modelling and Characterization of Zero-Bias Asymmetrical Spacer Layer Tunnel Diode Detectors

OS Abdulwahid[1], S Muttlak[1], J Sexton[1], KN Zainul Ariffin[1], MJ Kelly[2] and M Missous[1].
[1]School of Electrical and Electronic Engineering, the University of Manchester, United Kingdom; [2]The University of Cambridge, Cambridge, United Kingdom

17.30 A19_19 Experimentally Validated Physical Modelling of GaAs/AlAs Asymmetric Spacer Layer Tunnel Diodes

A Hadfield and M Missous.
School of Electrical & Electronic Engineering, The University of Manchester, Manchester, M13 9PL, United Kingdom

17.45 A19_20 Passivation of AlInAsSb Data Alloy Avalanche Photodiodes

C Guoa,[b], Y Lv[a], Y Ding[b],*, E Wasige[b], Z Niu[a].
[a]Institute of Semiconductors, Chinese Academy of Sciences, Beijing 100083, China; [b]School of Engineering, University of Glasgow, Glasgow, G12 8LT, UK,

Session 3: Posters & IET Publishing Reception (including drinks and buffet)
West Extension Building WX3.07/WX3.14; 18:00 – 20:00

A19_55 III-V Quantum dot materials and devices grown on on-axis (001) Si substrate

Z Liu[1]*, C Hantschmann[2], M Tang[1], Y Lu[1], J Park[1], M Liao[1], A Sanchez[3], R Beanland[3], M Martin[4], T Baron[4], S Chen[1], A Seeds[1], R Penty[2], I White[2], and H Liu[1]
[1] Department of Electronic and Electrical Engineering, University College London, London, WC1E 7JE, United Kingdom; [2] Centre for Photonic Systems, Department of Engineering, University of Cambridge, 9 JJ Thomson Avenue, Cambridge CB3 0FA, United Kingdom; [3] Department of Physics, University of Warwick, Coventry, CV4 7AL, United Kingdom; [4] Univ. Grenoble Alpes, CNRS, CEA-LETI, MINATEC, LTM, F-38054 Grenoble, France

A19_06 CW Laser for All Quantum Dot CW THz emission

G Bello, S Smirnov and E Rafailov.
Optoelectronics and Biomedical Photonics GroupAston Institute of Photonics Technologies, Aston University, Birmingham, B4 7ET

A19_11 Design conditions in the middle range for implementation of integrated ring resonator $LiNbO_3$ by direct laser writing

PL Pagano[1, 2], D Presti[1, 3], RR Peyton[1, 3], N Abadía[5,6], FA Videla[1,4], GA Torchia[1,3]
[1]Centro de Investigaciones Ópticas (CONICET-CICBA-UNLP), M.B. Gonnet (1897), Buenos Aires, Argentina; [2] Facultad de Ciencias Exactas, Departamento de Física, Universidad Nacional de La Plata– Argentina, Calle 115 y 47; [3] Depto. De Ciencia y Tecnología, Universidad Nacional de Quilmes Roque Sáenz Peña 352 – Bernal (1876) – Bs. As. – Argentina; [4] Facultad de Ingeniería, Universidad Nacional de la Plata, Depto de Ciencias Básicas.; [5]School of Physics and Astronomy, Cardiff University, Queen's Buildings, The Parade, Cardiff, CF24 3AA, United Kingdom; [6]Institute for Compound Semiconductors, Cardiff University, Queen's Buildings, The Parade, Cardiff, CF24 3AA, United Kingdom

A19_14 Ultrafast laser inscription: a key method available to a wide range of materials with high integration for 3D optical devices fabrication

V Guarepi[1], R Peyton[1,2], D Presti [1,2], D Biasetti[1], M Tejerina[3], F Videla[1] N Abadía[4,5] and GA Torchia[1,2]

[1]Centro de Investigaciones Ópticas, CONICET-CICBA-UNLP, Camino Centenario y 506, s/n, M.B. Gonnet (1897), Buenos Aires, República Argentin; [2]Departamento de Ciencia y Tecnología, Universidad Nacional de Quilmes, Roque Saénz Peña, 352, Bernal (1876), Buenos Aires, República Argentina; [3]Centro de Tecnología de Recursos Minerales y Cerámica (CONICET La Plata-CIC), CC nº 49, M.B. Gonnet (1897), Buenos Aires, República Argentina; [4]School of Physics and Astronomy, Cardiff University, Queen's Buildings, The Parade, Cardiff, CF24 3AA, United Kingdom; [5]Institute for Compound Semiconductors, Cardiff University, Queen's Buildings, The Parade, Cardiff, CF24 3AA, United Kingdom

A19_22 **3D Monte Carlo simulation of GaAs nanowire single-photon avalanche diodes**

H Li[1,2], S Xie[1*], and DL Huffaker[1]

[1]School of Physics and Astronomy, Cardiff University, Cardiff, UK; [2]School of Physics Science and Technology, Wuhan University, China

A19_31 **Designing optimized retro-reflecting electro-absorption modulators for free space optical datalinks.**

B Maglio[1], N Abadía[1], PM Smowton[1], C Quitana[2], G Erry[2], Y Thueux[2]

[1]Department of Physics, Cardiff University, Cardiff, CF24 3AA; [2]Airbus Group Innovations, Newport, NP10 8FZ

A19_54 **Vertical Cavity Surface Emitting Lasers for Miniature Atomic Clocks**

C Hentschel[1], S-J Gillgrass[1] S Shutts[1], DG Hayes[1], CP Allford[1], D Zaouris[2], M Haji[2], I Eddie[3], I Kostakis[4], M Missous[4], W Meredith[5], and PM Smowton[1]

[1]EPSRC Future Compound Semiconductor Manufacturing Hub, School of Physics and Astronomy, Cardiff University, Cardiff, UK; [2]Time and Frequency Metrology, National Physical Laboratory, Teddington, UK; [3]CST Global Ltd, Glasgow, UK; [4]ICS Ltd, Manchester, UK; [5]Compound Semiconductor Centre, Cardiff, UK

A19_51 **InP Quantum Dot Monolithically Mode-Locked Lasers Emitting at 740 nm**

Z Li[1], S Shutts[1], CP Allford[1], RS Alharbi[1], AB Krysa[2], PM Smowton[1].

[1]EPSRC Future Compound Semiconductor Manufacturing Hub, School of Physics and Astronomy, Cardiff University, Queen's Building, The Parade, Cardiff, UK, CF24 3AA; [2]EPSRC National Centre for III-V Technologies, University of Sheffield, Sheffield, S1 3JD

A19_09 **Design of a Y-branch in silicon-on-insulator based on simplified coherently coupled**

R Peyton[1, 2, †], D Presti[1, 2], F Videla[1, 3], N Abadía[4, 5] and GA Torchia[1, 2].

[1]Centro de Investigaciones Opticas (CONICET-CICBA-UNLP), M.B. Gonnet (1897), Buenos Aires, Argentina; [2]Departamento de Ciencia y Tecnologia, Universidad Nacional de Quilmes; [3]Facultad de Ingenieria, Universidad Nacional de la Plata, Depto de Ciencias Basica; [4]School of Physics and Astronomy, Cardiff University, Queen's Buildings, The Parade, Cardiff, CF24 3AA, United Kingdom; [5]Institute for Compound Semiconductors, Cardiff University, Queen's Buildings, The Parade, Cardiff, CF24 3AA, United Kingdom

A19_33 **Silicon Nitride Polarization Beam Splitters: A Review**

M Tosi[1, 2], A Fasciszewki1, N Abadía[4, 5] and PA Costanzo Caso[1, 2,3].

[1]Comisión Nacional de Energía Atómica (CNEA); [2] Instituto Balseiro, UNCuyo-CNEA, Av. Bustillo 9500, Bariloche (RN), Argentina; [3] Consejo Nacional de Investigaciones Científicas y Técnicas (CONICET), Argentina; [4] School of Physics and Astronomy, Cardiff University, Queen's Building, The Parade, Cardiff, CF24 3AA, United Kingdom; [5] Institute for Compound Semiconductors, Cardiff University, Queen's Building, The Parade, Cardiff, CF24 3AA, United Kingdom.

A19_24 **Latest advances in microresonator based frequency combs**

M Barturen[1, 2], N Abadía [3, 4], PA Costanzo Caso [2, 5, 6].

[1]Instituto de Tecnología, Universidad Argentina de la Empresa, Lima 775, (C1073AAO) Ciudad Autónoma de Buenos Aires, Argentina; [2] Consejo, Nacional de Investigaciones Científicas y Técnicas (CONICET), Argentina; [3]School of Physics and Astronomy, Cardiff University, Queen's Building, The Parade, Cardiff, CF24 3AA, United Kingdom; [4]Institute for Compound Semiconductors, Cardiff University, Queen's Building, The Parade, Cardiff, CF24 3AA, United Kingdom; [5]Instituto Balseiro, UNCuyo-CNEA, Av. Bustillo 9500, Bariloche (RN), Argentina; [6]Comisión Nacional de Energía Atómica (CNEA).

A19_44 **C-Band tunable laser modeling and simulation**

M Bustillos[1,2*], GF Rinalde[1,2], L Bulus[1,2,3], N Abadía[4,5,6], and PA Costanzo Caso[1,2,3#]
*[1]Instituto Balseiro, UNCuyo-CNEA, Av. Bustillo 9500, Bariloche (RN), Argentina; [2] Comisión Nacional de Energía Atómica (CNEA); [3] Consejo Nacional de Investigaciones Científicas y Técnicas (CONICET), Argentina; [4]Department of Electrical and Computer Engineering, McGill University, Montreal, Quebec, H3A 0E9, Canada; [5]School of Physics and Astronomy, Cardiff University, Queen's Building, The Parade, Cardiff, CF24 3AA, United Kingdom; [6]Institute for Compound Semiconductors, Cardiff University, Queen's Building, The Parade, Cardiff, CF24 3AA, United Kingdom*___

A19_41 Optical Switch using Beamsteering at 900 nm wavelength in GaAs / $Al_xGa_{(1-x)}As$ with High Extinction Ratio for Quantum Sensors

JL Moss, B Saleeb-Mousa, JO Maclean*, RP Campion, and CJ Mellor
School of Physics and Astronomy, University of Nottingham, University Park, Nottingham, NG7 2RD _____

Programme, Wednesday 17th April

Session 4: Lasers & Light Sources I

Law Building 0.22; 08:45 – 10:30

08.45 A19_12 **Unidirectional topological edge modes in nanowire-based kagomephotonic crystals**

S Wong[1], M Saba[2], O Hess[2], and SS Oh[1]

[1]School of Physics and Astronomy, Cardiff University, Cardiff CF24 3AA; [2]The Blackett Laboratory, Imperial College London, London SW7 2AZ, UK

09.00 A19_46 **Design, Fabrication and Characterisation of 980 nm Linearly Polarised Multi-Mode VCSELs for Ebium Doped Waveguide Amplifier Integration**

D Lei[1], N Babazadeh[2], J Sarma[3], DTD Childs[1], and RA Hogg[1]

[1]The University of Glasgow, Glasgow, G12 8LT UK; [2]The University of Sheffield, Western Bank, Sheffield, S10 2TN UK, [3]University of Bath, Claverton Down, Bath, BA2 7AY UK

09.15 A19_10 **Photonic Topological Insulator Lasers based on III-V Semiconductor Nanowires**

Y Gong, S Wong, DL Huffaker, SS Oh

School of Physics and Astronomy, Cardiff University, Cardiff, CF24 3AA, United Kingdom

09.30 A19_03 **Numerical Simulation of Photonic Microwave Generation in a Single Mode VCSEL**

C Xue[1, 2], S Ji[1], A Valle[3] and Y Hong[1]

[1]School of Electronic Engineering, Bangor University, Wales, LL57 1UT, UK; [2]School of Information and Communication Engineering, University of Electronic Science and Technology of China, Chengdu 611731, China; [3]Institution de Física de Cantabria (CSIC-Univ. de Cantabria), Avda. Los Castros s/n, E39005 Santander, Spain.

09.45 A19_45 **The Nature of Auger Recombination in Type-I Mid-Infrared Laser Diodes**

TD Eales[1], MC Amann[2], IP Marko[1], BA Ikyo[1], AR Adams[1], A Andrejew[2], K Vizbaras[2,3], L Shterengas[4], G Belenky[4], I Vurgaftman[5], JR Meyer[5], SJ Sweeney[1]

[1]Advanced Technology Institute and Department of Physics, University of Surrey, Guildford GU2 7XH, United Kingdom; [2]Walter Schottky Institut, Technische Universität München, Am Coulombwall 3, 85748 Garching, Germany; [3]Brolis Semiconductors UAB, Moletu pl. 73, Vilnius, Lithuania, LT-14259; [4]Department of Electrical and Computer Engineering, State University of New York at Stony Brook, New York 11794, USA; [5]US Naval Research Laboratory, 4555 Overlook Avenue SW, Washington DC 20375, USA.

10.00 A19_21 **Surface Recombination Effects in Transfer Printable Red Micro-LEDs**

J Browne[1], Z Li1, J Justice[1], A Gocalinska[1], E Pelucchi[1] and B Corbett[1]

[1]Tyndall National Institute, University College Cork, Lee Maltings, Dyke Parade, Cork, Ireland

10.15 A19_32 **An approach towards spin-injected edge-emitting semiconductor lasers**

N Jung[1], M Lindemann[1], J Ritzmann[2], S Webers[3,] A Ludwig[2], A Wieck[2], H Wende[3], NC Gerhardt[1] and MR Hofman[1]

[1]Photonics and Terahertz Technology, Ruhr University Bochum, 44780 Germany; [2]Angewandte Festkörperphysik, Ruhr University Bochum, 44780 Germany; [3]Faculty of Physics and Center for Nanointegration(CENIDE), University of DuisburgEssen, lotharstr. 1, Duisburg, Germany

10:30 – 11:15 Refreshment Break, Aberdare Hall

Session 5: Lasers & Light Sources II
Law Building 0.22; 11:15 – 13:00

11.15 A19_48 **Mode Coupling and Analysis in Laterally Coupled Vertical Cavities**

S Chen, H Francis, CH Ho, KJ Che, M Hopkinson, and CY Jin
Department of Electronic & Electrical Engineering, University of Sheffield

11.30 A19_30 **Temperature and Pressure Dependence of Low Threshold Current Type-II GaInAs/GaAsSb"W"-Lasers Emitting Around 1.25-μm**

D Duffy[1], IP Marko[1], TD Eales[1], C Fuchs[2], J Lehr[2], W Stolz[2] and SJ Sweeney[1]
[1]Advanced Technology Institute and Department of Physics, University of Surrey, Guildford, GU2 7XH, United Kingdom; [2]Materials Sciences Center and Department of Physics, Philipps-Universität Marburg, Renthof 5, 35032, Marburg, Germany

11.45 A19_49 **High Resolution Opitcal Spectrcopy of state-of-the-art Quantum-Dot Lasers for High Temperature Operation**

IME Butler[1, 2], N Babazadeh[1], R Baba[1], K Nishi[3], K Takemasa[3], M Sugawara[3], DTD Childs[1], RA Hogg[1]
[1]School of Engineering, University of Glasgow, Glasgow, G12 8LT, UK; [2]School of Mathematics and Physics, Queen's University Belfast, Belfast, BT7 1NN, UK; [3]QD Laser Inc, Keihin Bldg. 1F, 1-1 Minamiwataridacho, Kawasaki-ku, Kawasaki, Kanagawa 210-0855, JAPAN

12.00 A19_52 **Temperature Dependant Characteristics of P-doped Laser Devices**

L Jarvis[1], S Shutts[1], M Tang[2], H Liu[2] and PM Smowton[1]
[1]School of Physics and Astronomy, Cardiff University, The Parade, Cardiff, CF24 3AA, [2]Department of Electronic and Electrical Engineering, University College London, Torrington Place, WC1E 7JE

12.15 A19_28 **High-yield, low-density InAs/GaAs quantum dots as on-chip quantum light sources**

E Clarke, [1*] P Patil, [1] I Farrer,[1] B Royall,[2] AP Foster,[2] D Hallett,[2] DL Hurst,[2] P Kok,[2] F Liu,[2] AJ Brash,[2] J O'Hara,[2] LMPP Martins,[2] CL Phillips,[2] R Coles,[2] C Bentham,[2] N Prtljaga,[2] M Makhonin, [2] IE Itskevich, [3] LR Wilson, [2] AM Fox,[2] J Heffernan,[1] MS Skolnick[2]
[1]EPSRC National Epitaxy Facility, University of Sheffield, Sheffield S1 3JD, UK; [2]Department of Physics and Astronomy, University of Sheffield, Sheffield, S3 7RH, UK; [3]School of Engineering and Computer Science, University of Hull, Hull HU6 7RX, UK

12.30 A19_29 **Quantum dot-based optically pumped VCSELs with high-contrast periodic gratings**

T Fördös[1,4,5], E Clarke[1], P Patil[1], RJ Airey[1], N Babazadeh[1], C Ovenden[2], M Adams[3], I Henning[3], and J Heffernan[1,2]
[1]EPSRC National Epitaxy Facility, University of Sheffield, Sheffield, S1 3JD, United Kingdom; [2]Department of Electronic and Electrical Engineering, University of Sheffield, Sheffield S1 3JD, United Kingdom; [3]School of Computer Science and Electronic Engineering, University of Essex, Colchester, CO4 3SQ, United Knigdom; [4]Nanotechnology Centre, VŠB - Technical University of Ostrava, 17. listopadu 15, 708 00 Ostrava - Poruba, Czech Republic; [5]IT4Innovation, VŠB - Technical University of Ostrava, 17. listopadu 15, 708 00 Ostrava - Poruba, Czech Republic.

12.45 A19_15 **O-band InAs/GaAs quantum dot laser monolithically integrated on exact (001) Si substrate**

K Li[1]*, Z Liu[1], M Tang[1], M Liao[1], D Kim[1], H Deng[1], AM Sanchez[2], R Beanland[2], M Martin[3], T Baron[3], S Chen[1], J Wu[1], A Seeds[1] and H Liu[1]
[1]Department of Electronic and Electr–ical Engineering, University College London, London, WC1E 7JE, United Kingdom; [2]Department of Physics, University of Warwick, Coventry, CV4 7AL, United Kingdom; [3]Univ. Grenoble Alpes, CNRS, CEA-LETI, MINATEC, LTM, F-38054 Grenoble, France

13:00 – 14:00 Lunch, Aberdare Hall

Session 6: Integration Strategies & Approaches I
Law Building 0.22; 14:00 – 15:00

14.00 A19_47 Silicon and germanium mid-infrared platforms
J Soler Penadés[1], A Osman[1], A Sánchez-Postigo[2], Z Qu[1], Y Wu[1], CJ Stirling[1], DP Cheben[3], A Ortega-Moñux[2], JG Wangüemert-Pérez[2], M Nedeljkovic[1], GZ Mashanovich[1]
[1]Optoelectronics Research Centre, University of Southampton, Southampton, SO17 1BJ, UK; [2]Universidad de Málaga, ETSI Telecomunicación, Campus de Teatinos, 29071 Málaga, Spain; [3]National Research Council Canada, Building M-50, Ottawa, K1A 0R6 Canada

14.15 A19_01 Integrated Polarization Handling Devices
M Ghulam Saber[1,*] ,L Xu[1], RH Sagor[2], DV Plant[1], and N Abadía[1,3,4,]
[1]Department of Electrical and Computer Engineering, McGill University, Montreal, Quebec, H3A 0E9, Canada; [2]Department of Electrical and Electronic Engineering, Islamic University of Technology, Gazipur 1704, Bangladesh; [3]School of Physics and Astronomy, Cardiff University, Queen's Building, The Parade, Cardiff, CF24 3AA, United Kingdom; [4]Institute for Compound Semiconductors, Cardiff University, Queen's Building, The Parade, Cardiff, CF24 3AA, United Kingdom.

14.30 A19_04 Integration of Sub-wavelength Structures with Silicon Photonic Devices
Y D'Mello[1], S Bernal[1], DV Plant[1], and N Abadía[2,3]
[1]Department of Electrical and Computer Engineering, McGill University, Montreal, Quebec, H3A 0E9, Canada; [2]School of Physics and Astronomy, Cardiff University, Queen's Building, The Parade, Cardiff, CF24 3AA, United Kingdom; [3]Institute for Compound Semiconductors, Cardiff University, Queen's Building, The Parade, Cardiff, CF24 3AA, United Kingdom.

14.45 A19_18 Raman Scattering Effect on a QKD and High Speed Classical Data Hybrid Link
H Qin[1], A Wonfor[1], S Yang[1], RV Penty[1], IH White[1]
[1]Electrical Engineering Dept., University of Cambridge, 9 JJ Thomson Ave, Cambridge CB3 0FA

15:00 to 15:45 Refreshment Break, Aberdare Hall

Session 7: Integration Strategies & Approaches II
Law Building 0.22; 15:45 – 16:30

15.45 A19_40 Generating optical frequency combs via nano-scale all-optical modulators
H Francis, S Chen, KJ Che, M Hopkinson and CY Jin.
Department of Electrical and Electronic Engineering, University of Sheffield.

16.00 A19_53 Particle Manipulation and Control for Integrated Optoelectronic Microfluidics
D Giliyana*, E Le Boulbar, S Gillgrass and PM Smowton
School of Physics and Astronomy, Cardiff University, The Parade, Cardiff, CF24 3AA

16.15 A19_43 **Optically Controlled Millimetre-wave Switches with Coplanar Stepped-Impedance Lines**

Y Zhang, AW Pang and MJ Cryan
Department of Electrical and Electronic Engineering, University of Bristol, U.K

Session 7b: Discussion - Integration Strategies

Law Building 0.22; 16:30 – 17:30

Conference Banquet

National Museum Cardiff 18:00 onwards

Programme, Thursday 18th April

Session 8: Materials Development and Devices I

Room 0.22, Law Building; 08:45 - 10:45

08.45 A19_50 **Monolithic Growth of 1.5 µm InAs Quantum Dots Lasers on (001) Si and Material Studies**

Z Li[1], S Shutts[1], CP Allford[1], B Shi[2], W Luo[2], KM Lau[2] and PM Smowton[1]

[1]EPSRC Future Compound Semiconductor Manufacturing Hub, School of Physics and Astronomy, Cardiff University, Queen's Building, The Parade, Cardiff, UK, CF24 3AA; [2]Department of Electronic and Computer Engineering, Hong Kong University of Science and Technology,Clear Water Bay, Kowloon, Hong Kong

09.00 A19_05 **Sub-mm(>100µm) thick diamond layer on aluminium nitride for thermal management applications.**

S Mandal[1]*, JA Cuenca[1], H Bland[1], C Yuan[2], F Massabuau[3], JW Pomeroy[2], D Wallis[3,4], R Oliver[3], M Kuball[2], OA Williams[1]

[1]School of Physics and Astronomy, Cardiff University, Cardiff, UK, [2]Center for Device Thermography and Reliability, Bristol University, Bristol, UK, [3]Department of Materials Science & Metallurgy, University of Cambridge, Cambridge, UK, [4]School of Engineering, Cardiff University, Cardiff, UK

09.15 A19_26 **Angled Cage Etching for Integrated Photonics in GaN**

GP Gough[1,2], DM Beggs[2], RA Taylor[3], B Humphreys[4], AD Sobiesierski[5], S Shabbir[5], S Thomas[5], K Sun[5], AJ Bennett[5,6]

[1]Quantum Engineering Centre for Doctoral Training, Nanoscience and Quantum Information (NSQI) Building,University of Bristol, Tyndall Avenue, Bristol,BS8 1FD; [2] School of Physics and Astronomy, Cardiff University, Queen's Buildings, Cardiff, CF24 3AA, UK; [3] Department of Physics, University of Oxford, Clarendon Laboratory, Parks Road, Oxford, OX1 3PU, UK; [4] Seren Photonics, UK Technology Centre, Pencoed Technology Park, Bridgend, CF35 5HZ, UK; [5] Institute for Compound Semiconductors, Cardiff University, Queen's Buildings, Cardiff, CF24 3AA, UK; [6] School of Engineering, Cardiff University, Queen's Buildings, Cardiff, CF24 3AA, UK.

09.30 A19_35 **Growth, Fabrication and Characterization of Integrated Green HEMT-LED Devices**

Y Cai, Y Gong, J Bai, X Yu, C Zhu, V Esendag, KB Lee and T Wang

Department of Electronic and Electrical Engineering, University of Sheffield, Sheffield, S1 3JD

09.45 A19_37 **Nonpolar (11-20) InGaN/GaN light-emitting diodes overgrown on a micro-rod Template**

L Jiu, J Bai, N Poyiatzis, P Fletcher and T Wang

Department of Electronic and Electrical Engineering, University of Sheffield, Mappin Street, Sheffield, S1 3JD, United Kingdom

10.00 A19_13 **Optimization of thin Ge buffer layers on Silicon for integration of III-V on silicon Substrates**

J Yang[1], P Jurczak[1*], F Cui[1], K Li[1], M Tang[1], L Billiald[2] , R Beanland[2], AM Sanchez[2], and H Liu[1]

[1] Department of Electronic and Electrical Engineering, University College London, Torrington Place, WC1E 7JE London, United Kingdom, [2] Department of Physics, University of Warwick, CV4 7AL, Coventry, United Kingdom

10.15 A19_34 **Hybrid III–V/IV Nanowires: High-Quality Ge Shell Epitaxy on GaAs Cores**

H Zeng,[†,‖] X Yu,*[,†,‖] H Fonseka,[‡] JA Gott,[‡] M Tang,[†] Y Zhang,[†] AM Sanchez, [‡] and H Liu[†]

[†]Department of Electronic and Electrical Engineering, University College London, London WC1E 7JE, United Kingdom; [‡]Department of Physics, University of Warwick, Coventry CV4 7AL, United Kingdom

10.30 A19_16 **Novel Hydrogen Silsesquioxane Planarization for Electronic-Photonic Integrated Circuit Applications**

A Al-Moathin, L Hou, S Thoms, JH Marsh
School of Engineering, University of Glasgow, Glasgow G12 8QQ, U.K.

10:45 – 11:15 Refreshment Break, Aberdare Hall

Session 9: Materials Development and Devices II

Location: Room 0.22, Law Building; 11:15 - 12:45

11.15 A19_39 **AlInAs Gettering Layer for Resonant Tunnelling Diode Barrier Symmetry**

R Baba[1], BA Harrison[2], BJ Stevens[3], R Beanland[4], T Mukai[5], RA Hogg[1]
[1]The University of Glasgow, Glasgow, G12 8LT UK; [2]EPSRC National Epitaxy Facility, Sheffield, S3 7HQ UK; [3]IQE Europe Ltd., Cardiff CF3 0LW UK; [4]Integrity Scientific Ltd., Warwick, CV34 4JP UK; [5]ROHM Semiconductor Co. Ltd., Kyoto, 615-8585 Japan

11.30 A19_36 **A two-step method of growing (11-22) semi-polar GaN on (113) silicon**

Y Cai, S Shen, X Yu, X Zhao, L Jiu, C Zhu, J Bai and T Wang
Department of Electronic and Electrical Engineering, University of Sheffield, Sheffield, S1 3JD

11.45 A19_17 **Engineering the optical transitions in InAs/GaAsSb QDs using thin InAlAs layers**

A Salhi[1, 2], S Alshaibani[2], Y Alaskar[2], A Albadri[2], A Alyamani[2] and M Missous[1]
[1]School of Electrical and Electronic Engineering. The University of Manchester, Sackville Street, Manchester M13 9PL, United Kingdom; [2]National center for Nanotechnology and advanced materials, KACST, 11442 Riyadh, Saudi Arabia

12.00 A19_25 **Analytical model of optical amplification in strained Ge**

EE Orlova and RW Kelsall
Pollard Institute, School of Electronic and Electrical Engineering, University of Leeds, Leeds LS2 9JT, UK

12.15 A19_38 **Electroluminescence from GaAsBi/GaAs multiple quantum well devices – potential for broadband light source applications**

TBO Rockett[1], RD Richards[1]*, Y Liu[1], F Harun[1], Z Zhou[1], Y Gu[2], JR Willmott[1], and JPR David[1].
[1]University of Sheffield, Sheffield, South Yorkshire, S1 3JD, U, K[2]Shanghai Institute of Microsystem and Information Technology, Chinese Academy of Sciences, China

12.30 A19_27 **Dilute Magnetic Contact for a Spin GaN HEMT**

JE Evans[1], G Burwell[2], FC Langbein[3], SG Shermer[2], and K Kalna[4]
[1]Centre for NanoHealth & [2]College of Science, Physics, Swansea University, SA1 8EN, Wales, UK; [3]School of Computer Science and Informatics, Cardiff University, Cardiff CF24 3AA, Wales, UK; [4]Nanoelectronic Devices Computational Group, Swansea University, Swansea, SA1 8EN, Wales, UK

12:45 Lunch, Aberdare Hall

Conference Close

Abstract List

Numerical order

A19_01 Integrated Polarization Handling Devices

M Ghulam Saber[1,*], L Xu[1], RH Sagor[2], DV Plant[1], and N Abadía[1,3,4,]

[1]Department of Electrical and Computer Engineering, McGill University, Montreal, Quebec, H3A 0E9, Canada; [2]Department of Electrical and Electronic Engineering, Islamic University of Technology, Gazipur 1704, Bangladesh; [3]School of Physics and Astronomy, Cardiff University, Queen's Building, The Parade, Cardiff, CF24 3AA, United Kingdom; [4]Institute for Compound Semiconductors, Cardiff University, Queen's Building, The Parade, Cardiff, CF24 3AA, United Kingdom

A19_02 InGaAs-InP PIN-HBT Optoelectronic Integrated Circuit with Extended Bandwidth and High Optical Power Capability

SG Muttlak, OS Abdulwahid, J Sexton and M Missous.

School of Electrical and Electronic Engineering, University of Manchester, UK

A19_03 Numerical Simulation of Photonic Microwave Generation in a Single Mode VCSEL

C Xue[1, 2], S Ji[1], A Valle[3] and Y Hong[1]

[1]School of Electronic Engineering, Bangor University, Wales, LL57 1UT, UK; [2]School of Information and Communication Engineering, University of Electronic Science and Technology of China, Chengdu 611731, China; [3]Institution de Física de Cantabria (CSIC-Univ. de Cantabria), Avda. Los Castros s/n, E39005 Santander, Spain

A19_04 Integration of Sub-wavelength Structures with Silicon Photonic Devices

Y D'Mello[1], S Bernal[1], DV Plant[1], and N Abadía[2,3]

[1]Department of Electrical and Computer Engineering, McGill University, Montreal, Quebec, H3A 0E9, Canada; [2]School of Physics and Astronomy, Cardiff University, Queen's Building, The Parade, Cardiff, CF24 3AA, United Kingdom; [3]Institute for Compound Semiconductors, Cardiff University, Queen's Building, The Parade, Cardiff, CF24 3AA, United Kingdom

A19_05 Sub-mm (>100 μm) thick diamond layer on aluminium nitride for thermal management applications.

S Mandal[1]*, JA Cuenca[1], H Bland[1], C Yuan[2], F Massabuau[3], JW Pomeroy[2], D Wallis[3,4], R Oliver[3], M Kuball[2], OA Williams[1]

[1]School of Physics and Astronomy, Cardiff University, Cardiff, UK, [2]Center for Device Thermography and Reliability, Bristol University, Bristol, UK, [3]Department of Materials Science & Metallurgy, University of Cambridge, Cambridge, UK, [4]School of Engineering, Cardiff University, Cardiff, UK

A19_06 CW Laser for All Quantum Dot CW THz emission

G Bello, S Smirnov and E Rafailov.

Optoelectronics and Biomedical Photonics GroupAston Institute of Photonics Technologies, Aston University, Birmingham, B4 7ET

A19_07 Modelling and Characterization of Zero-Bias Asymmetrical Spacer Layer Tunnel Diode Detectors

OS Abdulwahid[1], S Muttlak[1], J Sexton[1], KN Zainul Ariffin[1], MJ Kelly[2] and M Missous[1].

[1]School of Electrical and Electronic Engineering, the University of Manchester, United Kingdom; [2]The University of Cambridge, Cambridge, United Kingdom

A19_08 Growth and characterization of long-wavelength Type-II InAs/GaSb superlattice infrared detectors

DCM Kwan[1], M Delmas[1], B Liang[2], D Huffaker[1,].

[1]School of Physics and Astronomy, Cardiff University, The Parade, Cardiff, CF24 3AA, UK; [2]California NanoSystem Institute, University of California, Loa Angeles, CA90095, USA

A19_09 Design of a Y-branch in silicon-on-insulator based on simplified coherently coupled

R Peyton[1, 2, †], D Presti[1, 2], F Videla[1, 3], N Abadía[4, 5] and GA Torchia[1, 2].
[1]Centro de Investigaciones Opticas (CONICET-CICBA-UNLP), M.B. Gonnet (1897), Buenos Aires, Argentina; [2]Departamento de Ciencia y Tecnologia, Universidad Nacional de Quilmes; [3]Facultad de Ingenieria, Universidad Nacional de la Plata, Depto de Ciencias Basica; [4]School of Physics and Astronomy, Cardiff University, Queen's Buildings, The Parade, Cardiff, CF24 3AA, United Kingdom; [5]Institute for Compound Semiconductors, Cardiff University, Queen's Buildings, The Parade, Cardiff, CF24 3AA, United Kingdom

A19_10 Photonic Topological Insulator Lasers based on III-V Semiconductor Nanowires

Y Gong, S Wong, DL Huffaker, SS Oh
School of Physics and Astronomy, Cardiff University, Cardiff, CF24 3AA, United Kingdom

A19_11 Design conditions in the middle range for implementation of integrated ring resonator $LiNbO_3$ by direct laser writing

PL Pagano[1, 2], D Presti[1, 3], RR Peyton[1, 3], N Abadía[5,6], FA Videla[1,4], GA Torchia[1,3]
[1]Centro de Investigaciones Ópticas (CONICET-CICBA-UNLP), M.B. Gonnet (1897), Buenos Aires, Argentina; [2] Facultad de Ciencias Exactas, Departamento de Física, Universidad Nacional de La Plata– Argentina, Calle 115 y 47; [3] Depto. De Ciencia y Tecnología, Universidad Nacional de Quilmes Roque Sáenz Peña 352 – Bernal (1876) – Bs. As. – Argentina; [4] Facultad de Ingeniería, Universidad Nacional de la Plata, Depto de Ciencias Básicas.; [5]School of Physics and Astronomy, Cardiff University, Queen's Buildings, The Parade, Cardiff, CF24 3AA, United Kingdom; [6]Institute for Compound Semiconductors, Cardiff University, Queen's Buildings, The Parade, Cardiff, CF24 3AA, United Kingdom

A19_12 Unidirectional topological edge modes in nanowire-based kagomephotonic crystals

S Wong[1], M Saba[2], O Hess[2], and SS Oh[1]
[1]School of Physics and Astronomy, Cardiff University, Cardiff CF24 3AA; [2]The Blackett Laboratory, Imperial College London, London SW7 2AZ, UK

A19_13 Optimization of thin Ge buffer layers on Silicon for integration of III-V on silicon Substrates

J Yang[1], P Jurczak[1*], F Cui[1], K Li[1], M Tang[1], L Billiald[2] , R Beanland[2], AM Sanchez[2], and H Liu[1]
[1] Department of Electronic and Electrical Engineering, University College London, Torrington Place, WC1E 7JE London, United Kingdom, [2] Department of Physics, University of Warwick, CV4 7AL, Coventry, United Kingdom

A19_14 Ultrafast laser inscription: a key method available to a wide range of materials with high integration for 3D optical devices fabrication

V Guarepi[1], R Peyton[1,2], D Presti [1,2], D Biasetti[1], M Tejerina[3], F Videla[1] N Abadía[4,5] and GA Torchia[1,2]
[1]Centro de Investigaciones Ópticas, CONICET-CICBA-UNLP, Camino Centenario y 506, s/n, M.B. Gonnet (1897), Buenos Aires, República Argentin; [2]Departamento de Ciencia y Tecnología, Universidad Nacional de Quilmes, Roque Saénz Peña, 352, Bernal (1876), Buenos Aires, República Argentina; [3]Centro de Tecnología de Recursos Minerales y Cerámica (CONICET La Plata-CIC), CC nº 49, M.B. Gonnet (1897), Buenos Aires, República Argentina; [4]School of Physics and Astronomy, Cardiff University, Queen's Buildings, The Parade, Cardiff, CF24 3AA, United Kingdom; [5]Institute for Compound Semiconductors, Cardiff University, Queen's Buildings, The Parade, Cardiff, CF24 3AA, United Kingdom

A19_15 O-band InAs/GaAs quantum dot laser monolithically integrated on exact (001) Si substrate

K Li[1]*, Z Liu[1], M Tang[1], M Liao[1], D Kim[1], H Deng[1], AM Sanchez[2], R Beanland[2], M Martin[3], T Baron[3], S Chen[1], J Wu[1], A Seeds[1] and H Liu[1]
[1]Department of Electronic and Electr–ical Engineering, University College London, London, WC1E 7JE, United Kingdom; [2]Department of Physics, University of Warwick, Coventry, CV4 7AL, United Kingdom; [3]Univ. Grenoble Alpes, CNRS, CEA-LETI, MINATEC, LTM, F-38054 Grenoble, France

A19_16 Novel Hydrogen Silsesquioxane Planarization for Electronic-Photonic Integrated Circuit Applications

A Al-Moathin, L Hou, S Thoms, JH Marsh
School of Engineering, University of Glasgow, Glasgow G12 8QQ, U.K

A19_17 Engineering the optical transitions in InAs/GaAsSb QDs using thin InAlAs layers

A Salhi[1, 2], S Alshaibani[2], Y Alaskar[2], A Albadri[2], A Alyamani[2] and M Missous[1]
[1]School of Electrical and Electronic Engineering. The University of Manchester, Sackville Street, Manchester M13 9PL, United Kingdom; [2]National center for Nanotechnology and advanced materials, KACST, 11442 Riyadh, Saudi Arabia

A19_18 Raman Scattering Effect on a QKD and High Speed Classical Data Hybrid Link

H Qin[1], A Wonfor[1], S Yang[1], RV Penty[1], IH White[1]
[1]Electrical Engineering Dept., University of Cambridge, 9 JJ Thomson Ave, Cambridge CB3 0FA

A19_19 Experimentally Validated Physical Modelling of GaAs/AlAs Asymmetric Spacer Layer Tunnel Diodes

A Hadfield and M Missous.
School of Electrical & Electronic Engineering, The University of Manchester, Manchester, M13 9PL, United Kingdom

A19_20 Passivation of AlInAsSb Data Alloy Avalanche Photodiodes

C Guoa,[a], Y Lv[a], Y Ding[b],*, E Wasige[b], Z Niu[a].
[a]Institute of Semiconductors, Chinese Academy of Sciences, Beijing 100083, China; [b]School of Engineering, University of Glasgow, Glasgow, G12 8LT, UK

A19_21 Surface Recombination Effects in Transfer Printable Red Micro-LEDs

J Browne[1], Z Li1, J Justice[1], A Gocalinska[1], E Pelucchi[1] and B Corbett[1]
[1]Tyndall National Institute, University College Cork, Lee Maltings, Dyke Parade, Cork, Ireland

A19_22 3D Monte Carlo simulation of GaAs nanowire single-photon avalanche diodes

H Li[1,2], S Xie[1*], and DL Huffaker[1]
[1]School of Physics and Astronomy, Cardiff University, Cardiff, UK; [2]School of Physics Science and Technology, Wuhan University, China

A19_23 $AlAs_{0.56}Sb_{0.44}$ avalanche photodiodes with high gain-bandwidth product over 300 GHz

S Xie[1], X Yi [2], BL Liang[3], CH Tan[2], JPR David[2] and DL Huffaker[1].
[1]School of Physics and Astronomy, Cardiff University, Cardiff; [2]Department of Electronic and Electrical Engineering, University of Sheffield; [3]California NanoSystems Institute, University of California-Los Angeles

A19_24 Latest advances in microresonator based frequency combs

M Barturen[1, 2], N Abadía [3, 4], PA Costanzo Caso [2, 5, 6].
[1]Instituto de Tecnología, Universidad Argentina de la Empresa, Lima 775, (C1073AAO) Ciudad Autónoma de Buenos Aires, Argentina, [2] Consejo, Nacional de Investigaciones Científicas y Técnicas (CONICET), Argentina.[3] School of Physics and Astronomy, Cardiff University, Queen's Building, The Parade, Cardiff, CF24 3AA, United Kingdom.[4] Institute for Compound Semiconductors, Cardiff University, Queen's Building, The Parade, Cardiff, CF24 3AA, United Kingdom.[5] Instituto Balseiro, UNCuyo-CNEA, Av. Bustillo 9500, Bariloche (RN), Argentina.[6] Comisión Nacional de Energía Atómica (CNEA).

A19_25 Analytical model of optical amplification in strained Ge

EE Orlova and RW Kelsall
Pollard Institute, School of Electronic and Electrical Engineering, University of Leeds, Leeds LS2 9JT, UK

A19_26 Angled Cage Etching for Integrated Photonics in GaN

GP Gough[1,2], DM Beggs[2], RA Taylor[3], B Humphreys[4], AD Sobiesierski[5], S Shabbir[5], S Thomas[5], K Sun[5], AJ Bennett[5,6]

[1]Quantum Engineering Centre for Doctoral Training, Nanoscience and Quantum Information (NSQI) Building,University of Bristol, Tyndall Avenue, Bristol,BS8 1FD; [2] School of Physics and Astronomy, Cardiff University, Queen's Buildings, Cardiff, CF24 3AA, UK; [3] Department of Physics, University of Oxford, Clarendon Laboratory, Parks Road, Oxford, OX1 3PU, UK; [4] Seren Photonics, UK Technology Centre, Pencoed Technology Park, Bridgend, CF35 5HZ, UK; [5] Institute for Compound Semiconductors, Cardiff University, Queen's Buildings, Cardiff, CF24 3AA, UK; [6] School of Engineering, Cardiff University, Queen's Buildings, Cardiff, CF24 3AA, UK

A19_27 Dilute Magnetic Contact for a Spin GaN HEMT

JE Evans[1], G Burwell[2], FC Langbein[3], SG Shermer[2], and K Kalna[4]

[1]Centre for NanoHealth & [2]College of Science, Physics, Swansea University, SA1 8EN, Wales, UK; [3]School of Computer Science and Informatics, Cardiff University, Cardiff CF24 3AA, Wales, UK; [4]Nanoelectronic Devices Computational Group, Swansea University, Swansea, SA1 8EN, Wales, UK

A19_28 High-yield, low-density InAs/GaAs quantum dots as on-chip quantum light sources

E Clarke, [1*] P Patil, [1] I Farrer,[1] B Royall,[2] AP Foster,[2] D Hallett,[2] DL Hurst,[2] P Kok,[2] F Liu,[2] AJ Brash,[2] J O'Hara,[2] LMPP Martins,[2] CL Phillips,[2] R Coles,[2] C Bentham,[2] N Prtljaga,[2] M Makhonin, [2] IE Itskevich, [3] LR Wilson, [2] AM Fox,[2] J Heffernan,[1] MS Skolnick[2]

[1]EPSRC National Epitaxy Facility, University of Sheffield, Sheffield S1 3JD, UK; [2]Department of Physics and Astronomy, University of Sheffield, Sheffield, S3 7RH, UK; [3]School of Engineering and Computer Science, University of Hull, Hull HU6 7RX, UK

A19_29 Quantum dot-based optically pumped VCSELs with high-contrast periodic gratings

T Fördös[1,4,5], E Clarke[1], P Patil[1], RJ Airey[1], N Babazadeh[1], C Ovenden[2], M Adams[3], I Henning[3], and J Heffernan[1,2]

[1]EPSRC National Epitaxy Facility, University of Sheffield, Sheffield, S1 3JD, United Kingdom; [2]Department of Electronic and Electrical Engineering, University of Sheffield, Sheffield S1 3JD, United Kingdom; [3]School of Computer Science and Electronic Engineering, University of Essex, Colchester, CO4 3SQ, United Knigdom; [4]Nanotechnology Centre, VŠB - Technical University of Ostrava, 17. listopadu 15, 708 00 Ostrava - Poruba, Czech Republic; [5]IT4Innovation, VŠB - Technical University of Ostrava, 17. listopadu 15, 708 00 Ostrava - Poruba, Czech Republic

A19_30 Temperature and Pressure Dependence of Low Threshold Current Type-II GaInAs/GaAsSb"W"-Lasers Emitting Around 1.25-μm

D Duffy[1], IP Marko[1], TD Eales[1], C Fuchs[2], J Lehr[2], W Stolz[2] and SJ Sweeney[1]

[1]Advanced Technology Institute and Department of Physics, University of Surrey, Guildford, GU2 7XH, United Kingdom; [2]Materials Sciences Center and Department of Physics, Philipps-Universität Marburg, Renthof 5, 35032, Marburg, Germany

A19_31 Designing optimized retro-reflecting electro-absorption modulators for free space optical datalinks.

B Maglio[1], N Abadía[1], PM Smowton[1], C Quitana[2], G Erry[2], Y Thueux[2]

[1]Department of Physics, Cardiff University, Cardiff, CF24 3AA; [2]Airbus Group Innovations, Newport, NP10 8FZ

A19_32 An approach towards spin-injected edge-emitting semiconductor lasers

N Jung[1], M Lindemann[1], J Ritzmann[2], S Webers[3,] A Ludwig[2], A Wieck[2], H Wende[3], NC Gerhardt[1] and MR Hofman[1]

[1]Photonics and Terahertz Technology, Ruhr University Bochum, 44780 Germany; [2]Angewandte Festkörperphysik, Ruhr University Bochum, 44780 Germany; [3]Faculty of Physics and Center for Nanointegration(CENIDE), University of DuisburgEssen, lotharstr. 1, Duisburg, Germany

A19_33 Silicon Nitride Polarization Beam Splitters: A Review

M Tosi[1, 2], A Fasciszewki[1], N Abadía[4, 5] and PA Costanzo Caso[1, 2,3].

[1]Comisión Nacional de Energía Atómica (CNEA); [2] Instituto Balseiro, UNCuyo-CNEA, Av. Bustillo 9500, Bariloche (RN), Argentina; [3] Consejo Nacional de Investigaciones Científicas y Técnicas (CONICET), Argentina; [4] School of Physics and

Astronomy, Cardiff University, Queen's Building, The Parade, Cardiff, CF24 3AA, United Kingdom; [5] Institute for Compound Semiconductors, Cardiff University, Queen's Building, The Parade, Cardiff, CF24 3AA, United Kingdom

A19_34 Hybrid III–V/IV Nanowires: High-Quality Ge Shell Epitaxy on GaAs Cores

H Zeng,[†,‖] X Yu,*[,†,‖] H Fonseka,[‡] JA Gott,[‡] M Tang,[†] Y Zhang,[†] AM Sanchez, [‡] and H Liu[†]
[†]Department of Electronic and Electrical Engineering, University College London, London WC1E 7JE, United Kingdom; [‡]Department of Physics, University of Warwick, Coventry CV4 7AL, United Kingdom

A19_35 Growth, Fabrication and Characterization of Integrated Green HEMT-LED Devices

Y Cai, Y Gong, J Bai, X Yu, C Zhu, V Esendag, KB Lee and T Wang
Department of Electronic and Electrical Engineering, University of Sheffield, Sheffield, S1 3JD

A19_36 A two-step method of growing (11-22) semi-polar GaN on (113) silicon

Y Cai, S Shen, X Yu, X Zhao, L Jiu, C Zhu, J Bai and T Wang
Department of Electronic and Electrical Engineering, University of Sheffield, Sheffield, S1 3JD

A19_37 Nonpolar (11-20) InGaN/GaN light-emitting diodes overgrown on a micro-rod Template

L Jiu, J Bai, N Poyiatzis, P Fletcher and T Wang
Department of Electronic and Electrical Engineering, University of Sheffield, Mappin Street, Sheffield, S1 3JD, United Kingdom

A19_38 Electroluminescence from GaAsBi/GaAs multiple quantum well devices – potential for broadband light source applications

TBO Rockett[1], RD Richards[1]*, Y Liu[1], F Harun[1], Z Zhou[1], Y Gu[2], JR Willmott[1], and JPR David[1].
[1]University of Sheffield, Sheffield, South Yorkshire, S1 3JD, U, K[2]Shanghai Institute of Microsystem and Information Technology, Chinese Academy of Sciences, China

A19_39 AlInAs Gettering Layer for Resonant Tunnelling Diode Barrier Symmetry

R Baba[1], BA Harrison[2], BJ Stevens[3], R Beanland[4], T Mukai[5], RA Hogg[1]
[1]The University of Glasgow, Glasgow, G12 8LT UK; [2]EPSRC National Epitaxy Facility, Sheffield, S3 7HQ UK; [3]IQE Europe Ltd., Cardiff CF3 0LW UK; [4]Integrity Scientific Ltd., Warwick, CV34 4JP UK; [5]ROHM Semiconductor Co. Ltd., Kyoto, 615-8585 Japan

A19_40 Generating optical frequency combs via nano-scale all-optical modulators

H Francis, S Chen, KJ Che, M Hopkinson and CY Jin.
Department of Electrical and Electronic Engineering, University of Sheffield

A19_41 Optical Switch using Beamsteering at 900 nm wavelength in GaAs / $Al_xGa_{(1-x)}As$ with High Extinction Ratio for Quantum Sensors

JL Moss, B Saleeb-Mousa, JO Maclean*, RP Campion, and CJ Mellor
School of Physics and Astronomy, University of Nottingham, University Park, Nottingham, NG7 2RD

A19_43 Optically Controlled Millimetre-wave Switches with Coplanar Stepped- Impedance Lines

Y Zhang, AW Pang and MJ Cryan
Department of Electrical and Electronic Engineering, University of Bristol, U.K

A19_44 C-Band tunable laser modeling and simulation

M Bustillos[1,2*], GF Rinalde[1,2], L Bulus[1,2,3], N Abadía[4,5,6], and PA Costanzo Caso[1,2,3#]
[1]Instituto Balseiro, UNCuyo-CNEA, Av. Bustillo 9500, Bariloche (RN), Argentina; [2] Comisión Nacional de Energía Atómica (CNEA); [3] Consejo Nacional de Investigaciones Científicas y Técnicas (CONICET), Argentina; [4]Department of Electrical and Computer Engineering, McGill University, Montreal, Quebec, H3A 0E9, Canada; [5]School of Physics and Astronomy, Cardiff University, Queen's Building, The Parade, Cardiff, CF24 3AA, United Kingdom; [6]Institute for Compound Semiconductors, Cardiff University, Queen's Building, The Parade, Cardiff, CF24 3AA, United Kingdom

A19_45 The Nature of Auger Recombination in Type-I Mid-Infrared Laser Diodes

TD Eales[1], MC Amann[2], IP Marko[1], BA Ikyo[1], AR Adams[1], A Andrejew[2], K Vizbaras[2,3], L Shterengas[4], G Belenky[4], I Vurgaftman[5], JR Meyer[5], SJ Sweeney[1]

[1]Advanced Technology Institute and Department of Physics, University of Surrey, Guildford GU2 7XH, United Kingdom; [2]Walter Schottky Institut, Technische Universität München, Am Coulombwall 3, 85748 Garching, Germany; [3]Brolis Semiconductors UAB, Moletu pl. 73, Vilnius, Lithuania, LT-14259; [4]Department of Electrical and Computer Engineering, State University of New York at Stony Brook, New York 11794, USA; [5]US Naval Research Laboratory, 4555 Overlook Avenue SW, Washington DC 20375, USA

A19_46 Design, Fabrication and Characterisation of 980 nm Linearly Polarised Multi-Mode VCSELs for Ebium Doped Waveguide Amplifier Integration

D Lei[1], N Babazadeh[2], J Sarma[3], DTD Childs[1], and RA Hogg[1]

[1]The University of Glasgow, Glasgow, G12 8LT UK; [2]The University of Sheffield, Western Bank, Sheffield, S10 2TN UK, [3]University of Bath, Claverton Down, Bath, BA2 7AY UK

A19_47 Silicon and germanium mid-infrared platforms

J Soler Penadés[1], A Osman[1], A Sánchez-Postigo[2], Z Qu[1], Y Wu[1], CJ Stirling[1], DP Cheben[3], A Ortega-Moñux[2], JG Wangüemert-Pérez[2], M Nedeljkovic[1], GZ Mashanovich[1]

[1]Optoelectronics Research Centre, University of Southampton, Southampton, SO17 1BJ, UK; [2]Universidad de Málaga, ETSI Telecomunicación, Campus de Teatinos, 29071 Málaga, Spain; [3]National Research Council Canada, Building M-50, Ottawa, K1A 0R6 Canada

A19_48 Mode Coupling and Analysis in Laterally Coupled Vertical Cavities

S Chen, H Francis, CH Ho, KJ Che, M Hopkinson, and CY Jin

Department of Electronic & Electrical Engineering, University of Sheffield

A19_49 High Resolution Opitcal Spectrcopy of state-of-the-art Quantum-Dot Lasers for High Temperature Operation

IME Butler[1, 2], N Babazadeh[1], R Baba[1], K Nishi[3], K Takemasa[3], M Sugawara[3], DTD Childs[1], RA Hogg[1]

[1]School of Engineering, University of Glasgow, Glasgow, G12 8LT, UK; [2]School of Mathematics and Physics, Queen's University Belfast, Belfast, BT7 1NN, UK; [3]QD Laser Inc, Keihin Bldg. 1F, 1-1 Minamiwataridacho, Kawasaki-ku, Kawasaki, Kanagawa 210-0855, JAPAN

A19_50 Monolithic Growth of 1.5 µm InAs Quantum Dots Lasers on (001) Si and Material Studies

Z Li[1], S Shutts[1], CP Allford[1], B Shi[2], W Luo[2], KM Lau[2] and PM Smowton[1]

[1]EPSRC Future Compound Semiconductor Manufacturing Hub, School of Physics and Astronomy, Cardiff University, Queen's Building, The Parade, Cardiff, UK, CF24 3AA; [2]Department of Electronic and Computer Engineering, Hong Kong University of Science and Technology,Clear Water Bay, Kowloon, Hong Kong

A19_51 InP Quantum Dot Monolithically Mode-Locked Lasers Emitting at 740 nm

Z Li[1], S Shutts[1], CP Allford[1], RS Alharbi[1], AB Krysa[2], PM Smowton[1].

[1]EPSRC Future Compound Semiconductor Manufacturing Hub, School of Physics and Astronomy, Cardiff University, Queen's Building, The Parade, Cardiff, UK, CF24 3AA; [2]EPSRC National Centre for III-V Technologies, University of Sheffield, Sheffield, S1 3JD

A19_52 Temperature Dependant Characteristics of P-doped Laser Devices

L Jarvis[1], S Shutts[1], M Tang[2], H Liu[2] and PM Smowton[1]

[1]School of Physics and Astronomy, Cardiff University, The Parade, Cardiff, CF24 3AA, [2]Department of Electronic and Electrical Engineering, University College London, Torrington Place, WC1E 7JE

A19_53 Particle Manipulation and Control for Integrated Optoelectronic Microfluidics

D Giliyana*, E Le Boulbar, S Gillgrass and PM Smowton
School of Physics and Astronomy, Cardiff University, The Parade, Cardiff, CF24 3AA

A19_54 Vertical Cavity Surface Emitting Lasers for Miniature Atomic Clocks

C Hentschel[1], S-J Gillgrass[1] S Shutts[1], DG Hayes[1], CP Allford[1], D Zaouris[2], M Haji[2], I Eddie[3], I Kostakis[4], M Missous[4], W Meredith[5], and PM Smowton[1]
[1]EPSRC Future Compound Semiconductor Manufacturing Hub, School of Physics and Astronomy, Cardiff University, Cardiff, UK; [2]Time and Frequency Metrology, National Physical Laboratory, Teddington, UK; [3]CST Global Ltd, Glasgow, UK; [4]ICS Ltd, Manchester, UK; [5]Compound Semiconductor Centre, Cardiff, UK

A19_55 III-V Quantum dot materials and devices grown on on-axis (001) Si substrate

Z Liu[1]*, C Hantschmann[2], M Tang[1], Y Lu[1], J Park[1], M Liao[1], A Sanchez[3], R Beanland[3], M Martin[4], T Baron[4], S Chen[1], A Seeds[1], R Penty[2], I White[2], and H Liu[1]
[1] Department of Electronic and Electrical Engineering, University College London, London, WC1E 7JE, United Kingdom; [2] Centre for Photonic Systems, Department of Engineering, University of Cambridge, 9 JJ Thomson Avenue, Cambridge CB3 0FA, United Kingdom; [3] Department of Physics, University of Warwick, Coventry, CV4 7AL, United Kingdom; [4] Univ. Grenoble Alpes, CNRS, CEA-LETI, MINATEC, LTM, F-38054 Grenoble, France

Abstracts

Session 1: Guest Speakers

Invited Utilization of Dielectrophoresis positioning and selection for Nanowire based Bio-Sensors

S. Laumier[1], N. Sedghi[1], A. Marshall[2], A. Krier[2], M. Bosi[3], I. Sandall[1]*

*[1]Department of Electrical Engineering and Electronics, The University of Liverpool, Brownlow Hill, Liverpool, L69 3GJ, UK; [2]Physics Department, Lancaster University, Lancaster, LA1 4YB, UK; [3]IMEM-CNR, Institute, Parma, Italy *Ian.Sandall@Liverpool.ac.uk*

When the molecules of interest interact with the surface of the nanowires there is a resultant change in the conductivity of the nanowire allowing specific molecules to be detected selectively. As such nanowire based microfluidic devices have been demonstrated as flow rate sensors and for the detection of specific chemical and biological molecules. While much of this work has focused on use of silicon nanowires or carbon nanotubes, indium arsenide based wires are also of interest due to their high carrier motilities and the presence of a surface charge accumulation layer making them more sensitive to their ionic environment. To date such devices have been realized by removing the NWs from their host substrate and using expensive and time consuming pick and place techniques (i.e. utilizing SEM and AFM techniques) to deposit the NWs onto the microfluidic structures.

In this talk we will discuss recent work where we have utilized dielectrophoresis, which allows us to control and position individual nanowires electronically. During a dielectrophertic process (DEP), a polarizable nano-object is subjected to a non-uniform alternating electric field, the intrinsic charges separate and accumulate at the surface to form a dipole, which then experiences a force dependent on the gradient of the electric field. This results in the self-assembly of the dipoles across the electrode gap. As a first step, we have investigated the relationship between the DEP process parameters and the quality of the captured NWs, allowing us to select only the high quality NWs.

We have subsequently fabricated Schottky Diodes and Field Effect Transistors from these nanowires and investigated the relationships between measurable device properties and the physical quality of the nanowires. Finally we will discuss how these devices can be integrated with microfluidic structures to enable them to be used as a potential sensing platform.

*Invited*Photonic Integrated Circuits for Terahertz Photonics

L Hou and J Marsh
School of Engineering, University of Glasgow, Glasgow, G12 8QQ, U.K

THz radiation (0.1-10 THz) has many applications which include medical imaging, spectroscopy, security screening, detection of hidden explosives, remote sensing of chemical and atmosphere, high-bit-rate optical fibre communications, ultrafast optical data processing and optical computing. Many applications of THz radiation require sources that are compact, low-cost, and operate at room temperature. Photonic integrated circuits (PICs) are the next logical step in the world of optics and will meet the above requirements of THz applications. Here introduce the following Terahertz photonics' components based on PIC: PIC-based fully integrated optoelectronic synthesizer for THz communications which can be tuned continuously over the range of 0.254 THz to 2.723 THz by photomixing techniques and has a degree of redundancy, making it suitable for applications such as inter-satellite communications, where high reliability is mandatory; 820 GHz beat signal using laterally-coupled dual-grating distributed feedback lasers (DFBs) integrated with electroabsroption modulator with different periods of the gratings on each side of the DFB ridge waveguide; THz signal production based on dual wavelength DFB laser using two-section phase-shifted sampled Bragg grating (2PS-SBG) with a π phase-shifted seed grating filling half of the sampling period; THz source production based on sampled grating DBR (SGDBR) mode locked lasers (MLLs) which offer far superior reproducibility, controllability, and a wider operation range than all other reported mode-locked THz laser diodes; PIC-based phased array THz emitter to improve photodiode conversion efficiency and power saturation, beam steering will be accomplished using an optical beam forming network, a technique that eliminates the need for true time delay switch.

Invited III/V Nano-ridge Engineering for novel Device Integration on (001) Si

Bernardette Kunert
Imec, Kapeldreef 75, B-3001 Leuven, Belgium

The monolithic hetero-epitaxial deposition is the most promising approach in III/V integration on Si. It meets the high requirements of cost-efficiency and scalability although facing the challenges of misfit defect formation due to the large lattice mismatch. A well-known method to achieve a high III/V crystal quality in hetero-epitaxy is selective area growth in narrow trenches fabricated on (001) Si substrates. Strain induced misfit defects are confined inside the trench close to the Si-III/V interface by so-called aspect ratio trapping (ART). The pronounced growth out of trenches together with an engineered nano-ridge shape lead to an enlarged III/V nano-ridge volume, which can be used for novel III/V device architectures on Si. In this presentation I will explain this unique III/V nano-ridge engineering approach and evaluate the challenges and opportunities in epitaxial growth and new device design specifically for Silicon Photonics.

Abstracts

Session 2: Photodetectors

A19_08 Growth and characterization of long-wavelength Type-II InAs/GaSb superlattice infrared detectors

DCM Kwan[1], M Delmas[1], B Liang[2], D Huffaker[1,].
[1]School of Physics and Astronomy, Cardiff University, The Parade, Cardiff, CF24 3AA, UK; [2]California NanoSystem Institute, University of California, Loa Angeles, CA90095, USA

The present study compares the material quality and device performance of long-wavelength infrared (LWIR) Type-II InAs/GaSb superlattice (SL) p-i-n photodiodes grown on GaSb p-type substrates by molecular beam epitaxy (MBE). It is well known that the energy gap of broken gap (type-II) materials, such as InAs/GaSb SLs, can be tuned by varying the SL composition and thickness. This has allowed many research groups to develop InAs/GaSb infrared (IR) detectors capable of operating in the short- to (very) long-wavelength infrared spectral ranges. For LWIR applications (8 – 12 µm), a SL period composed of 14 monolayers (ML) InAs and 7 ML GaSb, with a cut-off wavelength of approximately 10.5 µm at 77K, is used in most studies despite not having demonstrated a significant advantage over alternative period compositions and thicknesses. Comparative studies of the 14 ML InAs/ 7 ML GaSb SL with alternative compositions and thicknesses have, so far, been relatively narrow in scope and are therefore of limited use in optimisation.
In this communication, InAs/GaSb p-i-n diodes consisting of X ML InAs/ Y ML GaSb (where X/Y = 7/4, 10/4, 12/4, 14/4 and 14/7) were studied. Note that the 7/4 sample has a cut-off wavelength in the mid-wavelength infrared spectral range and, for this work, is used for comparison. The material quality of each sample was evaluated using a combination of atomic force microscopy, X-ray Diffraction and Photoluminescence (PL) spectroscopy. PL measurements at temperatures ranging from 77K to room temperature allowed for verification of the SL bandgap tunability as well as the determination of the Varshni parameters and activation energies. Single pixel devices were also fabricated using a standard photolithography process. The electrical performance (I-V) of each of these devices was then determined as a function of temperature and dark current levels at the state-of-the-art have been obtained for LWIR SL p-i-n photodiodes.

Acknowledgements: The authors would like to acknowledge the financial support provided by the Sêr Cymru National Research Network in Advanced Engineering and Materials and by the EPSRC for the Future Compound Semiconductor Manufacturing Hub, reference number EP/P006973/1.

A19_02 InGaAs-InP PIN-HBT Optoelectronic Integrated Circuit with Extended Bandwidth and High Optical Power Capability

SG Muttlak, OS Abdulwahid, J Sexton and M Missous. saad.muttlak@manchester.ac.uk
School of Electrical and Electronic Engineering, University of Manchester, UK

The increase trend in data traffic as a result of the huge-demands for ultra-high data rates in telecom and datacom is a key-driver for developing low-cost, mass produced, optoelectronic integrated photoreceiver (OEIC) operating at 10Gb/s and beyond. Among all photoreceivers, the InP/InGaAs material technology utilizing heterojunction bipolar transistors (HBTs) and PIN-photodiode is the most studied and the one holding most promise as a low cost OEIC. A monolithically integrated OEIC consisting of a Transimpedance Amplifier (TIA) and PIN/Avalanche photodiodes requires minimizing the feature size of the active devices to a few micrometers for high-speed operation. This is however usually at the expense of poor yield process and an increase in the cost of the manufactured photoreceivers. In addition, conventional front-end amplifiers circuit configurations still suffer from a poor overload performance at high optical power of >0dBm due to the use of large resistor feedback parameter values which are necessary for high gain and low noise operation. The direct consequences of such an issue are low system reliability and nearly zero amplification characteristics contributing to a detrimental impact on the dynamic range. This predominantly occurs in short-haul intercity communication systems, in which an optical amplifier is not used. An effective way to broaden the dynamic range without sacrificing the sensitivity of the photoreceiver (i.e. amplifier gain) is based on exploiting a multiple feedback loop TIA amplifier (MFB-TIA). This topology does not only help in further extending the receiver's frequency bandwidth but it also improves the optical overload performance to reach ~2dBm.

The work reported here is concerned with investigating InP/InGaAs HBT based MFB front-end TIA amplifier monolithically integrated with a PIN-photodiode targeted for intercity optical link operating at over 10Gb/s. The photodiode and HBT were successfully fabricated, with the former utilizing the base and collector regions of the HBT. The experimental results showed dc responsivity and quantum efficiency of the PIN without AR coatings of 0.5 A/W and 0.45 respectively. Due to the specific design of the InP-InGaAs epilayer structures, and considering the trade-off between high performance PIN and the heterostructure transistor, a 10□10μm^2 emitter mesa size HBT achieved an f_T and f_{max} of 54 and 57GHz respectively which are amply adequate of low cost integrated 10Gb/s optical receiver. Further minimizing the HBT mesa area to 4□4μm^2 can lead to over 100 GHz cut-off frequencies. The TIA module showed an approximately flat transimpedance gain of 45dBΩ with an electrical bandwidth exceeding 18GHz while the fully integrated photoreceiver has an optical bandwidth of 14GHz which is theoretically sufficient for up to 20 Gb/s operation. The simulated eye diagram provided a clearly open eye diagram without any observation of inter-symbol interference for 10 and 20 Gb/s operation. Detailed characterization and modelling of the components and OEICs and their optimization for high data rate communication systems will be presented.

A19_23 $AlAs_{0.56}Sb_{0.44}$ avalanche photodiodes with high gain-bandwidth product over300 GHz

S Xie[1], X Yi [2], BL Liang[3], CH Tan[2], JPR David[2] and DL Huffaker[1]. xies1@cardiff.ac.uk
[1]School of Physics and Astronomy, Cardiff University, Cardiff; [2]Department of Electronic and Electrical Engineering, University of Sheffield; [3]California NanoSystems Institute, University of California-Los Angeles

Ultrafast and high-efficiency photodetectors are among the sought-after elements in modern optical networks. Avalanche photodiodes (APDs) with higher sensitivity compared to conventional photodetector technologies have been considered as a key component enabling a small footprint and low power consumption in optical receivers.

Today's telecommunication based InGaAs APDs have utilised InP or InAlAs as the avalanche gain material. Due to their broadly similar electron and hole ionisation coefficients (α and β respectively), the devices have limited gain-bandwidth product (GBP) that is below 300 GHz [1]. This hampers the devices in use at 25 Gb/s system or above. Silicon APD has a high GBP of 340 GHz [2] for its favorable α/β ratio, but silicon cannot detect wavelength above 1100 nm. A new promising alternative avalanche material is $AlAs_{0.56}Sb_{0.44}$ (hereafter AlAsSb) which can be grown latticed match to InP and compatible with the current InGaAs technology for 1310/1550 nm detection.

We recently demonstrated that AlAsSb could be grown as a digital alloy within its wide miscibility gap and it has a larger α/β ratio exceeding silicon [3]. In this work, we performed a theoretical modelling to investigate the GBP performance in AlAsSb APD by a random path length model [4]. The electron and hole ionisation coefficients [3] are used to compute the carrier impact ionisation probability in AlAsSb. The results shows that AlAsSb APD have a high GBP over 300 GHz, which is suitable for high speed optical system operation (e.g. ≥25 Gb/s).

Reference :

[1] S. Xie, et al. IEEE Photon. Tech. Letter., **27** (16), 1745(2015).
[2] Y. Kang, et al. Nature Photonics. **3**, 59-63 (2009).
[3] X. Yi, et al. Scientific Reports. **8**, 9107 (2018).
[4] D. S. Ong, et al. J. Appl. Phys., **83**, 3426 (1998).

A19_07 Modelling and Characterization of Zero-Bias Asymmetrical Spacer Layer Tunnel Diode Detectors

O S Abdulwahid[1], S Muttlak[1], J Sexton[1], K N Zainul Ariffin[1], MJ Kelly[2] and M Missous[1].

[1]School of Electrical and Electronic Engineering, the University of Manchester, United Kingdom, [2]The University of Cambridge, Cambridge, United Kingdom

The last two decades have seen a growing trend towards designing high-frequency detectors for imaging and communication systems that have the ability to accommodate the huge demand for high data rate wireless communication devices in anticipation of the Internet of Things (IoT) applications. Highly sensitive and linear detectors are required to reduce the gain of the low noise amplifier in the detector chain. To date, Schottky diodes represent the best technological choice due to their very high cut-off frequencies, good dynamic range, small size, and low cost. The sensitivity of detector is directly related to the curvature coefficient value (K_V) of the non-linear diode used to extract the DC component from the received RF signal. Such a key parameter is limited to K_V < q/nkT for a Schottky or Planar Doped Barrier (PDB) diodes [1]. Tunnel diodes, on the other hand, show a very weak temperature dependence of their I-V characteristics. It was verified in [2, 3], that the Asymmetrical Spacer Layer Tunnel (ASPAT) diode has very stable I-V characteristics over a wide temperature range (77-398)K. This work reports on zero-bias GaAs/AlAs Asymmetric Spacer Layer Tunnel (ASPAT) diode detectors with a curvature coefficient of $22V^{-1}$ for 6×6µm^2 mesa area size. However, a smaller feature size of 3×3µm^2 has a very promising curvature coefficient exceeding $78V^{-1}$. The measured I-V characteristics of the ASPAT diodes show that the curvature coefficient increases when the device mesa area gets smaller. The detector was fabricated exploiting a 6×6µm^2 28Å AlAs barrier ASPAT device and experimentally tested in the frequency band 4 to 18GHz at various input RF powers. The maximum measured sensitivity is 3650V/W at 11GHz for a -27 dBm incident RF power as shown in figure 1. Furthermore, the calculated noise equivalent power is 5.5 pW/$\sqrt{Hz}$ for this large area device. The results reported here validate the model which can be used to design and fabricate low cost, low power, temperature insensitive high-frequency tunnel diode detector in a range of applications. Other performances of the fabricated zero-bias ASPAT detector will be discussed in details.

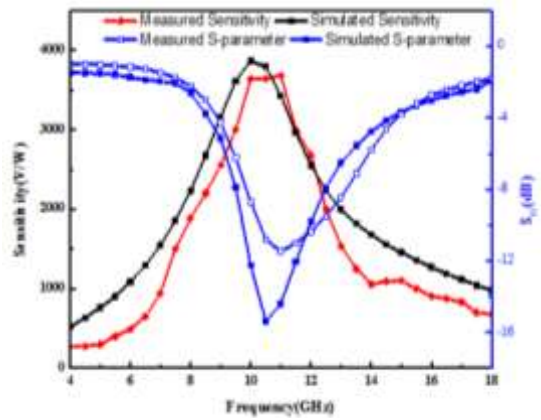

Figure 1: Measured and simulated S_{11} reflection and sensitivity of 6×6µm^2 28Å AlAs zero-bias ASPAT diode detector at -

[1] S. M. Sze and K. K. Ng, Physics of semiconductor devices. John wiley & sons, 2006.
[2] M. R. Abdullah, Y. Wang, J. Sexton, M. Missous, and M. Kelly, "GaAs/AlAs tunnelling structure: Temperature dependence of ASPAT detectors," in Millimeter Waves and THz Technology Workshop (UCMMT), 2015 8th UK, Europe, China, 2015, pp. 1-4: IEEE.
[3] Y. Wang, M. R. R. Abdullah, J. Sexton, and M. Missous, "Temperature dependence characteristics of In0. 53Ga0. 47As/AlAs asymmetric spacer-layer tunnel (ASPAT) diode detectors," in Millimeter Waves and THz Technology Workshop (UCMMT), 2015 8th UK, Europe, China, 2015, pp. 1-4: IEEE.

A19_19 Experimentally Validated Physical Modelling of GaAs/AlAs Asymmetric Spacer Layer Tunnel Diodes

A Hadfield and M Missous. andrew.hadfield-4@postgrad.manchester.ac.uk,
School of Electrical & Electronic Engineering, The University of Manchester, Manchester, M13 9PL, United Kingdom

Quantum-based devices have received a great deal of attention due to their potential use in the field of Gb/s wireless data transmission, imaging and biomedical applications. One such device is the Asymetric Spacer Layer Tunnel Diodes (ASPAT). The structure of this device is formed from a very thin single barrier with asymmetrical undoped spacer layers. The ratio of the asymmetrical spacer layers is 40:1. As a result of this unequal structure, the ASPAT exhibits an asymmetric I-V characteristic making it suitable for use as a zero-bias microwave detector. Due to the quantum nature of the device, the ASPAT shows greater temperature independence over both Schottky and Planar Doped Barrier (PDB) diodes without sacrificing sensitivity or dynamic range.

In this work physical models of GaAs/AlAs ASPAT Diodes with various mesa sizes ($3x3\mu m^2$, $4x4\mu m^2$, $5x5\mu m^2$ and $6x6\ \mu m^2$) and thin 2.8nm AlAs barriers were created using Silvaco ATLAS software. Current-Voltage characteristics of these ASPAT designs were obtained using the ATLAS semiconductor-insulator semiconductor model. The simulated results were validated against measured results of fabricated ASPATs with the same epitaxial designs [1]. The model showed good scaling with device mesa area and good matching to both current and resistance of the fabricated devices. The effects of traps at the GaAs/AlAs interface will be discussed in this work. Once an experimentally validated model of the ASPAT was produced new ASPAT designs were simulated to study the effects of thinning the AlAs barrier and modifying the doping of the contact layers.

[1] *K. N. Zainul Ariffin* et al*., "Investigations of Asymmetric Spacer Tunnel Layer Diodes for High-Frequency Applications," in* IEEE Transactions on Electron Devices*, vol. 65, no. 1, pp. 64-71, Jan. 2018. doi: 10.1109/TED.2017.2777803*

A19_20 Passivation of AlInAsSb Data Alloy Avalanche Photodiodes

C Guoa,[a], Y Lv[a], Y Ding[b],*, E Wasige[b], Z Niu[a]. ying.ding@glasgow.ac.uk
[a]*Institute of Semiconductors, Chinese Academy of Sciences, Beijing 100083, China;* [b]*School of Engineering, University of Glasgow, Glasgow, G12 8LT, UK*

Conventionally, the performance of avalanche photodiodes (APDs) are limited by the lateral surface leakage, mainly caused by interfacial traps, dangling bonds, and conductive oxides. In this work, in order to suppress the lateral surface leakage, various methods of passivation, including applying SiO2 as the dielectric layers, sulfuration treatment and SU8 coating, have been investigated for AlxInyAsGb high gain separate absorption, grading, charge, and multiplication (SAGCM) avalanche photodiode (APD). The AlxInyAsGb quaternary alloy based on GaSb APD was grown by molecular beam epitaxy (MBE). Also, the properties of APD have been systematically explored by typical capacitance-voltage (C-V) and current-voltage (I-V) approaches. Consequently, the CV measurement results the CV modeling for 200μm diameter mesa device fit the modeling curve well. The punchthrough voltage is about -30V. Before punchthrough, the capacitance is determined by the 122nm charge layer. Besides, as to the results of IV measurement, for APDs of the same size, different passivation processes influence the dark current slightly in normal temperature. However, under lower temperature (<210K), when the surface leakage dominants among the causation of dark current, the suppression of dark current caused by different passivation processes varies obviously. According to the IV measuring, sulfide passivation can restrain surface leakage most, three orders of magnitude less than that of the unpassivated one, for SACGM APDs in low temperature of 77K. Comparison with dark current, the passivation layer have an effect on photocurrent of APDs apparently. In the meanwhile, there is a linear relationship between the geometric size of APDs mesas and current. The relationships between current and the diameter of circle devices passivated by sulfuration show in the **Fig 1**. (a) and (b) are for photocurrent and dark current respectively

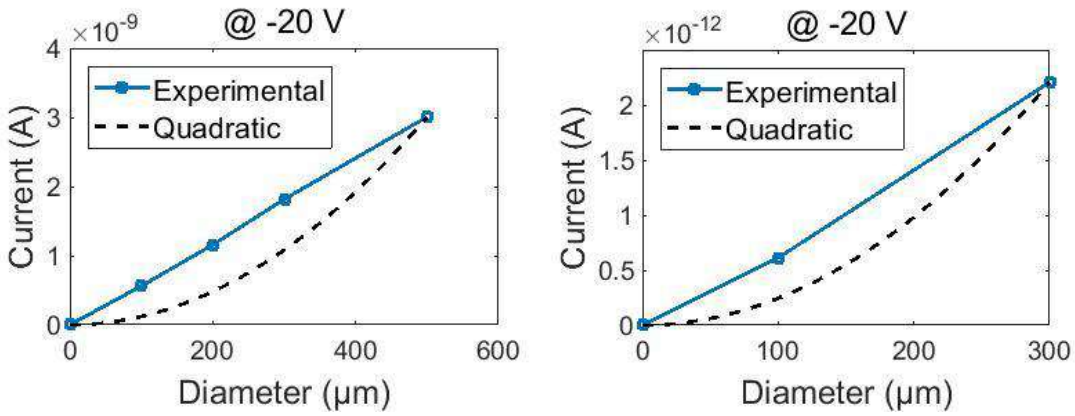

Fig 1. Current versus the diameter of pixel device with sulfuration passivation. (a) The photocurrent; (b) The dark current.

Abstracts

Session 3: Posters

A19_55 III-V Quantum dot materials and devices grown on on-axis (001) Si substrate

Z Liu[1]*, C Hantschmann[2], M Tang[1], Y Lu[1], J Park[1], M Liao[1], A Sanchez[3], R Beanland[3], M Martin[4], T Baron[4], S Chen[1], A Seeds[1], R Penty[2], I White[2], and H Liu[1] zizhuo.liu.16@ucl.ac.uk

[1] Department of Electronic and Electrical Engineering, University College London, London, WC1E 7JE, United Kingdom [2] Centre for Photonic Systems, Department of Engineering, University of Cambridge, 9 JJ Thomson Avenue, Cambridge CB3 0FA, United Kingdom, [3] Department of Physics, University of Warwick, Coventry, CV4 7AL, United Kingdom, [4] Univ. Grenoble Alpes, CNRS, CEA-LETI, MINATEC, LTM, F-38054 Grenoble, France

Silicon photonics combining the PICs on Si platform emerged to overcome the networking bottlenecks and reduce the cost of data-centres. However, the efficient and reliable Si-based laser source is still not realized monolithic growth. The main issue is threading dislocations (TDs) caused by the lattice mismatch between III-V material and Si. Due to quantum dot (QD) structure has the advantage of high defect tolerance, QDs have been expected to be the gain medium for laser devices monolithic grown on the Si. In this paper, Si-based QD laser devices and quantum well (QW) devices under the same growth and fabrication conditions are compared. The TD density of both QD and QW samples are around $5\times10^{7}cm^{-2}$ after the growth of 4 sets of DFLs on GaAs/Si virtual substrate. Each DFL consists of 5 periods of 10 nm/10 nm $In_{0.18}Ga_{0.82}As$/GaAs SLSs and 300 nm GaAs. Five layers of InAs/GaAs DWELL structures separated by 40 nm GaAs spacer layer was grown as the active region of QD samples. The QW samples have the same thickness which contain 5 periods of 8 nm $In_{0.15}Ga_{0.85}As$ QWs spaced by 40 nm GaAs spacer layer. Temperature-dependent PL intensities of InAs/GaAs QD and InGaAs/GaAs QW samples were measured from 20 K to 300 K. The thermal activation energy of both QD and QW material is estimated in Fig. 1(a), the value of QD material (240.7meV) is nearly 7 times higher than that of QW material (35meV), indicating that the carriers in QD material have a higher barrier to transit to the continuum. As shown in Fig.1 (b), the series resistance of two samples are similar obviously, and QD laser shows high performance with single-facet output power over 100mW under continuous-wave (CW) operation at room temperature, in contrast, there is no lasing behaviour for the QW laser device. The result demonstrates that the outstanding carrier capture ability and dislocation insensitivity of QD is promising for laser devices monolithically grown on Si.

Fig. 1 (a) Temperature-dependent integrated PL intensities of QD and QW samples; (b) RT and CW L-I-V curve of a QD and a QW laser with same fabrication process and same growth conditions

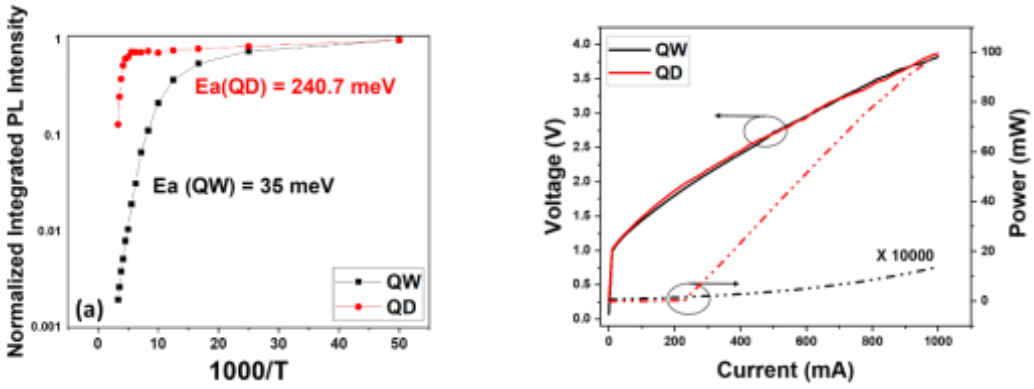

A19_06 CW Laser for All Quantum Dot CW THz emission

G Bello, S Smirnov and E Rafailov.
Optoelectronics and Biomedical Photonics GroupAston Institute of Photonics Technologies, Aston University, Birmingham, B4 7ET

Abstract
A continuous wave (CW) terahertz source emitting in a broad frequency range (1-5THz) is promising towards achieving a compact, high power, room temperature terahertz source that will be of immense importance to terahertz applications in spectroscopy, communication, sensing, and imaging.
A tunable continuous-wave Quantum Dot external cavity laser emitting at two frequencies has been demonstrated and characterised for continuous wave terahertz emission. The external cavity QD Laser has been characterised with tunability of 152nm and a tuning range from 1143nm -1295.8nm that lies within the THz difference frequency.

Introduction
Terahertz (THz) refers to the region in the electromagnetic spectrum that is defined from around 300GHz – 10THz in frequency and 1mm- 100µm in wavelength; it lies right between the microwave and optical infrared frequencies. Based on classical electrodynamics, the terahertz region is the highest frequency where emission of electromagnetic radiations can be achieved using an electric dipole. This has made it challenging to realise high-frequency antennas, especially at terahertz frequencies, which is because common architectures used at microwave frequencies present extremely high losses at high frequencies due to the strong dielectric absorption.

CW Laser for All Quantum Dot CW THz emission
The InAs/GaAs QD laser is in quasi-littrow configuration with an external cavity comprising of a beam splitter and two diffraction gratings for wavelength tunability to enable the generation of CW THz in a Photoconductive antenna based on photo mixing technique employed by Ksenia et al [1].
The QD structure used for the laser was grown on GaAs substrate and consists of 10 non-identical layers of InAs Quantum dots grown by molecular beam epitaxy in the Strantski-Krastanow mode, which has shown benefits in fabricating dislocation free Quantum dots. Using single arm the QD Laser has a tunability of 152nm as shown in Fig (a) and a dual frequency operation was obtained as demonstrated in Fig (b).

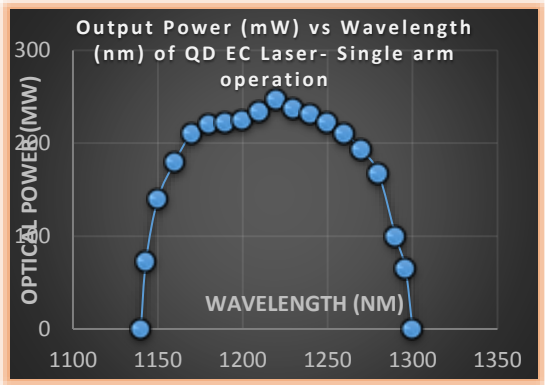

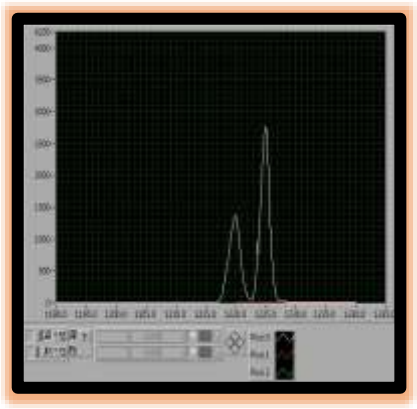

From left to right Fig (a) Single arm operation Fig (b) Dual-frequency operation

References
[1] K. A. Fedorova, A. Gorodetsky, E. U. Rafailov, and S. Member, "Compact All-Quantum-Dot-Based Tunable THz Laser Source," IEEE J. Sel. Top. Quantum Electron., vol. 23, no. 4, 2017.

A19_11 Design conditions in the middle range for implementation of integrated ring resonator $LiNbO_3$ by direct laser writing

PL Pagano[1, 2], D Presti[1, 3], RR Peyton[1, 3], N Abadía[5,6], FA Videla[1,4], GA Torchia[1,3]

[1] Centro de Investigaciones Ópticas (CONICET-CICBA-UNLP), M.B. Gonnet (1897), Buenos Aires, Argentina, [2] Facultad de Ciencias Exactas, Departamento de Física, Universidad Nacional de La Plata– Argentina, Calle 115 y 47 , [3] Depto. De Ciencia y Tecnología, Universidad Nacional de Quilmes Roque Sáenz Peña 352 – Bernal (1876) – Bs. As. – Argentina, [4] Facultad de Ingeniería, Universidad Nacional de la Plata, Depto de Ciencias Básicas., [5]School of Physics and Astronomy, Cardiff University, Queen's Buildings, The Parade, Cardiff, CF24 3AA, United Kingdom, [6]Institute for Compound Semiconductors, Cardiff University, Queen's Buildings, The Parade, Cardiff, CF24 3AA, United Kingdom

Fiber ring resonators have demonstrated to be useful for a variety of applications especially in the field of inertial navigation. As a typical requirement, these devices have a free spectral range (FSR) of 3pm and resolution of few °/h being with a radius ranging in the centimeter scale [1][2]. Unfortunately, they are too bulky and power consuming. For integrated ring design, due to the resolution, radius dimensions must be as larger as possible around 1cm. Their main features resolution about 10°/h, FSR of 10 pm and a quality factor about 10^6 [3]. Simulation software for integrated optical circuits and implementation techniques are indeed challenging. The first, are memory and time constrained, normally based on Finite Differential Time Domain (FDTD) or Beam Propagation Method (BPM). FDTD allows back-propagation, but BeamProp tool (part of RSOFT suite, BPM based) does not, however enable to simulate larger rings than FDTD (r < 200 □m).

As implementation technique to fabricate large rings, we choose Femtosecond Laser Direct Writing [5] on Lithium Niobate crystals ($LiNbO_3$) a typical used electro optical material. An important issue of this method is to optimize the tracing of multiple straight lines to represent waveguides with some bending degree, so in this sense it is relevant to define how the curves will be plotted by this approach. In this paper, we tried BPM as a convenient tool to simulate rings and analyze preliminary results of propagation on waveguides fabricated whose geometry corresponds to inscribed polygons where each double track [5] segment is a side. Because of bending losses, it is important to select a suitable splice angle between tracks [6][7]. Additionally, based on simplified coherent coupling [8],[4] and in the hope of some relaxation of the splice angle condition, we believe it is possible to reduce the number of sides. Several strategies to compute large ring resonator (over 5 mm radii) extracted from the literature will be presented in this work and then they will be compared with our design and calculations approach used in this paper.

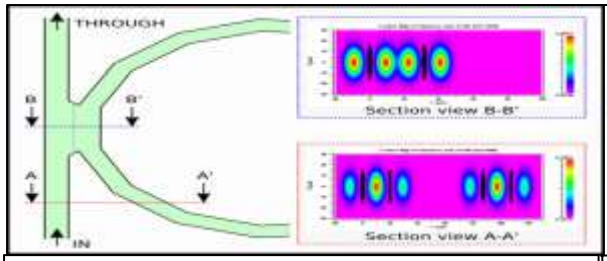

Detail of the tracks geometry and refractive index distribution closest to the coupling region. Black lines bounds the guiding zone (green).

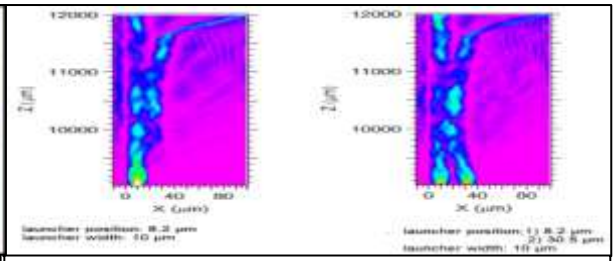

Field injected split up between a curved and straight waveguide (left). Splitting up and re-coupling light (right). It can be appreciated evanescent field.

References:[1] Ciminelli et Al High performance InP ring resonator for new generation monolithically integrated optical Gyroscopes Meas. Sci. Technol. 20 027002 (2009) [2] Vladimir Vukmirica Interferometric fiber optic gyroscopes Principle of operation and basic parameters determination, Scientific Technical Review,Vol.LVIII,No.3-4,(2008).[3] Caterina Ciminelli, Francesco Dell'Olio, Mario N. Armenise, Francisco M. Soares, and Wolfgang Passenberg, High performance InP ring resonator for new generation monolithically integrated optical gyroscopes, Optics Express, 21, 556 (2013).[4] Peyton, R, V Guarepi, F Videla, and G A Torchia. Key Kinematic Parameters in a Low-Loss Power Splitter Written by Femtosecond Laser Micromachining. Journal of Micromechanics and Microengineering 28, 055011 (2018). [5]Chen F, de Aldana JRV. Optical waveguides in crystalline dielectric materials produced by femtosecond-laser micromachining. Laser & Photonics Reviews 7;8(2):251–75 (2013). [6] Taylor H F Losses at corner bends in dielectric waveguides, Appl. Optics. 13 642-647 (1974). [7] Hutcheson L, White I A and Burke J J Comparison of bending losses in integrated optical circuits, Opt. Lett. 5 276-278 (1980). [8] Johnson L. and Leonberger F. Low-loss LiNbO3 waveguide bends with coherent coupling Opt. Lett. 8 111-113 (1983).

A19_14 Ultrafast laser inscription: a key method available to a wide range of materials with high integration for 3D optical devices fabrication

V Guarepi[1] , R Peyton[1,2], D Presti [1,2]D Biasetti[1], M Tejerina[3], F Videla[1] N Abadía[4,5] and GA Torchia[1,2] * gustavot@ciop.unlp.edu.ar

[1]Centro de Investigaciones Ópticas, CONICET-CICBA-UNLP, Camino Centenario y 506, s/n, M.B. Gonnet (1897), Buenos Aires, República Argentin, [2] Departamento de Ciencia y Tecnología, Universidad Nacional de Quilmes, Roque Saénz Peña, 352, Bernal (1876), Buenos Aires, República Argentina, [3] Centro de Tecnología de Recursos Minerales y Cerámica (CONICET La Plata-CIC), CC nº 49, M.B. Gonnet (1897), Buenos Aires, República Argentina[4]School of Physics and Astronomy, Cardiff University, Queen's Buildings, The Parade, Cardiff, CF24 3AA, United Kingdom, [5]Institute for Compound Semiconductors, Cardiff University, Queen's Buildings, The Parade, Cardiff, CF24 3AA, United Kingdom

In the last years a nontraditional method to fabricate optical circuits in materials has been fruitfully emerged. This technique promises great potential but up to now have not reach the development mature as standard manufacturing technology such as Silicon platform or Titanium diffusion. The method is based on the interaction of ultra-short pulses of laser with optical materials and it was introduced two decades ago from a pioneer paper written by K. Hirao et al. [1]. That article showed that using a femtosecond laser pulse system it is possible to modify in a precise and permanent way the optical properties of a transparent material. This process allows the direct writing of guiding structures, commonly known as of waveguides which are the base of optical circuits. As advantages of this fabrication approach we can mention it can be applied to a wide range of passive and active optical materials. Besides, this method can be implemented in a single step process and allows the fabrication of three dimensional waveguiding structures. Furthermore, femtosecond laser writing is a cheaper technology so it not needs conventional lithography and etching techniques which demands expensive and complex rooms. Additionally, it is important to point out that 3D architecture boosts optical integration since the conventional methods use flat guiding structures [2-3].

In this paper, on one hand, we present the state of art of fundamental studies related to the ultrafast laser-matter interaction with optical materials in order to fabricate suitable and efficient wave-guiding structures. In particular, we present and discuss about micro-Raman and luminescence experiments used to link these results with the main characteristics and the optical performance of the written waveguides. Computational modeling and spectroscopic analysis have been used to support the experimental data obtained in pure and doped Lithium Niobate crystals [4-5]. On the other hand, we show passive integrated devices made in Lithium Niobate. In this sense, signal deviator, couplers, 2D and 3D power splitters have been properly designed so in this contribution we present the fabricated devices made by fs laser writing technique and their guiding performance [6].

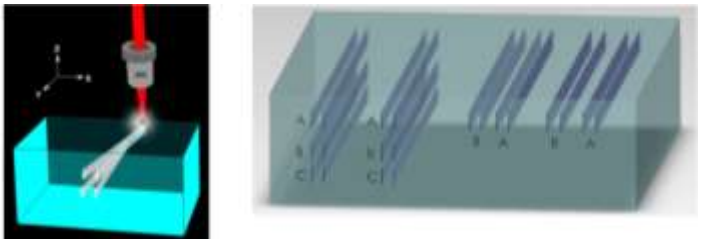

Figure 1: (a) Schematic 3D writing of 1x4 power splitter by using ultra-short laser pulses. (b) This picture represents a scheme of 3D waveguides array written by this technique.

References: [1] K. M. Davis, K. Miura, N. Sugimoto, and K. Hirao, Writing waveguides in glass with a femtosecond laser, Opt. Lett. 21, 1729, (1996). [2] R. Osellame, G. Cerullo, and R. Ramponi, Femtosecond laser micromachining: photonic and microfluidic devices in transparent materials (Springer Science & Business Media, (2012). [3] F. Chen and J. V. de Aldana, Laser & Photonics Reviews, Optical waveguides in crystalline dielectric materials produced by femtosecond laser micromachining, 8, 251 (2014). [4] MR Tejerina, D Jaque, GA Torchia, A 2D μ-Raman analysis of low repetition rate femto-waveguides in lithium niobate by using a finite element model, Optical Materials 36 (5), 936-940 (2014). [5] DA Biasetti, GA Torchia, E Cantelar, Luminescent features in double-track type II waveguides made in Er/Yb: LiNbO3 by Ultrafast Laser Inscription Optical Materials, 88, 680-688 (2019). 6] R Peyton, V Guarepi, F Videla, GA Torchia Key kinematic parameters in a low-loss power splitter written by femtosecond laser micromachining, Journal of Micromechanics and Microengineering 28 (5), 055011 (2018).

A19_22 3D Monte Carlo simulation of GaAs nanowire single-photon avalanche diodes

H Li[1,2], S Xie[1*], and DL Huffaker[1] xies1@cardiff.ac.uk
[1]School of Physics and Astronomy, Cardiff University, Cardiff, UK, 2School of Physics Science and Technology, Wuhan University, China

Single photon avalanche photodiodes (SPADs) at near infrared wavelength are vital optical components used for various applications, such as 3D mapping system [1], time-of-flight scanners [2] and light detection and ranging (LiDAR) [3]. Recently GaAs nanowire SPAD has been attracted more attention in single photon detection at this spectrum due to their drastically reduced volume leading to an extremely small afterpulsing probability and low dark count rate [4]. However models accurately interpreting the avalanche breakdown performances of GaAs nanowire SPAD are still lacking.
In this work, we for the first time developed a sophisticated 3D Monte Carlo model for GaAs nanowire SPAD that is capable of predicting the avalanche multiplication process, breakdown probability, mean time to breakdown and timing jitter. Model validation includes ionisation coefficient and avalanche multiplication with the experimental data. The simulated devices structures are with PN junction and under different doping concentration and carrier injection. These results can be used as instructions for high performance device design and optimization.

Reference

[1] Ackerman, E. et al, IEEE Spectrum 2016, 53 (10), 14-14.
[2] Lussana, R. et al. Opt. Express 2015, 23 (19), 24962-24973.
[3] Williams, G. M. et al, Defense and Security Symposium, SPIE: 2006; p 14.
[4] Farrell, A. et al. Nano Lett. 2019, 19, 582−590

A19_31 Designing optimized retro-reflecting electro-absorption modulators for free space optical datalinks.

B Maglio[1], N Abadía[1], PM Smowton[1], C Quitana[2], G Erry[2], Y Thueux[2]
[1]Department of Physics, Cardiff University, Cardiff, CF24 3AA, [2]Airbus Group Innovations, Newport, NP10 8FZ

Free space optics (FSO) uses light to transmit information wirelessly through free space or an atmospheric medium, and benefits from increased data rates, no spectrum license, and simple installation. Datalinks comprising of two transceivers have demonstrated excellent performance [1]. However, as need for more lightweight, compact systems increases, research into reflecting light at its angle of incidence using modulating retro-reflectors (MRR) has gained prevalence. Predominantly, surface-normal electro-absorption modulators, exploiting the quantum confined Stark effect, have shown promise with peak extinction ratios of 7.5 dBs (NRL [2]) and data rates of 200 Mbps (ACREO/Airbus [3]). Applications include small satellites, UAVs, and drones, with another advantage of signals being undetectable and un-jammable. Numerous papers have proposed improvements on these systems by modifying macroscopic features like tracking systems, lens configurations and transceiver combinations. Here, we describe a computational model to predict band structure, absorption, and optical confinement to enhance the modulator itself. A generic algorithm will allow the selection of parameters such as conduction band-offsets, size and number of quantum wells to be optimized. These developments will be implemented at a materials level to improve the capabilities of the modulator. This model will be adaptable to Ge/SiGe as well as many III-V systems.

References

[1] W. S. Rabinovich *et al.*, "Free-space optical communications research and demonstrations at the US Naval Research Laboratory," *Appl. Opt.*, vol. 54, no. 31, p. F189, Nov. 2015.
[2] W. S. Rabinovich *et al.*, "Free space quantum key distribution using modulating retro-reflectors," *Opt. Express*, vol. 26, no. 9, p. 11331, 2018.
[3] C. Quintana *et al.*, "High Speed Electro-Absorption Modulator for Long Range Retroreflective Free Space Optics," *IEEE Photonics Technol. Lett.*, vol. 29, no. 9, pp. 707–710, 2017.

A19_54 Vertical Cavity Surface Emitting Lasers for Miniature Atomic Clocks

C Hentschel[1], S-J Gillgrass[1], S Shutts[1], DG Hayes[1], CP Allford[1], D Zaouris[2], M Haji[2], I Eddie[3], I Kostakis[4], M Missous[4], W Meredith[5], and PM Smowton[1]

[1]EPSRC Future Compound Semiconductor Manufacturing Hub, School of Physics and Astronomy, Cardiff University, Cardiff, UK; [2]Time and Frequency Metrology, National Physical Laboratory, Teddington, UK; [3]CST Global Ltd, Glasgow, UK; [4]ICS Ltd, Manchester, UK; [5]Compound Semiconductor Centre, Cardiff, UK

Due to their reliability, low power consumption, and stable single mode emission, vertical cavity surface emitting lasers (VCSELs) are a commonly used laser source in miniature atomic clocks. However, VCSELs operating at the 894.6nm wavelength are typically not available commercially, and generally do not meet the narrow linewidth, polarisation stability, and high temperature operation requirements. Here we outline the key design considerations and fabrication steps required to meet the specification, and present preliminary results which highlight the performance of our devices.

Epitaxial structures have been designed to meet the specification target for miniature atomic clocks which utilise a caesium vapour cell. Key design parameters include linewidth, threshold gain, gain peak wavelength, and cavity resonance for emission at 894.6nm when operating close to the temperature required for the clock (70˚C). The polarisation, which is inherently unstable in a conventional VCSEL, can be controlled through several means, one of which includes the geometry of an oxide aperture. As well as providing sufficient current and optical confinement, the aperture can be designed to favour emission in a particular polarisation, stable over a wide current range. We report on devices measured with selective oxidation of buried thin Al0.98GaAs layers using various mesa geometries, and present oxidation studies carried out at temperatures of around 350-400°C with an AET ALOX furnace, where the selective oxidation process of an individual layer was monitored in-situ with a wavelength-selectable infrared optical setup.

The VCSEL devices were screened at the wafer level using a Keysight semiconductor parameter analyser with an automatic prober, which enabled fast characterization of the DC diode properties. The same measurement system is also capable of wafer mapping small-signal S-parameters to 120 GHz, and electro-optic modulation up to 67 GHz. The modulation characteristics of VCSELs will be presented, in addition to the nearfield mode profile, emission wavelength, and optical power versus current (P-I) characteristics of several discrete devices, measured as a function of temperature.

Figure 1. Infrared image of a typical VCSEL oxide aperture used in this study. The P-I characteristics of a similar device is shown in Fig. 2.

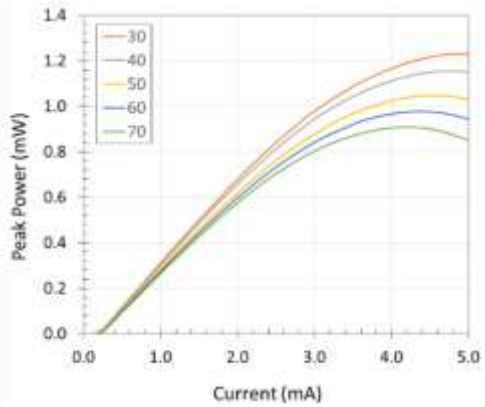

Figure 2. P-I curve of a typical device from 30-70°C. The device has a low threshold of 0.25±0.05mA at 70°C.

A19_51 InP Quantum Dot Monolithically Mode-Locked Lasers Emitting at 740 nm

Z Li[1], S Shutts[1], CP Allford[1], RS Alharbi[1], AB Krysa[2], PM Smowton[1]. LiZ74@cardiff.ac.uk
[1]EPSRC Future Compound Semiconductor Manufacturing Hub, School of Physics and Astronomy, Cardiff University, Queen's Building, The Parade, Cardiff, UK, CF24 3AA; [2]EPSRC National Centre for III-V Technologies, University of Sheffield, Sheffield, S1 3JD.

Semiconductor monolithic mode-locked lasers (MLL) emitting in the visible to near infrared region are required for their small footprint and low cost, having particularly importance for biomedical applications. Inhomogeneously broadened QD materials feature a broad optical gain bandwidths which are suitable for achieving ultrashort pulse mode-locking [1]. We demonstrated, for the first time, monolithic mode-locking using InP/GaInP quantum dots as the active region that can be extended to cover the 630 – 780nm wavelength range [2].

Figure 1 (A) gives the structure grown by MOCVD on n-GaAs (100) substrates oriented 10° off toward <111>. InP QDs were covered by lattice-matched GaInP quantum wells and separated by AlGaInP barriers, with AlInP cladding layers forming the rest of the waveguide. Figure 1 (B) shows the diagram of the passive mode-locked lasers with 2µm wide shallow-etched ridges. These ridges were planarised by BCB, then p-type and n-type contact metals were deposited on the top and bottom sides correspondingly. The sample was then cleaved into two cavity lengths, of 2mm and 3mm, where the saturated absorber (SA) section was 0.4mm and 0.6mm respectively. Light-current (L-I) curves of the 3mm long device are shown in Figure 1 (C), with the insertion showing the lasing spectrum when device was mode-locked, with 60mA gain current and 1.7V reverse bias on the SA. Figure 2 shows the RF frequency signal from a fast photodiode for the 2mm long (blue) and 3mm long (red) mode-locked lasers, where repetition frequencies of 15.21GHz and 12.5GHz are observed, which correspond to the calculated frequencies for these cavity lengths. In conclusion, we achieved the first monolithic MLLs using InP/GaInP QD material system, and demonstrated different repetition frequencies with two cavity lengths.

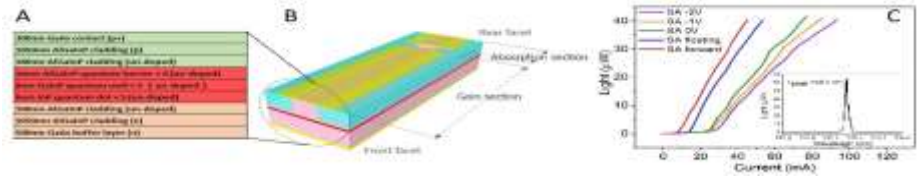

Figure 1,(A) InP/GaInP QD mode-locked laser structure, (B) Diagram of passive mode-locked lasers,(C) L-I curves of 3mm long mode-locked laser, the inserted showing the lasing spectrum under mode-locked condition (I_{gain} = 60 mA and VSA = -1.7 V)

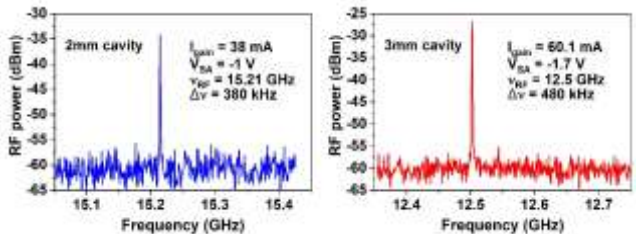

Figure 2, RF signals of 2mm long (blue) and 3mm (red) long devices, showing the corresponding repetition frequency of 15.21GHz and 12.5GHz at indicated operation condition.

[1] E. U. Rafailov, M. A. Cataluna, W. Sibbett, "Mode-locked quantum-dot lasers", Nature Photonics, 1, 395–401 (2007)
[2] S. Shutts, S.N. Elliott, P.M. Smowton, A.B. Krysa, "Exploring the wavelength range of InP/AlGaInP QDs and application to dual-state lasing", Semiconductor Science and Technology, Vol. 30 (4), 044002 (2015)

A19_09 Design of a Y-branch in silicon-on-insulator based on simplified coherently coupled

R Peyton[1, 2, †], D Presti[1, 2], F Videla[1, 3], N Abadía[4, 5] and GA Torchia[1, 2]. robertop@ciop.unlp.edu.ar

[1]Centro de Investigaciones Opticas (CONICET-CICBA-UNLP), M.B. Gonnet (1897), Buenos Aires, Argentina; [2]Departamento de Ciencia y Tecnologia, Universidad Nacional de Quilmes; [3]Facultad de Ingenieria, Universidad Nacional de la Plata, Depto de Ciencias Basica; [4]School of Physics and Astronomy, Cardiff University, Queen's Buildings, The Parade, Cardiff, CF24 3AA, United Kingdom; [5]Institute for Compound Semiconductors, Cardiff University, Queen's Buildings, The Parade, Cardiff, CF24 3AA, United Kingdom

Currently, silicon photonic technology has a significant importance in optical communications systems since its small footprint devices, CMOS process compatibility and high integration level. In particular, we focus on silicon-on-insulator (SOI) which is the most popular platform for that purpose [1]. he high refractive index contrast between silicon and silica layers makes possible submicron waveguides and tight bends, also state-ofthe-art electronics industry foundry processes can be exploited. However, unlike electronic circuits where electrical routing can be accomplished flexibly, optical routing is limited either for optical conditions or technological limitation. Each design must be performed taking into account the design rules of a CMOS process. For example, many fundamental components (e.g. Y-branch) used in integrated photonics show better performance if sharp corners and spline interpolation are employed, but usually they violate the design rules described fabrication process details [2]. In order to solve the issues, geometries based on simplified coherently coupled, multi-sectional bends and smoothed corners can be conducted.

Coherent coupling is a technique to bend light through small straight waveguides with sharp bending. Several studies have already reported on deviators and splitters with low-loss, compact and efficient devices, compared with other types of geometries. Physically, decoupled light in a curve can be coupled back into a subsequent curve if the difference between the phase of modes (guided and unguided) is an odd multiple of π. Bending loss is an oscillatory function that depends strongly on section length, effective refractive index and wavelength, due to coupling between guided and radiated modes [3-5]. In this work we design a Y-branch (see figure 1) using the coherent coupling theory and friendly geometries with modern CMOS photonics process, particularly on silicon-on-insulator platform. Finally, we utilize an optimization algorithm for reducing the excess loss, wavelength sensitivity, and footprint. In this paper, the state of art of the splitters design in SOI platform will be discussed and then compared with the results obtained in this paper.

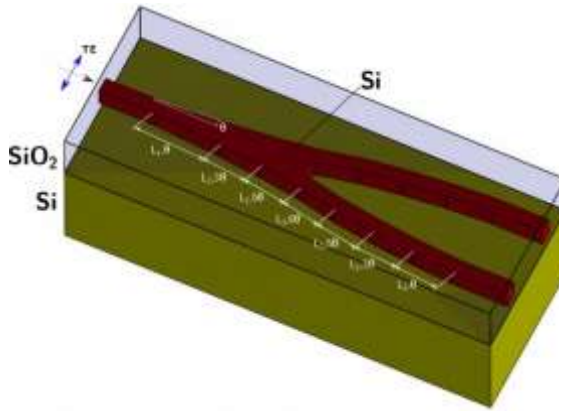

Figure 1: Schematic of the proposed Y-branch based on simplified coherently coupled

References

[1] L. C. Kimerling, "Silicon photonics and interconnects: Roadmap for implementation," 2012 Optical Interconnects Conference, May 2012. [2] Y. Zhang, S. Yang, A. E.-J. Lim, G.-Q. Lo, C. Galland, T. Baehr-Jones, and M. Hochberg, "A compact and low loss Y-junction for submicron silicon waveguide," Optics Express, vol. 21, no. 1, p. 1310, Jan. 2013. [3] H. F. Taylor, "Power Loss at Directional Change in Dielectric Waveguides," Applied Optics, vol. 13, no. 3, p. 642, Mar. 1974. [4] Jenn-Jia Su and Way-Seen Wang, "Novel coherently coupled multisectional bending optical waveguide," IEEE Photonics Technology Letters, vol. 14, no. 8, pp. 1112–1114, Aug. 2002. [5] R. Peyton, V. Guarepi, F. Videla, and G. A. Torchia, "Key kinematic parameters in a low-loss power splitter written by femtosecondlaser micromachining," Journal of Micromechanics and Microengineering, vol. 28, no. 5, p. 055011, Mar. 2018.

A19_33 Silicon Nitride Polarization Beam Splitters: A Review

M Tosi[1, 2], A Fasciszewki1, N Abadía[4, 5] and PA Costanzo Caso[1, 2,3] mauricio.tosi@ib.edu.ar
[1]Comisión Nacional de Energía Atómica (CNEA); [2] Instituto Balseiro, UNCuyo-CNEA, Av. Bustillo 9500, Bariloche (RN), Argentina; [3] Consejo Nacional de Investigaciones Científicas y Técnicas (CONICET), Argentina; [4] School of Physics and Astronomy, Cardiff University, Queen's Building, The Parade, Cardiff, CF24 3AA, United Kingdom; [5] Institute for Compound Semiconductors, Cardiff University, Queen's Building, The Parade, Cardiff, CF24 3AA, United Kingdom.

In the last few years, silicon photonics has become one of the most important platforms for the development of photonic integrated circuits (PICs). Silicon-on-insulator (SOI) is the main technology used for passive photonic devices in optical communication applications [1]. However, the high refractive index-contrast of SOI ($\Delta n \approx 2$) makes the required nm-scale fabrication process a real challenge. As counterpart silicon nitride (Si3N4) based waveguides with a moderate index-contrast ($\Delta n \approx 0.5$) provides a more simpler alternative for optical devices. They have the additional advantage of presenting higher transparency in a broadband wavelength region [2, 3], making them suitable for other applications such as biophotonics and sensing. Polarization management is required for both, to avoid undesired polarization mode dispersion (PMD) and to improve the spectral efficiency employing dual polarization in coherent communications system [4].
In this work we first review different designs of polarization beam splitters (PBS) using Si3N4 platform. We analyze different approaches of PBS based on directional couplers (DC) [5] and interferometers [6, 7]. Then, we propose a different approach for a broadband PBS operating in the whole C-band, which is based on a multi-mode interferometer (MMI). We develop an analytical model and the numerical simulations of the device, and finally, we compare the results with state of the art devices.

Fig 1: Examples of different designs of PBS: (a) DC-based PSB with phase control stage and (b) 1 × 2 MMI-based PSB.

Ref.	IL (dB)	BW (nm)	ER (dB)	Wavelength (nm)	Tech.	Platform
[5]	0.6	95	>10	1260-1355	DC	Si_3N_4
[9]	~1	100	~12	1470-1570	DC	SOI
[6]	0.13	80	>20	1530-1610	MZI	Si_3N_4
[7]	0.5	100	>20	1500-1600	MMI	Si_3N_4
[8]	1	35	>17	1530-1565	MMI	Si_3N_4/SOI

Table 1: State of the art of integrated PBS. Abbreviations: IL Insertion Loss, BW Bandwidth, ER Extinction Rate, MZI Mach-Zehnder Interferometer.

References

[1]D. Thomson, A. Zilkie, J. E. Bowers, T. Komljenovic, G. T. Reed, et al.: "Roadmap on silicon photonics", Journal of Optics, 2016, vol. 18, p. 073003. [2]P. Muñoz, G. Micó, L. Bru, D. Pastor, D. Pérez, et al.: "Silicon Nitride Photonic Integration Platforms for Visible, Near-Infrared and Mid-Infrared Applications", Sensors, 2017, vol. 17, p. 2088. [3] A. Rahim, E. Ryckeboer, A. Z. Subramanian, S. Clemmen, B. Kuyken, et al. "Expanding the Silicon Photonics Portfolio With Silicon Nitride Photonic Integrated Circuits", Journal of Lightwave Technology, 2017, vol. 35, pp. 639-649. [4]D. Dai, L. Liu, S. Gao, D.-X. Xu y S. He, "Polarization management for silicon photonic integrated circuits", Laser & Photonics Reviews, 2012, vol. 7, pp. 303-328. [5]S. Guerber, C. Alonso-Ramos, D. Perez-Galacho, X. L. Roux, N. Vulliet, et al.: "Design and integration of an O-band silicon nitride AWG for CWDM applications", 2017 IEEE 14th International Conference on Group IV Photonics (GFP), 2017. [6]S. Gao, Y. Wang, K. Wang y E. Skafidas, "High Efficient, Compact and Broadband 2x2 Polarization Beam Splitter on Silicon Nitride", Conference on Lasers and Electro-Optics, 2016. [7]M. Teng, S. Kim, K. Han, B. Niu, Y. Lee y M. Qi, "Silicon Nitride Polarization Beam Splitter Based on MMI with Phase Delay Line", Conference on Lasers and Electro-Optics, 2017. [8] X. Sun, J. S. Aitchison, and M. Mojahedi, "Realization of an ultra-compact polarization beam splitter using asymmetric MMI based on silicon nitride / silicon-on-insulator platform," Opt. Express 25, 8296-8305, 2017. [9] F. Zhang, H. Yun, Y. Wang, Z. Lu, L. Chrostowski, and N. A. F. Jaeger, "Compact broadband polarization beam splitter using a symmetric directional coupler with sinusoidal bends" Opt. Lett. 42, 235-238, 2017

A19_24 Latest advances in microresonator based frequency combs

M Barturen[1, 2], N Abadía [3, 4], PA Costanzo Caso [2, 5, 6]. mbarturen@uade.edu.ar

[1]Instituto de Tecnología, Universidad Argentina de la Empresa, Lima 775, (C1073AAO) Ciudad Autónoma de Buenos Aires, Argentina; [2] Consejo, Nacional de Investigaciones Científicas y Técnicas (CONICET), Argentina; [3]School of Physics and Astronomy, Cardiff University, Queen's Building, The Parade, Cardiff, CF24 3AA, United Kingdom; [4]Institute for Compound Semiconductors, Cardiff University, Queen's Building, The Parade, Cardiff, CF24 3AA, United Kingdom; [5]Instituto Balseiro, UNCuyo-CNEA, Av. Bustillo 9500, Bariloche (RN), Argentina; [6]Comisión Nacional de Energía Atómica (CNEA)

In the evolutive path of frequency combs, microresonator based frequency combs pumped with continuous wave, have come up as a promising alternative to the femtosecond laser scenario. These photonic devices offer the advantages of a unique compact footprint and pave the way to monolithic electronic integration, which is a promise of expanding the already vast number of applications. Related to the materials composing the resonators, two interesting advances have been recently made. The first one is related to the incorporation of 2D materials to the resonators and the second one is associated with the usage of materials with quadratic nonlinearity instead of the third one to produce combs.

On the one hand, the addition of 2D materials to the resonators has been proposed with the aim of manipulating the resonator's effective index by electrical means, once it is built. After the fabrication process, many parameters are fixed in the resonator. Among these, we can find the resonance frequency and the coupling strength to the bus waveguide which exerts significant influence on the comb extinction properties. This is why different techniques, like thermal and electric tuning [1,2] have been used to modify the resonator's effective index and materials like graphene have been incorporated to the devices.

On the other hand, one natural evolution of kerr combs is found in quadratic combs [3]. The quadratic nonlinearity has several features different from those found in Kerr nonlinearity. First the quadratic nonlinear materials have a larger nonlinearity than the Kerr nonlinearity and require a lower pump power. This reduces the necessary intensity inside the cavity and allows a larger system size, which is suitable for generating denser comb spectra. Such features of quadratic nonlinearity are useful for not only conventional photonics but also quantum information processing. In this work, we will review the latest advances in these two areas including thermal tuning of the extinction features, incorporation of 2D materials like graphene to manipulate the extinction characteristics, power consumption reduction and quadratic nonlinearity based frequency combs among others.

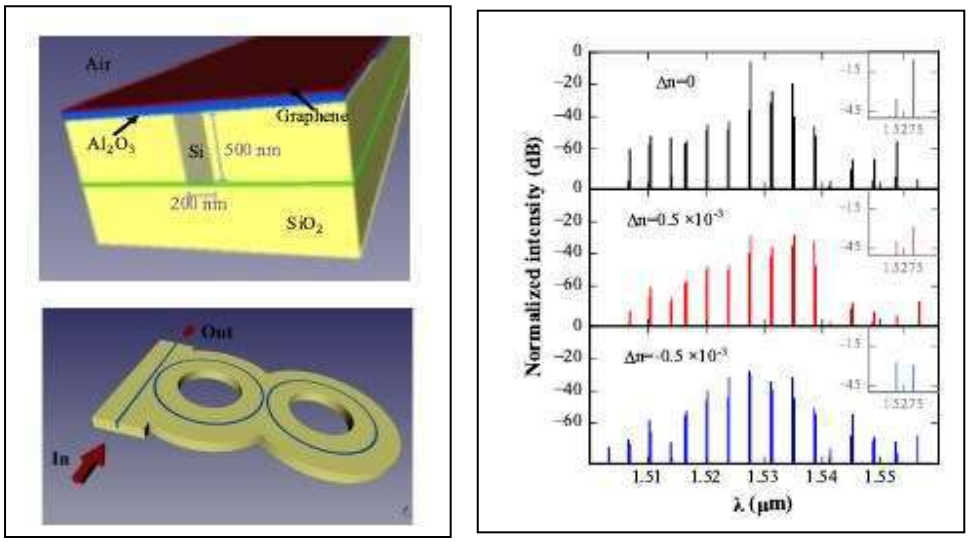

Figure 1: a) Waveguide structure including a graphene layer. b) Coupled resonators structure c) Comb obtained when the waveguide effective index is changed in Δn.

References

[1] Miller, S. A., Okawachi, Y., Ramelow, S., Luke, K., Dutt, A., Farsi, A., ... & Lipson, M. (2015). Tunable frequency combs based ondual microring resonators. Optics express, 23(16), 21527-21540. [2] Barturen, M., Abadía, N., Milano, J., Caso, P. A. C., & Plant, D. V. (2018). Manipulation of extinction features in frequency combs through the usage of graphene. Optics express, 26(12), 15490-15502. [3] Ikuta, R., Asano, M., Tani, R., Yamamoto, T., & Imoto, N. (2018). Frequency comb generation in a quadratic nonlinear waveguide resonator. Optics express, 26(12), 15551-15558.

A19_44 C-Band tunable laser modeling and simulation

M Bustillos[1,2*], GF Rinalde[1,2], L Bulus[1,2,3], N Abadía[4,5,6], and PA Costanzo Caso[1,2,3]

*marvin.bustillos@ib.edu.ar

[1] Instituto Balseiro, UNCuyo-CNEA, Av. Bustillo 9500, Bariloche (RN), Argentina. [2] Comisión Nacional de Energía Atómica (CNEA). [3] Consejo Nacional de Investigaciones Científicas y Técnicas (CONICET), Argentina. [4]Department of Electrical and Computer Engineering, McGill University, Montreal, Quebec, H3A 0E9, Canada. [5]School of Physics and Astronomy, Cardiff University, Queen's Building, The Parade, Cardiff, CF24 3AA, United Kingdom. [6]Institute for Compound Semiconductors, Cardiff University, Queen's Building, The Parade, Cardiff, CF24 3AA, United Kingdom

Today's internet transport capacity is supported by technologies such as Wavelength Division Multiplexing (WDM). Such technologies allow an increase in network capacity at reasonable costs, and tunable lasers are key elements in these and future architectures, since they provide the flexibility that WDM-based networks need [1,2].

This paper presents an insight into the modeling and numerical simulation of a Y-branch widely tunable laser, which is intended for modern optical communications networks such as DWDM systems. The modeled laser is a Distributed Bragg Reflector (DBR) that uses the Vernier effect to extend the tuning range in order to cover the entire C-band. The main objective for the model and simulations is the design and implementation of control algorithms for wavelength and output power of the laser.

In the model, it was considered the different components of the laser such as the Bragg reflectors, phase adjustment section, resonator and the active medium. The structure of the laser is shown in Fig. 1(a). For the Bragg reflectors, the matrix theory of multilayer optics was used to obtain the reflectance spectrum [3], which is shown in Fig. 1(b) (top). The intensity transfer function of the resonator was obtained and it was considered the phase adjustment section in the model. The reflectance spectrum of the Bragg gratings along with the resonator´s light intensity and the active medium gain can be used to find the loss and gain inside the resonator, shown in Fig. 1(b) (middle) . All the component expressions were used to numerically solve the rate equation that governs the photon flux density inside the resonator, which can be used to ultimately find the output power spectrum, shown in fig. 1(b) (bottom). Finally, Fig. 1(c) shows the wavelength tunability of the laser by considering a variation of the Bragg reflectors, which are controlled by the injection current. Theo retical and numerical results are in very good agreement with experimental measurements.

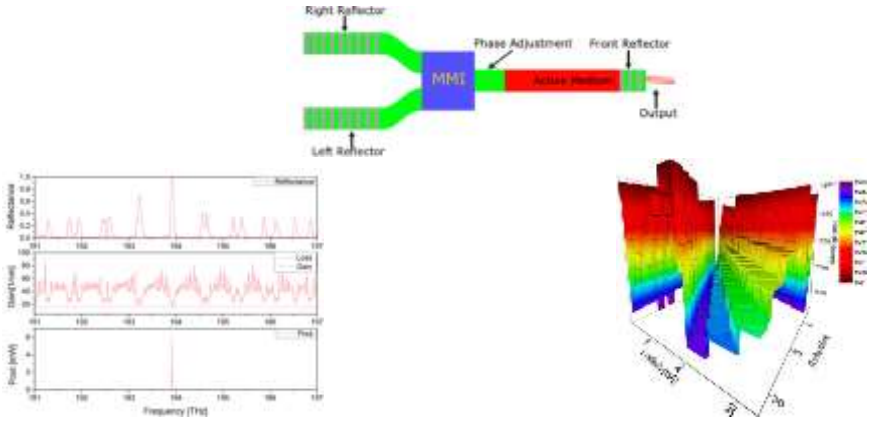

Fig. 1: (a) Y-branch tunable laser scheme, (b) Bragg Reflectors reflectance(top), Gain and losses inside the resonator(center) and output power(bottom), (c) Bragg reflectors current sweep.

References

[1] R. Plastow, "Emerging tunable laser applications in optical networks", Lightwave Magazine, vol 17, no. 3, March (2000). **[2]** H. Guan, et. al, "Widely-tunable, narrow-linewidth III-V/silicon hybrid external-cavity laser for coherent Communication," Vol. 26, Issue 7, pp. 7920-7933 (2018). **[3]** Saleh, B. E. A., Teich, M. C., "Fundamentals Of Photonics", 978-0-471-35832-9, second edition, Hoboken, New Jersey, USA: John Whiley & Sons (2007).

A19_41 Optical Switch using Beamsteering at 900 nm wavelength in GaAs / $Al_xGa_{(1-x)}As$ with High Extinction Ratio for Quantum Sensors

JL Moss, B Saleeb-Mousa, JO Maclean*, RP Campion, and CJ Mellor

Jessica.Maclean@nottingham.ac.uk

School of Physics and Astronomy, University of Nottingham, University Park, Nottingham, NG7 2RD

III-V semiconductor photonic waveguides confine high intensities of light (MW cm-2) in active and passive devices and are attractive for compact, lightweight sensing and communications photonic circuits. The fabrication of low loss waveguides at short wavelengths is challenging as a result of the alloy systems required and the fabrication precision necessary. We previously demonstrated single-mode, polarisation-maintaining semiconductor rib waveguides in the AlxGa(1-x)As III-V semiconductor alloy at the wavelength of 780 nm [1] which were designed for a quantum sensor using transitions of 87Rb cold atoms. We present a semiconductor device for high extinction ratio optical switching at 900 nm wavelength using dynamic refractive index modulation by current injection of a few mA. The device consists of a symmetric slab waveguide with steering and beam-sorting section. The epitaxial p-i-n structure was grown on a semi-insulating GaAs wafer using elemental sources of Ga, Al and As, on semi-insulating GaAs 50 mm diameter substrates by in-house Molecular Beam Epitaxy (MBE). Growth temperatures and flux ratios were optimised for the designed composition, low defect density and low unintentional dopant concentrations. The device process development involved the optimisation of photolithography for n- and p-type contact steps, mesa isolation steps using plasma etching, and device passivation and encapsulation using bis-cyclo-butene (BCB). The results of contact resistance measurements and planarisation measurements will be presented. A dedicated optical test set-up was designed for measuring the switching speed. This was used to compare the performance with commercially-fabricated 780 nm acousto-optic modulator devices. Future work will aim to test devices nanofabricated from a new epitaxial design for 780 nm optical switching and will integrate the devices in optical-fibre-based cold atom sensing experiments [2].

Acknowledgement: We wish to acknowledge funding from UK Quantum Technologies Hub for Sensors and Metrology, EP/M013294/1.

[1] “III-V semiconductor waveguides for photonic functionality at 780 nm”, **Jessica O. Maclean**, Mark T. Greenaway, Richard P. Campion, Tadas Pyragius, T. Mark Fromhold, Anthony J. Kent and Christopher J. Mellor, Proc. SPIE 8988, Integrated Optics: Devices, Materials, and Technologies XVIII, 898805 (March 8, 2014); doi: 10.1117/12.2039898, Volume 8988 Integrated Optics: Devices, Materials and Technologies XVIII

[2] “iSense: A Technology Platform for Cold Atom Based Quantum Technologies”, Kai Bongs, Jon Malcolm, Clemens Ramelloo, Lingxiao Zhu, Vincent Boyer, Tristan Valenzuela, **Jessica Maclean**, Anton Piccardo-Selg, Chris Mellor, Thomas Fernholz, Mark Fromhold, Peter Krüger, Ortwin Hellmig, Alexander Grote, Soren Dörscher, Hannes Duncker, Patrick Windpassinger, Klaus Sengstock, Christoph Becker, Bruno Pelle, Adelle Hilico, Marie-Christine Angonin, Peter Wolf, Franck Pereira Dos Santos, Andrea Bertoldi, Philippe Bouyer, Marella de Angelis, Marco Prevedelli, Nicola Poli, Fiodor, Sorrentino, Guglielmo Tino, Simon Stellmer, Florian Schreck, Manuel Popp, Waldemar Herr, Theis Wendrich, Wolfgang Ertmer, Ernst Rasel, Christian Kürbis, Achim Peters, Andreas Wicht, Optics InfoBase Conference Papers [1-55752-995-7] (2014)

Abstracts

Session 4: Lasers & Light Sources I

A19_12 Unidirectional topological edge modes in nanowire-based kagomephotonic crystals

S Wong[1], M Saba[2], O Hess[2], and SS Oh[1] wongs16@cardiff.ac.uk
[1]*School of Physics and Astronomy, Cardiff University, Cardiff CF24 3AA;* [2]*The Blackett Laboratory, Imperial College London, London SW7 2AZ, UK*

Back-reflection of light in optical devices occuring due to bendings, fabrication defects or temperature variations is a current problem that reduces the performances of the devices. Recently, it has been shown that photonic topological insulators can exhibit topological egde modes at the interface between two topologically inequivalent photonic crystals [1]. These modes propagate in onlyone direction and are robust against perturbations making possible to fabricate a one-way waveguide. Plenty of topologically non-trivial photonic designs have been proposed using nonreciprocal system [2], complex metamaterials [3] or perturbed photonic crystals [4], etc. However, the aforementioned photonic topological insulators are either complicated to fabricate, do need strong magnetic field or intrinsically suffer from back-reflection due to the symmetry breaking at the interface. Here, we propose a reciprocal photonic topological insluator based on the geometry of the crystal which is a Kagome lattice composed of nanowires [5]. We theoretically and numerically show that it has a non-trivial topology resulting in chiral edge modes which do not intrisically suffer from back-scattering at the interface but sensitive to its termination. Furthermore, the modes are shown to be robust against sharp bendings, dislocations and missing nanowires.
The design of the proposed photonic topological insulator is very simple making the structures easily fabricable with many conventional techniques such as selective-area epitaxy, electron-beam patterning, etc. Furthermore, using III-V semiconductor nanowires, it opens the possibility to design a new type of semiconductor laser using a one-way waveguide with extemely low loss.

This work is part-funded by the European Regional Development Fund through the Welsh Government.

References:

[1] L. Lu, J. D. Joannopoulos, and M. Solja˘cic. Topological states in photonic systems. Nature Physics, 12:626–629, 2016.
[2] F. D. M. Haldane and S. Raghu. Possible realization of directional optical waveguides in photonic crystals with broken time-reversal symmetry. Phys. Rev. Lett., 100:013904, 2008.
[3] A. B. Khanikaev, S. H. Mousavi, W. K. Tse, M. Kargarian, A. H. MacDonald, and G. Shvets. Photonic topological insulators. Nature materials, 12(3):233, 2013.
[4] L. H. Wu and X. Hu. Scheme for achieving a topological photonic crystal by using dielectric material. Phys. Rev. Lett., 114:223901, 2015.
[5] M. Mekata. Kagome: The Story of the Basketweave Lattice. Physics Today, 56(2):12, February 2003.

A19_46 Design, Fabrication and Characterisation of 980 nm Linearly Polarised Multi-Mode VCSELs for Ebium Doped Waveguide Amplifier Integration

D Lei[1], N Babazadeh[2], J Sarma[3], DTD Childs[1], and RA Hogg[1]
[1]The University of Glasgow, Glasgow, G12 8LT UK; [2]The University of Sheffield, Western Bank, Sheffield, S10 2TN UK, [3]University of Bath, Claverton Down, Bath, BA2 7AY UK

The temporal selection of degenerate polarisation modes in vertical cavity surface emitting lasers (VCSELs) is an issue in many applications. Our application lies in solutions to providing an optical pump for a novel erbium doped planar waveguide amplifier (EDWA). This application requires multimode VCSELs with (time integrated) stable linear polarization (LP) to match the polarization requirements of coupler elements and so pump the Er^{3+} glass elements efficiently.
For single-mode VCSELs, these modes occur at any azimuthal angle due to cylindrical symmetry. What is more, the direction of polarization can jump between angles with varying injection current for individual devices. Here we describe the design, fabrication and characterisation of multimode VCSELs with fixed linear polarization based upon a low cost manufacturing approach. This is based on an approach employed to pin the polarization of a single mode VCSELs [1]. The control of polarisation in multimode VCSELs has been explored using surface gratings [2], but by contrast, our method is a simpler approach. Our multimode VCSEL design is shown schematically in Fig.1 (a) and (b) and a microscope image of the realised device is in Fig. 1(c). Our device utilizes deeply etched trenches that simultaneously provide n-side contact from the top surface *and* polarisation pinning.
Figure 2(a) and (b) present typical power (CW and pulsed) and angular polarisation dependence of the emitted power (CW) of our device. The emission shows preferential polarization oriented parallel to the etched trench direction and this is stable with injected current increasing. Fig.2 (c) plots the extinction ratio of the device emission showing an extinction ratio of ~3 above threshold.

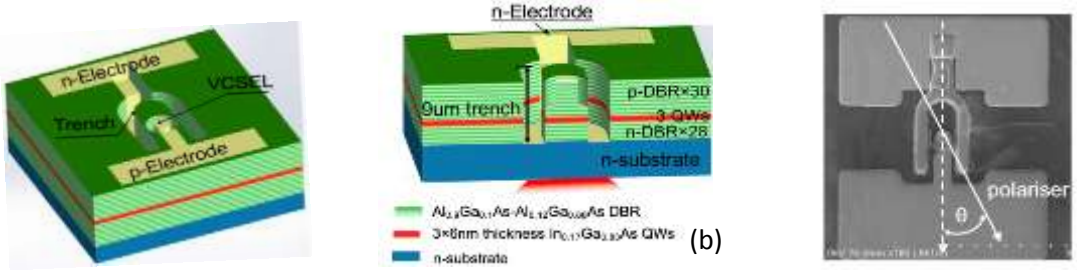

Fig. 1. (a),(b) Schematics and epitaxial structure of substrate-emitting VCSEL device, and (c) SEM of the realised device showing definition of polarisation angle, θ (=angle to parallel of etched trenches).

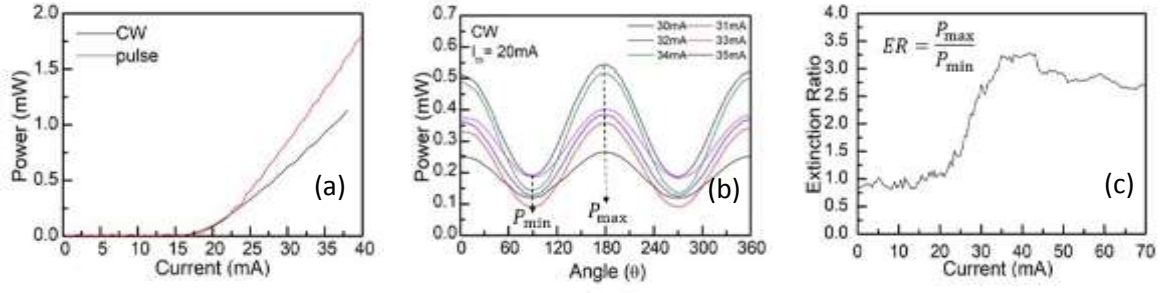

Fig. 2. (a) 40um diameter p contact VCSEL P-I curve for pulsed and CW operation; (b) Emitted power as a function of polarisation;

REFERENCES:
[1] P. Dowd et al., "Complete polarisation control of GaAs gain-guided top-surface emitting vertical cavity lasers," Electron. Lett., vol. 33, no. 15, p. 1315, 1997. [2]P. Debernardi, "Surface gratings for polarization control of single- and multi-mode oxide-confined vertical-cavity surface emitting lasers," Opt. Commun., vol. 246, no. 4–6, pp. 511–519, 2004.
Acknowledgemet: This work was carried out under EPSRC EP/M015165/1.

A19_10 Photonic Topological Insulator Lasers based on III-V Semiconductor Nanowires

Y Gong, S Wong, DL Huffaker, SS Oh OhS2@cardiff.ac.uk
School of Physics and Astronomy, Cardiff University, Cardiff, CF24 3AA, United Kingdom

A remarkable feature of topological insulators is generation of conducting edge states that propagate scatter-free even in the presence of large impurities [1]. This has opened up a new avenue for families of optical devices with extremely small propagation and bending losses due to the robust, scatter-free light propagation. Thus, topological protection has been extensively studied in magneto-optic photonic crystals [2-3] and metamaterials [4-5].

In this work, we apply the topological insulator concept to a photonic crystal structure made of dielectric rods and propose a new type of photonic topological insulator (PTI) lasers theoretically. For the demostration, we designed InGaAs nanowires PTI lasers and simulated the band structure and light propagation using 3D finite-difference time-domain method. Our simulation results clearly shows that edge modes from the InGaAs PTI lasers has exceptional light directionality and one-way waveguide with extremely low loss (Fig. 1). We believe the III-V semiconductor nanowire based-waveguide will enable highly efficient, low threshold and ultrastable lasers that are robust to defects and disorder.

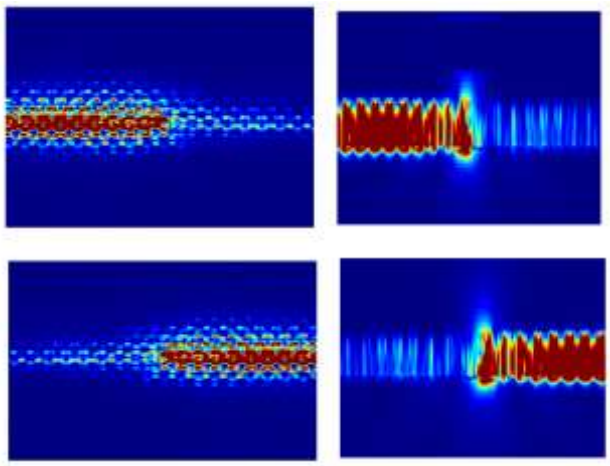

Key words: Nanophotonics; Photonic Topological Insulator; Semiconductor Nanowires

References:

[1] L. Lu, J. D. Joannopoulos, and M. Soljacic, “Topological photonics,” Nat. Photonics 8(11), 821–829 (2014).
[2] S. Barik, H. Miyake, W. DeGottardi, E. Waks, and M. Hafezi, “Two-dimensionally confined topological edge states in photonic crystals,” New J. Phys. 18(11), 113013 (2016).
[3] L.-H. Wu and X. Hu, “Scheme for achieving a topological photonic crystal by using dielectric material,” Phys.Rev. Lett. 114(22), 223901 (2015).
[4] W. Gao, M. Lawrence, B. Yang, F. Liu, F. Fang, B. Béri, J. Li, and S. Zhang, “Topological photonic phase in chiral hyperbolic metamaterials,” Phys. Rev. Lett. 114(3), 037402 (2015).
[5] A. Shaltout, A. Kildishev, and V. Shalaev, “Time-varying metasurfaces and Lorentz non-reciprocity,” Opt. Mater. Express 5(11), 2459–2467 (2015).

A19_03 Numerical Simulation of Photonic Microwave Generation in a Single ModeVCSEL

C Xue[1, 2], S Ji[1], A Valle[3] and Y Hong[1]
[1]School of Electronic Engineering, Bangor University, Wales, LL57 1UT, UK; [2]School of Information and Communication Engineering, University of Electronic Science and Technology of China, Chengdu 611731, China; [3]Institution de Física de Cantabria (CSIC-Univ. de Cantabria), Avda. Los Castros s/n, E39005 Santander, Spain

Photonic microwave generation based on period one (P1) dynamics in semiconductor lasers has received considerable interests due to many advantages. 100 GHz frequency of the photonic microwave has generated based on P1 dynamic in DFB lasers [1]. Such research activities have extended to low-cost vertical-cavity surface-emitting lasers (VCSELs) due to many advantages of VCSELs. We have experimentally demonstrated a widely continually tunable photonic microwave generation based on P1 in an optically injected VCSEL [2]. In [2], two local maximum microwave powers at the two detuning frequencies with a fixed injection power have been observed, which has not been shown in DFB lasers. The numerical simulation results [3] indicate that this is because the VCSEL polarization plays a role on the dynamics, where the two local maximum microwave powers are due to the excitation of both linear polarizations with small amplitudes and with out-of-phase. In this paper, we investigate in detail the effect of specific parameters associated with VCSELs on the characteristics of the generated microwave based on P1 dynamic.

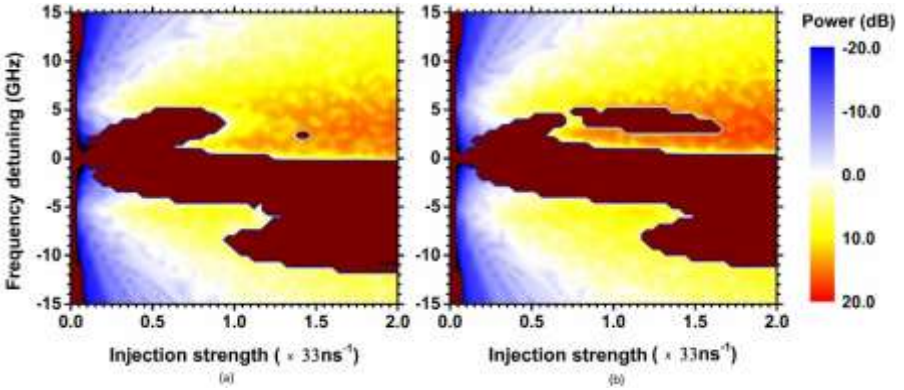

Fig. 3 Maps of the generated microwave power as a function of the injection strength and frequency detuning. The linear dichroism γ_a = (a) 0.21 ns^{-1}; (b) 5 ns^{-1}.

Fig. 1 shows the simulation results of the generated microwave power as a function of the injection strength and frequency detuning with the different values of the linear dichroism γ_a. In the maps, the VCSEL operates at P1 dynamic except wine colour areas. In Fig. 1(a), when the injection strength is between 31.5 ns^{-1} and 40 ns^{-1}, two local maximum microwave powers at the two detuning frequencies are observed, which are qualitatively agreed with the experimental results [2]. When the injection strength is increased to more than 40 ns^{-1}, two local maximum microwave powers disappear. However, for the VCSEL with higher γ_a, as shown in Fig. 1(b), no two local maximum microwave powers are observed within the injection strength ranges of 0 and 66 ns^{-1}. The results also show that γ_a also affects the P1 dynamic region. The effect of the linear birefringence parameter on the generated microwaves has also been studied, but no significant effect is found.

References

[1] S.-C. Chan et al., Opt. Lett., **31**, p. 2254, 2006; [2] S. Ji, et al., Opt. Express, **25**, p. 19863, 2017;
[3] A. Valle, et al., IEEE Photon. Technol. Lett. **25**, p. 1266, 2018.

A19_45 The Nature of Auger Recombination in Type-I Mid-Infrared Laser Diodes

TD Eales[1], MC Amann[2], IP Marko[1], BA Ikyo[1], AR Adams[1], A Andrejew[2], K Vizbaras[2,3], L Shterengas[4], G Belenky[4], I Vurgaftman[5], JR Meyer[5], SJ Sweeney[1]

[1]Advanced Technology Institute and Department of Physics, University of Surrey, Guildford GU2 7XH, United Kingdom; [2]Walter Schottky Institut, Technische Universität München, Am Coulombwall 3, 85748 Garching, Germany; [3]Brolis Semiconductors UAB, Moletu pl. 73, Vilnius, Lithuania, LT-14259; [4]Department of Electrical and Computer Engineering, State University of New York at Stony Brook, New York 11794, USA; [5]US Naval Research Laboratory, 4555 Overlook Avenue SW, Washington DC 20375, USA

Type-I quantum well (QW) lasers based on the GaSb material system show attractive characteristics in the mid-infrared [1]. However, as the wavelength (λ) increases in the range of 2-4 µm their performance begins to deteriorate due to increasing Auger recombination [2]. In the Auger process, the energy released from an electron-hole recombination is transferred to a third carrier. In order to develop strategies to suppress Auger recombination, it is crucial to understand the magnitude and nature of the dominant Auger recombination pathway, and their dependencies on the operating λ and temperature (T). In QW structures two fundamentally different Auger process can occur [3]. In an activated Auger process Fig (a), initial and final carrier states are confined to the plane of the QW. Then the recombination rate depends exponentially on T because it is determined by an activation energy, which is a consequence of energy and momentum conservation. In a thresholdless Auger process, Fig. (b), the initial carrier states can exist near the band edge (bottom of conduction/valence band) and the third carrier is excited into the continuum of unbound states in a direction perpendicular to the plane of the well. Without an activation energy, the thresholdless Auger process exhibits only a weak T dependence. In this work, we report on the T and λ dependence of the threshold current density (J_{th}) of type-I QW devices operating in range 1.95-3.2 µm. From T-dependent measurements, we find that radiative recombination dominates from low T up to a break point temperature [4]. Beyond this break point the temperature sensitivity of J_{th} increases rapidly, Fig. (c) indicating the onset of a strongly temperature-sensitive activated Auger process. Using hydrostatic pressure, we tuned the operating λ of the lasers in order to probe the λ dependence of the Auger coefficient. Modelling the gain and loss characteristics of the lasers allowed the threshold carrier density (n_{th}) to be determined. Since the carrier density calculations depend sensitively on the threshold gain, we undertook segmented contact measurements to experimentally determine the optical loss. By extracting the experimentally-determined radiative component of J_{th} and assuming the remaining non-radiative current $J_{nr}=Cn_{th}^3$, C and its λ dependence were calculated. It is interesting to consider the consequences of these results for quantum dot lasers.

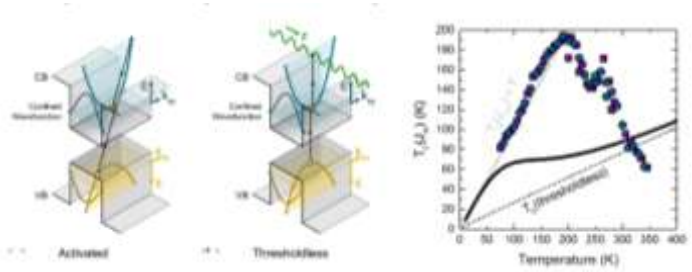

References

[1] S. D. Sifferman, H. P. Nair, R. Salas, N. T. Sheehan, S. J. Maddox, A. M. Crook, and S. R. Bank, "Highly Strained Mid-Infrared Type-I Diode Lasers on GaSb," IEEE J. Sel. Top. Quantum Electron., vol. **21**, no. 6, pp. 1–10, 2015. [2] T. D. Eales, I. P. Marko, B. A. Ikyo, A. R. Adams, S. Arafin, S. Sprengel, M. C. Amann, and S. J. Sweeney, "Wavelength Dependence of Efficiency Limiting Mechanisms in Type-I Mid-Infrared GaInAsSb/GaSb Lasers," IEEE J. Sel. Top. Quantum Electron., vol. 23, no. **6**, pp. 1–1, 2017. [3] R. I. Taylor, R. A Abram, M. G. Burt, and C. Smith, "A detailed study of Auger recombination in 1.3 um InGaAsP/InP quantum wells and quantum well wires," Semicond. Sci. Technol., vol. **5**, no. 1, pp. 90–104, 1990. [4] S. J. Sweeney, A. Phillips, A. R. Adams, E. P. O'Reilly, and P. J. A. Thijs, "The effect of temperature dependent processes on the performance of 1.5-µm compressively strained InGaAs (P) MQW semiconductor diode lasers," Photonics Technol. Lett., vol. 10, no. **8**, pp. 1076–1078, 1998.

A19_21 Surface Recombination Effects in Transfer Printable Red Micro-LEDs

J Browne[1], Z Li[1], J Justice[1], A Gocalinska[1], E Pelucchi[1] and B Corbett[1]
[1]Tyndall National Institute, University College Cork, Lee Maltings, Dyke Parade, Cork, Ireland

Non-radiative recombination at exposed p-n junctions is particularly relevant for III-V semiconductor light emitting devices being detrimental to efficient device operation due to the loss of carriers [1]. As the device size decreases and the perimeter to area ratio increases this issue becomes more pronounced. This is of particular relevance for (Al)GaInP devices as small and efficient red micro-LEDs are required for displays and many other applications.

The effect of surface recombination can be seen in the electrical domain by comparing the current voltage characteristics from devices of different sizes. Smaller devices draw a higher current density than larger devices at a given voltage. This can be seen in Figure 1 for samples fabricated from three different epitaxial structures; one with a bulk p-n junction and two with 3 quantum wells (QW) grown on different orientations. The QW samples show reduced surface leakage in comparison with the bulk p-n sample. Quantifying the effects of the surface on the optical emission is complicated by the presence of a GaAs substrate which absorbs red light. This restricts optical measurements of devices with the substrate in place. To address this we removed the devices from their GaAs substrates and transferred them on a glass slide. Measurement of the light output through the glass is shown in Figure 2. At low injection current there is a slow turn-on for the bulk p-n sample as carriers are recombining non-radiatively at low injected current. This corresponds with the higher surface leakage indicated by electrical measurements. Higher output powers are measured for the bulk sample due to the limited number of QWs used. At high current density heating causes the output power to saturate.

Micro-transfer-printing allows for the engineered separation of devices from their native substrate and placement onto a transparent donor substrate. Transfer-printing allows for much greater flexibility in integration schemes over flip-chip or wafer bonding. Selective etching of a sacrificial layer is needed and in conjunction with a tethering mechanism enables pick up and placement of individual device coupons. In Figure 3 fabricated transferable red emitting micro-LEDs with resist tethers are shown prior to undercutting of the sacrificial layer. This work is part funded by Science Foundation Ireland under 12/RC/2276 (IPIC).

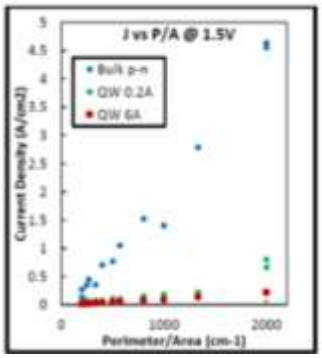

Fig 1: Current density vs. perimeter to area ratio for bulk and quantum well red-emitting samples at a forward bias of 1.5 V.

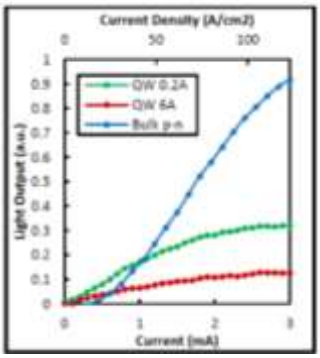

Fig 2: Output power vs. current density for 50µm diameter circular mesa LEDs with substrate removed.

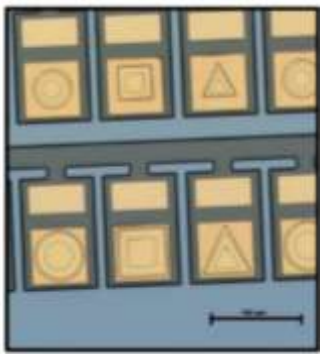

Fig 3: Micrograph of fabricated AlGaInP LEDs with different mesa sizes and shapes with resist tether prior to undercut etch. Each coupon (device) is 80 µm x 120 µm.

References

[1] E.J. Radauscher et al., Proc. SPIE, 10124, (2017)

A19_32 An approach towards spin-injected edge-emitting semiconductor lasers

N Jung[1], M Lindemann[1], J Ritzmann[2], S Webers[3], A Ludwig[2], A Wieck[2], H Wende[3], NC Gerhardt[1] and MR Hofman[1]

[1]Photonics and Terahertz Technology, Ruhr University Bochum, 44780 Germany; [2]Angewandte Festkörperphysik, Ruhr University Bochum, 44780 Germany; [3]Faculty of Physics and Center for Nanointegration(CENIDE), University of DuisburgEssen, lotharstr. 1, Duisburg, Germany

We have developed and grown an electrically spin-pumped room-temperature edge-emitting semiconductor laser. The spin-structure consists of a GaAs/AlGaAs heterostructure with a ferromagnetic Fe layer on top. An MgO tunnel barrier is embedded to provide a suitable spin-injection efficiency.

Recently spin-optoelectronic devices have gained more and more attention. These devices use the direct connection between the carrier spin and the photon spin upon radiative recombination in order to generate a spin-controlled net circular polarization degree for light emission. Spin-optoelectronic devices offer several advantages like reduced threshold, faster modulation dynamics, enhanced emission intensities and full polarization control. However, they are only interesting for applications if they operate at room temperature and without a large external magnetic field. [1, 2]

In general, spin-injection into a semiconductor, can be provided by a ferromagnetic layer. But in a standard ohmic contact between the ferromagnetic layer and the semiconductor, the large conductivity mismatch leads to an almost negligible spin-injection efficiency. The spin-injection efficiency can be increased by an insulating tunnel barrier (e. g. MgO) embedded between ferromagnetic contact and semiconductor. [1]

Furthermore, spin-injected semiconductor lasers can be achieved either in an edge-emitting geometry or in a vertical geometry. The edge-emitting laser (EEL) has a rather easy geometry whereas the vertical-cavity surface-emitting laser (VCSEL) has a rather complicated structure. Inside EELs with active regions containing quantum wells, the optical selection rules lead to a linearly polarized laser emission parallel or perpendicular to the waveguide plane. The VCSEL, on the other hand, is a laterally isotropic device with almost perfect circular symmetry which leads to weak pinning of the polarization state. [1]

The main disadvantage for an electrically pumped spin-VCSEL is the long spin-injection path length (in average $\gg$3µm [3]) which overcomes the spin relaxation length [4] by orders of magnitude. Thus, electrical spin pumping is challenging. In comparison, the spin-injection path length of an EEL is rather short (<500nm) and more suitable. Recently an electrical spin-injection from a FeCo/MgO Shottky tunnel barrier into an electrically pumped spin polariton diode laser has been demonstrated [5].

Our first attempt to realize a spin-EEL at room-temperature was made with a GaAs/AlGaAs heterostructure (Fig. 1) epitaxially grown on a 625µm GaAs:Zn substrate. An MgO tunnel barrier was grown on top, followed by a ferromagnetic compound of Fe57, Fe and Au. The results of the first measurements will be presented and further improvements and measurements will be discussed.

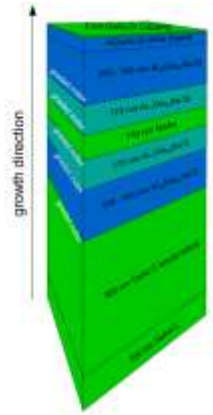

Fig 1*:* GaAs/AlGaAs heterostructure

References

[1] N. C. Gerhardt, and M. R. Hofmann, Adv. Opt. Technol. 2012, 268949 (2012)

[2] M. Lindemann, T. Pusch, R. Michalzik, N. C. Gerhardt and M. R: Hofmann, Appl. Phys. Lett. 108, 042404 (2016)

[3] D. Basu, D. Saha, and P. Battacharya, Phys. Rev. Lett. 102, 093904 (2009)

[4] H. Soldat, M. Li, N. C. Gerhardt, M. R. Hofmann, A. Ludwig, A. Ebbert, D. Reuter, A. D. Wieck, F. Stromberg, W. Keune, and H. Wende, Appl. Phys. Lett. 99, 051102 (2011)

[5] A. Bhattacharya, M. Z. Baten, I. Iorsh, T. Frost, A. Kavokin, and P. Battacharya, Phys. Rev. Lett. 119, 067701 (2017)

Abstracts

Session 5: Lasers & Light Sources II

A19_48 Mode Coupling and Analysis in Laterally Coupled Vertical Cavities

S Chen, H Francis, CH Ho, KJ Che, M Hopkinson, and CY Jin
Department of Electronic & Electrical Engineering, University of Sheffield

Recently, the coupled cavity system has been intensively studied in view of its ability to dynamically control the coupling state; a feature which is of interest for the realization of functional photonic circuits, e.g. optical buffers [1], single mode lasers [2] and Q factor control by cavities [3] [4]. Here we propose a laterally coupled vertical cavity system with two identical square vertical cavities coupled via a narrow bridge. Using GaAs/AlAs vertical cavities holds the advantages for the efficient overlap between light field and emitters, easy fabrication, and the convenience to optical excitation and collection. By carrying a systematic study on this laterally coupled vertical cavity system, we aim to open the possibility of constructing novel photonic devices for quantum information applications.
A theoretical model has been built to analyse the resonant modes of a single cavity with different lateral sizes. By combining the transfer-matrix method and Maxwell equations both the transverse and longitudinal field was calculated. As presented in Fig. 1, the calculated results match well with the experimentally observed position of the cavity modes. Room temperature PL measurements were taken on coupled cavities with a narrow bridge which has varying length and width. Fig. 1c and 1d show that by decreasing the channel length, the wavelength splitting between the fundamental modes increases, as expected for the stronger coupling strength between the two cavities. This provides us a potential mechanism for cavity detuning and Q factor control in vertical cavity systems

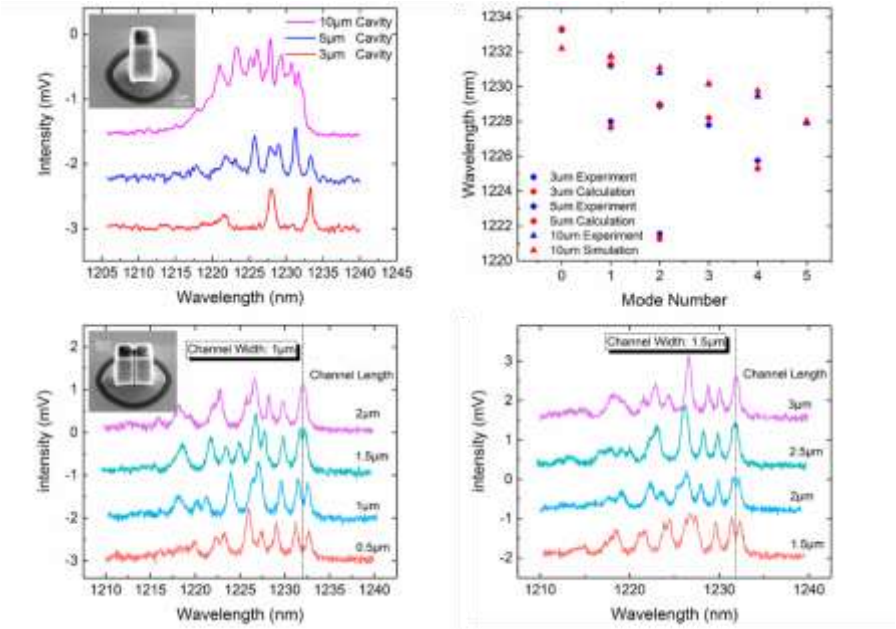

Figure 1. (a) PL spectrum of single square cavities with various sizes. The inset is the SEM image of a square cavity with size of 3μm, composed of two GaAs/Al0.8Ga0.2As Bragg mirrors separated by a GaAs λ-layer; (b) Measured and calculated wavelength of cavity modes as a function of the mode order number; (c) the PL spectrum of coupled cavity modes with varying channel lengths L, the inset shows the SEM image of two coupled square cavities with 3 μm size; (d) the PL spectrum of coupled cavity modes with varying channel lengths L at a fixed channel width W=1.5 μm.

[1] W. Yoshiki, Y. Honda, T. Tetsumoto, K. Furusawa, N. Sekine, and T. Tanabe, Sci. Rep. **7**, (2017). [2] X.W. Ma, Y.Z. Huang, Y.D. Yang, J.L. Xiao, H.Z. Weng, and Z.X. Xiao, Appl. Phys. Lett. **109**, 071102 (2016). [3]Y. Tanaka, J. Upham, T. Nagashima, T. Sugiya, T. Asano, and S. Noda, Nat. Mater. **6**, 862 (2007). [4] C.-Y. Jin, R. Johne, M. Y. Swinkels, T. B. Hoang, L. Midolo, P. J. van Veldhoven, and A. Fiore, Nat. Nanotechnol. **9**, 886 (2014). [5] T. F. Krauss, in *AIP Conf. Proc.* (AIP, Erice (Sicily), 2001), pp. 89–98.

A19_30 Temperature and Pressure Dependence of Low Threshold Current Type-II GaInAs/GaAsSb"W"-Lasers Emitting Around 1.25-μm

D Duffy[1], IP Marko[1], TD Eales[1], C Fuchs[2], J Lehr[2], W Stolz[2] and SJ Sweeney[1]
[1]*Advanced Technology Institute and Department of Physics, University of Surrey, Guildford, GU2 7XH, United Kingdom;*
[2]*Materials Sciences Center and Department of Physics, Philipps-Universität Marburg, Renthof 5, 35032, Marburg, Germany*

The development of more efficient and temperature stable semiconductor lasers in the near-infrared (NIR) is important for the future of energy saving data communications networks. While there has been considerable success using type-I quantum well (QW) and quantum dot based approaches[1,2], devices remain limited by fundamental non-radiative recombination processes such as Auger recombination, carrier leakage and defect-related recombination associated with less mature material growth[3]. A possible way forward to reduce Auger recombination is to use type-II heterostructures, where the electrons and holes are spatially confined in separate QWs. In the mid-infrared, this approach using so-called "W"-structures is well established, providing flexible control of operating wavelength and band parameters[4], and has shown some evidence of reducing Auger recombination5. These structures have recently been demonstrated in the near-infrared with InGaAs/GaAsSb type-II "W"-QW laser structures (see Fig.) emitting in the 1.2-1.3μm range, exhibiting low threshold current densities and a relatively low temperature sensitivity[6]. However, much of the physics underpinning the current understanding of type-II structures is not well-established, with most theoretical models based upon theory developed for simpler type-I structures which may not adequately describe type-II structures. In order to further improve the performance of these structures an improved understanding of the characteristics and main limiting processes occurring in these "W" devices is essential.

In this work, we investigate the physical properties of NIR InGaAs/GaAsSb-based type-II "W"-lasers comparing their performance with conventional type-I InGaAsP/InP devices using a combination of temperature and hydrostatic pressure dependence techniques. The type-II devices exhibit very low room temperature threshold current densities of around 100-300Acm^{-2}, pulsed (at a duty cycle of 0.4%) output powers greater than 1W for 100μm wide stripes and a characteristic temperature, T0, of ≈ 90K around room temperature. Optical gain studies indicate a high modal gain and relatively low optical loss. Further discussion of the device characteristics and their potential for near-infrared applications will be discussed.

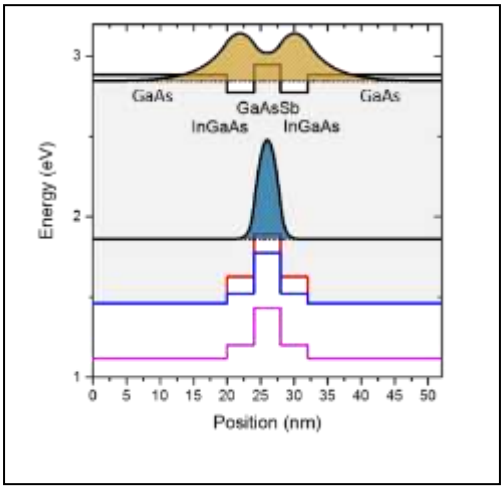

[1] V. M. Ustinov and A. E. Zhukov, *Semicond. Sci. Technol.*, vol. 15, no. 8, 2000.
[2] N. Tansu, J. Y. Yeh, and L. J. Mawst, *Appl. Phys. Lett.*, vol. 82, no. 23, pp. 4038–4040, 2003.
[3] I. P. Marko and S. J. Sweeney, *Semicond. Sci. Technol.*, vol. 33, no. 11, 2018.
[4] J. R. Meyer et al., *Appl. Phys. Lett.*, vol. 67, p. 757, 1995.
[5] G. G. Zegrya and A. D. Andreev, *Appl. Phys. Lett.*, vol. 67, no. 1995, p. 2681, 1995.
[6] C. Fuchs *et al.*, *Sci. Rep.*, vol. 8, no. 1, pp. 8–13, 2018.

A19_49 High Resolution Opitcal Spectrcopy of state-of-the-art Quantum-Dot Lasers for High Temperature Operation

IME Butler[1, 2], N Babazadeh[1], R Baba[1], K Nishi[3], K Takemasa[3], M Sugawara[3], DTD Childs[1], RA Hogg[1]
Iain.Butler@glasgow.ac.uk
[1]School of Engineering, University of Glasgow, Glasgow, G12 8LT, UK; [2]School of Mathematics and Physics, Queen's University Belfast, Belfast, BT7 1NN, UK; [3]QD Laser Inc, Keihin Bldg. 1F, 1-1 Minamiwataridacho, Kawasaki-ku, Kawasaki, Kanagawa 210-0855, JAPAN

Stranski–Krastanov (SK) growth of self-assembled quantum dot (QD) lasers have been the subject of significant research over the last 30 years due to the prediction, and realisation of their temperature insensitivity [1,2]. They have been offered commercially for the past decade finding applications in a wide range of industries such as optical communications and sensing, with an interest towards cooler-free and high temperature operation.

We present a temperature dependence characterisation of a state-of-the-art QD laser chip utilising a test apparatus that has been developed which enables laser characterisation and spectroscopy to be completed at a wide range of environmental temperatures (15K to >600K). Figure 1 shows optical power-current characteristics between 50K and 450K. Whilst slope efficiencies at low temperatures (below 325K) are similar [3], at higher temperatures a reduction of slope efficiency is observed. However, in the 25K before lasing ceases an increase of efficiency is seen. No lasing is observed above 420K with super-luminescence (indicating positive net modal gain) until 450K.

Gain spectra and spontaneous emission can be obtained using the Hakki-Paoli high resolution spectroscopy method [4]. Figure 2 shows gain spectra at 300K and 400K. We show that 450K is the hottest environmental temperature where positive gain is possible for this given chip, the junction temperature as yet unknown. Analysis of gain spectra shows a 13x decrease in efficiency, in comparison to 300K to 450K, resulting a shorter carrier lifetime due to the thermal escape of carriers. In this work we discuss these characteristics in-depth with a view to the applicability of QD lasers for use at high temperatures. We indicate where future improvements could be made to extend the operating temperature range of these devices.

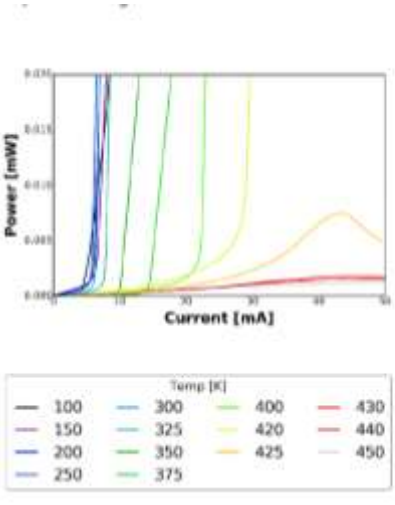

Figure 1. Temperature dependence of optical power-current characteristics of the quantum dot laser

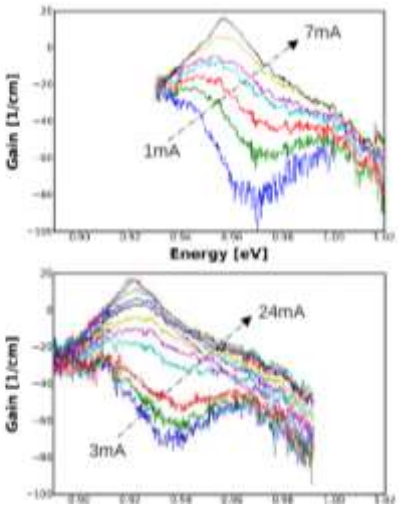

Figure 2. Gain spectra of the quantum dot laser at 300K and 400K.

[1] Y. Arakawa & H. Sakaki, Appl. Phys. Lett. 40, (1982)
[2] N. Kirsaedter et al., Electron. Lett. 30, (1994) [3] M. Sugawara et al., Phys. Rev. B 61, (2000) [4] B. Hakki & T. Paoli, J. of Appl. Phys. 44, 4113 (1973)
This work was supported by the Engineering and Physical Sciences Research Council (grant number EP/L015323/1).

A19_52 Temperature Dependant Characteristics of P-doped Laser Devices

L Jarvis[1], S Shutts[1], M Tang[2], H Liu[2] and PM Smowton[1] jarvislk@cardiff.ac.uk
[1]School of Engineering, University of Glasgow, Glasgow, G12 8LT, UK; [2]School of Mathematics and Physics, Queen's University Belfast, Belfast, BT7 1NN, UK; [3]QD Laser Inc, Keihin Bldg. 1F, 1-1 Minamiwataridacho, Kawasaki-ku, Kawasaki, Kanagawa 210-0855, JAPAN

This work examines 1.3µm InAs Quantum Dot lasers with varying levels of p-doping and cavity lengths grown on GaAs substrates. The resulting effects are non-linear so can be best understood by examining a range of combinations to understand their operation and find regimes of potential benefit. The structures are made into broad area lasing devices with a contact stripe of 100µm. To understand the resulting behaviour devices are mounted in a cryostat and characteristics recorded from 200 – 400K.

Current density as a function of temperature was analysed and the results are explained by considering two regimes of carrier distribution, random/non-thermal and thermal, this conclusion is supported from evidence from the threshold current density, spectral width and slope efficiency, all as a function of temperature. Non-thermal regimes are considered beneficial for applications such as mode-locking as they broaden the spectrum, enabling shorter pulse duration [1]. These distributions are commonly found at lower temperatures [2]. Here we discuss devices with p-type doping that show evidence of non-thermal populations at temperatures above 300K.

P-type modulation doping adds a number of holes close to the device's active region to counter inefficiencies brought about by valence band asymmetry. Higher levels of p-doping cause excited electron energy states to be relatively depopulated as the quasi-Fermi levels are shifted towards the valence states, accommodating more charge carriers before thermalization takes place. Longer cavities require lower threshold current densities to lase, which also extends the thermal regime to higher temperatures.

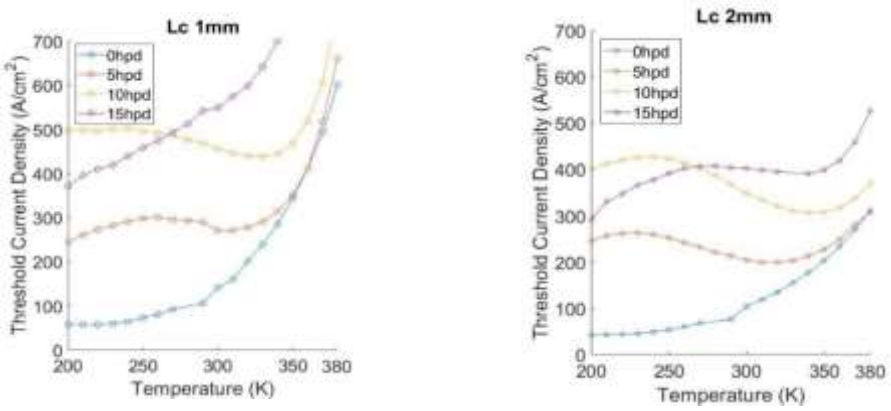

***Figures**: Threshold current density as a function of temperature.*

The local minima in threshold current density occurs as the carriers become thermally distributed [3]. This minima occurs at higher temperatures for higher doping and longer cavities so non thermal operation becomes possible at room temperature.

[1] P. Finch, P. Blood, P. M. Smowton, A. Sobiesierski, R. M. Gwilliam and I. O'Driscoll, *Femtosecond pulse generation in passively mode locked InAs quantum dot lasers,* Applied Physics Letters 2013
[2] M. Grundmann and D. Bimberg, Theory of random population for quantum dots, Phys. Rev. B 55, 1997
[3] Peter M. Smowton ; Ian C. Sandall ; David J. Mowbray ; Hui Yun Liu ; Mark *Hopkinson Temperature-Dependent Gain and Threshold in P-Doped Quantum Dot Lasers*, IEEE Journal of Selected Topics in Quantum Electronics 2007

A19_28 High-yield, low-density InAs/GaAs quantum dots as on-chip quantum light sources

E Clarke, [1*] P Patil, [1] I Farrer,[1] B Royall,[2] AP Foster,[2] D Hallett,[2] DL Hurst,[2] P Kok,[2] F Liu,[2] AJ Brash,[2] J O'Hara,[2] LMPP Martins,[2] CL Phillips,[2] R Coles,[2] C Bentham,[2] N Prtljaga,[2] M Makhonin, [2] IE Itskevich, [3] LR Wilson, [2] AM Fox,[2] J Heffernan,[1] MS Skolnick[2] edmund.clarke@sheffield.ac.uk

[1]EPSRC National Epitaxy Facility, University of Sheffield, Sheffield S1 3JD, UK; [2]Department of Physics and Astronomy, University of Sheffield, Sheffield, S3 7RH, UK; [3]School of Engineering and Computer Science, University of Hull, Hull HU6 7RX, UK

Single InAs/GaAs quantum dots (QDs) are promising as sources of on-demand non-classical light, due to their stable, sharp emission lines and the ability for on-chip integration into GaAs-based devices and quantum optical circuits. Recent advances in the optical control of QDs, such as resonance fluorescence (RF), has resulted in significant enhancements in the coherence of photons from QDs, vital for quantum information processing applications, but this places new demands on the optical properties of the QD, particularly its emission linewidth.

We present strategies for growth of high-quality InAs/GaAs QDs and their incorporation into device structures. Use of very low InAs growth rates or control over the InAs coverage provides QDs with uniform low density across a whole wafer, necessary to isolate single QD emission, while maintaining a narrow emission linewidth as low as 2 μeV (at 4 K). Wavelength control can be achieved by either using In-flush or InGaAs-capping techniques, giving QDs with a range of low temperature emission wavelengths from 900 to >1300 nm. Incorporation of low density QDs into freestanding, air-clad GaAs waveguide p-i-n devices allows the demonstration of elements for a quantum optical circuit. Antibunched emission is observed from a QD in the waveguide and cross-correlation measurements of the output ports of a directional coupler acting as a beam splitter indicates single photon beam splitting[1]. RF is also demonstrated from a QD embedded in a similar waveguide, with QD coherence enhanced by more than a factor of 4 compared to off-resonant excitation[2]. Electrical control of the charge state, wavelength tuning of the RF and a power-dependent waveguide transmission extinction of up to 40 ± 2% controlled by a single QD is observed[3]. Using the Purcell effect to shorten the radiative lifetime in a waveguide-coupled QD-photonic crystal cavity system (to 22.7 ps) provides near-lifetime-limited single photon emission with high indistinguishablility (93.9%) over a timescale of 2 ns (corresponding to 20 photon emission events at a driving rate of 10 GHz), which shows potential for high repetition rate single photon sources[4].

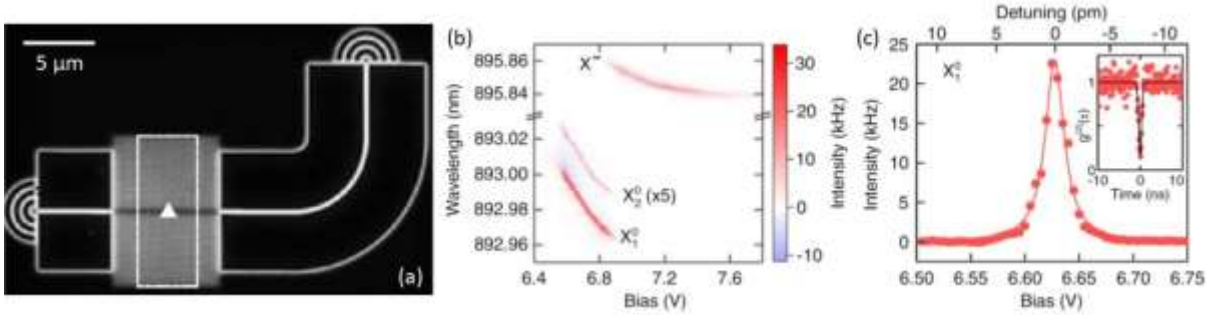

Figure: (a) Scanning electron microscope image of waveguide pin device, with triangle indicating position of QD within slow light section of a photonic crystal waveguide, (b) RF intensity as a function of wavelength and bias for neutral fine-structure-split states X_0 and charged state X^- of a single QD, (c) swept-bias RF spectrum from neutral exciton at fixed excitation wavelength, inset: second-order correlation function for photons scattered from X_0 spectral line. Figure from reference [3].

1. N. Prtljaga, R. J. Coles, J. O'Hara, B. Royall, E. Clarke, A. M . Fox, M. S. Skolnick, Appl. Phys. Lett. **104**, 231107 (2014)
2. M. N. Makhonin, J. E. Dixon, R. J. Coles, B. Royall, I. J. Luxmoore, E. Clarke, M. Hugues, M .S. Skolnick, A. M. Fox, Nano Lett. **14**, 6997 (2014)
3.D. Hallett, A. P. Foster, D. L. Hurst, B. Royall, P. Kok, E. Clarke, I. E. Itskevich, A. M. Fox, M. S. Skolnick, L. R. Wilson, Optica **5**, 644 (2018)
4. F. Liu, A. J. Brash, J. O'Hara, L. M. P. P. Martins, C. L. Phillips, R. J. Coles, B. Royall, E. Clarke, C. Bentham, N. Prtljaga, I. E. Itskevich, L. R. Wilson, M. S. Skolnick, A. M. Fox, Nature Nano. **13**, 835 (2018)

A19_29 Quantum dot-based optically pumped VCSELs with high-contrast periodic gratings

T Fördös[1,4,5], E Clarke[1], P Patil[1], RJ Airey[1], N Babazadeh[1], C Ovenden[2], M Adams[3], I Henning[3], and J Heffernan[1,2]

[1]EPSRC National Epitaxy Facility, University of Sheffield, Sheffield, S1 3JD, United Kingdom; [2]Department of Electronic and Electrical Engineering, University of Sheffield, Sheffield S1 3JD, United Kingdom; [3]School of Computer Science and Electronic Engineering, University of Essex, Colchester, CO4 3SQ, United Knigdom; [4]Nanotechnology Centre, VŠB - Technical University of Ostrava, 17. listopadu 15, 708 00 Ostrava - Poruba, Czech Republic; [5]IT4Innovation, VŠB - Technical University of Ostrava, 17. listopadu 15, 708 00 Ostrava - Poruba, Czech Republic.

Research on quantum dot-based vertical-cavity surface-emitting lasers (QD-VCSELs) for O-band telecoms window applications is a relatively new direction within optoelectronics. The use of QD gain materials in VCSELs provides additional advantages such as lower threshold, high gain, and longer spin life-time, which plays a crucial role in challenging spin-controlled lasers. We have previously demonstrated the first room temperature QD-based optically pumped VECSEL operating at 1305 nm, with a compact cavity using an HR-coated fiber as the top mirror and the bottom Distributed Bragg Reflector (DBR) consisting of 25 pairs of GaAs/AlAs with an active region consisting of 15 quantum dot-in-a-well (DWELL) InAs/InGaAs layers [1]. We discuss optimization of the active region in order to maximize the overall gain of the device by incorporating multiple QD layers while maintaining coincident emission of those layers.

For full cavity VCSELs comprising both bottom and top mirrors, there are advantages for device fabrication if the thickness of the top mirror can be reduced. One of possible solutions is to replace the semiconductor-based DBR, usually GaAs/Al(Ga)As pairs, with a dielectric-based DBR. We report the QD-VCSEL structure with a top DBR consisting of only 11 dielectric SiO2/Si3N4 pairs, grown by inductively-coupled plasma chemical vapour deposition (ICPCVD). By varying of growth parameters of SiNx, an increased refractive index contrast can be achieved, further reducing the number of DBR pairs required to reach high reflectivity. Spectroscopic ellipsometry has been applied to study dielectric SiO2/SiNx and to evaluate varying optical constants, which have been fitted in the transparent spectral range using the Cauchy dispersion relation, suggesting a greater than 50% reduction in the number of required DBR pairs is possible.

The most significant reduction of the resonator thickness can be achieved by the incorporation of a high-contrast 1D periodic grating [2] such as shown in inset of Fig. 1a. In such a structure, the in-plane waves cannot propagate in the in-plane direction due to a stop band arising from a large index contrast. The calculated reflectivity spectra for Si3N4 surrounded by air based on rigorous coupled-wave analysis (RCWA) for transverse-electric (TE-) polarization is shown in Fig. 1a. The area marked by black circle shows the high-reflectivity zone in the near-λ region, where the grating structure can be designed for QD-VCSEL mirror applications. Fig. 1b. shows the increased bandgap that can be achieved for a SiNx grating with $n = 2.84$.

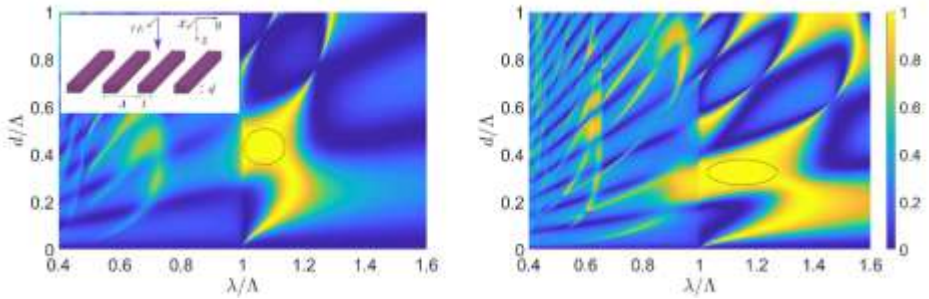

Figure 4: a) The calculated reflectivity spectra for Si_3N_4 ($\boldsymbol{n = 1.99}$) grating sorrounded by air with $\boldsymbol{\Lambda = 1.25\ \mu m}$ and $\boldsymbol{t = 0.5\Lambda}$. Inset: schematic of 1D periodic grating. Blue arrow shows the incident light with transversal electric (TE) polarization. b) The calculated reflectivity spectra for SiN_x grating with $\boldsymbol{n = 2.84}$.

[1] S. S. Alharthi, E. Clarke, I. D. Henning and M. J. Adams, "1305-nm Quantum Dot Vertical-External-Cavity Surface-Emitting Laser," *IEEE Photon. Technol. Lett.* **27**, 1489 (2015). [2] C. J. Chang-Hasnain and W. Yang, "High-contrast gratings for integrated optoelectronics," Adv. Opt. Photon. **4**, 379-440 (2012)

A19_15 O-band InAs/GaAs quantum dot laser monolithically integrated on exact (001) Si substrate

K Li[1]*, Z Liu[1], M Tang[1], M Liao[1], D Kim[1], H Deng[1], AM Sanchez[2], R Beanland[2], M Martin[3], T Baron[3], S Chen[1], J Wu[1], A Seeds[1] and H Liu[1] keshuang.li.17@ucl.ac.uk

[1]Department of Electronic and Electrical Engineering, University College London, London, WC1E 7JE, United Kingdom; [2]Department of Physics, University of Warwick, Coventry, CV4 7AL, United Kingdom; [3]Univ. Grenoble Alpes, CNRS, CEA-LETI, MINATEC, LTM, F-38054 Grenoble, France.

The concept of high-performance electrically pumped laser monolithically integrated on Si substrate have attracted enormous research interests as a promising approach of on-chip optical source for Si photonics. In this paper, an electrically pumped continuous-wave InAs/GaAs quantum dot (QD) laser with low threshold current density has been demonstrated on a complementary metal-oxide-semiconductor (CMOS) compatible Si exact (001) substrate by using III-As buffer layer. As shown in Fig. 1 (a), four repeats of $In_{0.18}Ga_{0.82}As$/GaAs strained-layer superlattices dislocation filter layers are well performed to annihilate threading dislocations with total buffer thickness of ~2µm. The active region of laser is consisted of five repeats of InAs/GaAs dot-in-well structure, realising a room temperature peak photoluminescence emission of ~1308 nm with a linewidth of ~32 meV. A comparison of room temperature PL results of InAs/GaAs QD on Si exact (001) and native GaAs substrates is shown in Fig. 1 (b), the inset image shows an AFM image of uncapped InAs/GaAs QD layer with about ~4×10^{10} cm^{-2} dot density. The laser samples are fabricated into 50µm×3mm broad-area laser devices. The characteristics of laser devices are all measured under continuous-wave. As shown in the inset image of Fig. 1 (c), The threshold current density (J_{th}) as low as ~160 A/cm^2 has been achieved at room temperature. A single facet output power of 48 mW is obtained at an injection current density of 500 A/cm^2 without any thermal rollover. The calculated slope efficiency and external differential quantum efficiency are achieved of ~0.095 W/A and 9.95 %, respectively. In addition, Fig. 1 (c) presents the light-current (LI) characteristics of InAs/GaAs QD laser on Si exact (001). The J_{th} increases with the rising of operation temperature and laser operation is observed up to 52 ºC. The characteristic temperature (T_0) obtained is ~60.8 K between 16 ºC to 36 ºC. These promising results suggest that O-band InAs/GaAs QD laser could have great potential in order to develop a high-performance monolithically integrated on-chip optical source for Si photonics.

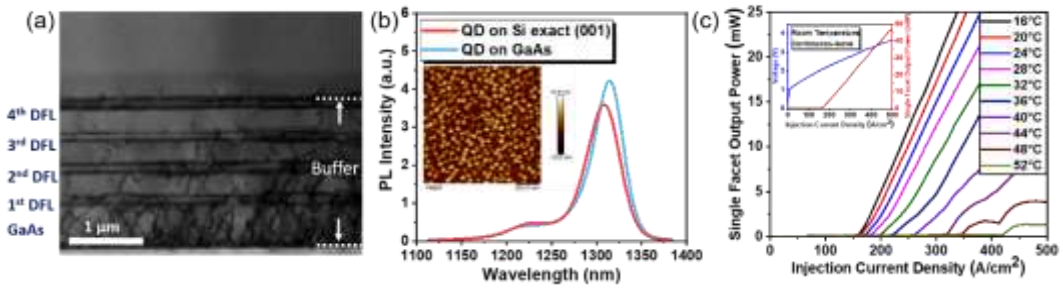

Fig. 1 (a) Cross-sectional TEM image for whole buffer; (b) A comparison of room temperature PL results, inset: an AFM image of uncapped InAs/GaAs QD layer; (c) LI characteristics of InAs/GaAs QD laser grown on Si exact (001) at various operation temperature, inset: LIV characteristic at room temperature.

Abstracts

Session 6: Integration Strategies & Approaches I

A19_47 Silicon and germanium mid-infrared platforms

J Soler Penadés[1], A Osman[1], A Sánchez-Postigo[2], Z Qu[1], Y Wu[1], CJ Stirling[1], DP Cheben[3], A Ortega-Moñux[2], JG Wangüemert-Pérez[2], M Nedeljkovic[1], GZ Mashanovich[1]
[1]Optoelectronics Research Centre, University of Southampton, Southampton, SO17 1BJ, UK; [2]Universidad de Málaga, ETSI Telecomunicación, Campus de Teatinos, 29071 Málaga, Spain; [3]National Research Council Canada, Building M-50, Ottawa, K1A 0R6 Canada

Silicon-on-insulator (SOI) as the most popular material platform in silicon photonics can be used up to 4 μm [1] due to large loss of the buried oxide layer at longer wavelengths [2]. Although a number of photonic devices and circuits have been reported in this platform with performances matching those in the much more established near-IR silicon photonics [e.g. 3], there is a large wavelength range in the mid-IR that contains strong absorption fingerprints of many molecules and substances where the SOI cannot be used. Therefore, alternative material platforms are needed.
One of them is suspended Si. Suspended silicon devices can be fabricated by removing the buried oxide layer (BOX). This can be achieved by either forming rib waveguides, etching holes on both sides of the rib, and removing the BOX with HF. Alternatively, suspended Si devices can be fabricated by performing only one dry etch step to form a subwavelength grating lateral cladding and subsequently removing the BOX with HF [4]. The latter approach is simpler, more robust and can result in more sensitive devices for sensing applications than the former. We have demonstrated a library of Si suspended devices at 3.8 μm [5] and 7.7 μm [6] achieving losses in the range of 0.8 dB/cm and 3.1 dB/cm, respectively.
Similar approach can be applied to germanium. Suspended rib Ge waveguides were fabricated by first depositing Ge on thin SOI wafers using RPCVD (reduced pressure chemical vapour deposition) and subsequently dry etching holes in Ge and wet etching SiO2 and Si. We have recently demonstrated suspended Ge waveguides operating at 7.7 μm with a propagation loss of 2.65 dB/cm [7]
The germanium-on-silicon platform has also been investigated and we have fabricated and characterised devices up to 8.5 μm [8-12]. A 3 micrometer thick Ge on Si was used to demonstrate waveguides, modulators, couplers, filters and multiplexers [8-12].

REFERENCES

[1] M. Nedeljkovic et al., Optical Materials Express 3, 1205 (2013).
[2] E. D. Palik, Handbook of Optical Constants of Solids, Vol. 1, London: Academic, London, 1985.
[3] M. Nedeljkovic et al., IEEE Photonics Technology Letters 28, 528 (2016).
[4] J. Soler Penades et al., Optics Letters 39, 5661 (2014).
[5] J. Soler Penades et al., Optics Express 24, 22908 (2016).
[6] J. Soler Penadés et al., Optics Letters 43, 795 (2018).
[7] A. Osman et al., Optics Letters 43, 5997 (2018).
[8] M. Nedeljkovic et al., IEEE Photonics Technology Letters 27, 1040 (2015).
[9] B. Troia et al., Optics Letters 41, 610 (2016).
[10] C. Alonso-Ramos et al., Optics Letters 41, 4324 (2016).
[11] G. Z. Mashanovich et al., Journal of Lightwave Technology 35, 624 (2017).
[12] M. Nedeljkovic et al., Optics Express 25, 27431 (2017).

A19_01 Integrated Polarization Handling Devices

M Ghulam Saber[1,*] ,L Xu[1], RH Sagor[2], DV Plant[1], and N Abadía[1,3,4,]

[1]Department of Electrical and Computer Engineering, McGill University, Montreal, Quebec, H3A 0E9, Canada; [2]Department of Electrical and Electronic Engineering, Islamic University of Technology, Gazipur 1704, Bangladesh; [3]School of Physics and Astronomy, Cardiff University, Queen's Building, The Parade, Cardiff, CF24 3AA, United Kingdom; [4]Institute for Compound Semiconductors, Cardiff University, Queen's Building, The Parade, Cardiff, CF24 3AA, United Kingdom

The demand for integrated photonic solutions for applications such as optical communications is increasing due to the advantages of integration in terms of size, cost and energy consumption compared to the discrete architectures [1]. Over the years, integrated photonic circuits have been built in different material platforms among which the indium phosphide (InP) and the silicon-on-insulator (SOI) technologies are the most popular [2]. Both platforms try to improve actual optical communication systems. Controlling the polarization within the integrated circuit will: (1) avoid polarization sensitivity which leads to unacceptable dispersion in many applications, (2) increase the capacity of optical links like in the optical coherent receiver

Consequently, polarization handling devices are required for many applications. To solve the issues (1) and (2) already mentioned, we have developed several solutions in InP and SOI technologies using different approaches. *E.g.* in Fig. 1(a) we demonstrated a InP polarization beam splitter (PBS) [3] which is tolerant to fabrication imperfections. On the other hand, we did several devices on SOI technology: we demonstrated polarization beam splitters using sub-wavelength structures [4] and photonic crystals [5]. They are represented in Fig. 1(b-c).

To further reduce the footprint of the devices, we developed CMOS-compatible integrated plasmonic polarizers that are of particular interest in dealing with the polarization dispersion in different parts of the chip. One example is the one based on plasmonic gratings [6] and highly doped silicon [7] represented in Fig. (d) and (e) respectively.

We will present the current state-of-the-art of integrated polarization beam splitters and polarizers, and present our current developments and latest results on this field.

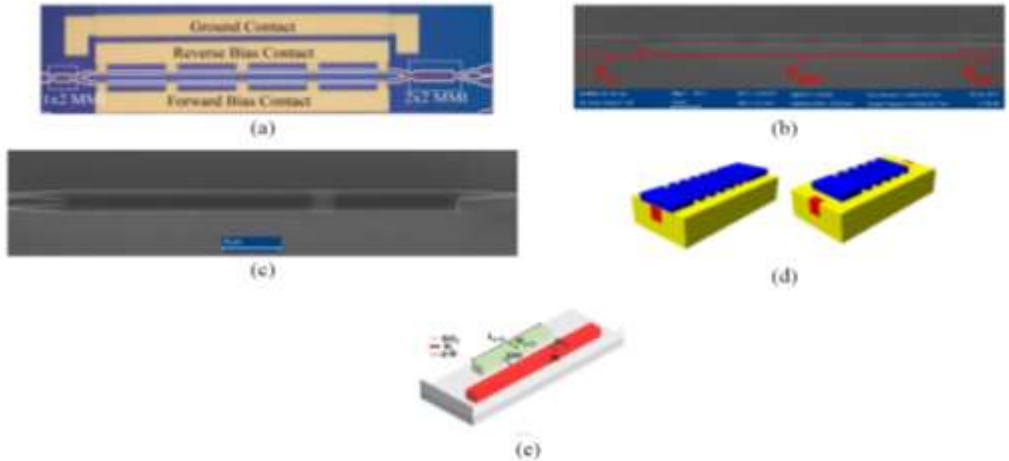

Fig. 1: (a) MZI-based InP PBS, (b) Sub-wavelength PBS, (c) Photonic crystal based PBS, (d) polarizer based on plasmonic grating and (e) polarizer based on highly doped silicon.

References [1] Thomson, D., Zilkie, A., Bowers, J.E., Komljenovic, T., Reed, G.T., et al.: 'Roadmap on silicon photonics', Journal of Optics, 2016, 18, (7), pp. 073003 [2] Liang, D., Bowers, J.: 'Photonic integration: Si or InP substrates?', Electronics Letters, 2009, 45, (12), pp. 578–581 [3] Abadía, N., Dai, X., Lu, Q., Guo, W.H., Patel, D., Plant, D.V., et al.: 'Highly fabrication tolerant inp based polarization beam splitter based on pin structure', Optics Express, 2017, 25, (9), pp. 10070–10077 [4] Xu, L., Wang, Y., Kumar, A., Patel, D., El.Fiky, E., Xing, Z., et al.: 'Polarization beam splitter based on MMI coupler with SWG birefringence engineering on SOI', IEEE Photonics Technology Letters, 2018, 30, (4), pp. 403–406 [5] Xu, L.,Wang, Y., El.Fiky, E., Mao, D., Kumar, A., Xing, Z., et al.: 'Compact broadband polarization beam splitter based on multimode interference coupler with internal photonic crystal for the soi platform', Journal of Lightwave Technology, 2019, [6] Abadía, N., Saber, M.G., Bello, F., Samani, A., El.Fiky, E.,Wang, Y., et al.: 'CMOS compatible multi-band plasmonic TE-pass polarizer', Optics Express, 2018, 26,(23), pp. 30292–30304 [7] Saber, M.G., Abadía, N., Plant, D.V.: 'CMOS compatible all-silicon TM pass polarizer based on highly doped silicon waveguide', Optics Express, 2018, 26, (16), pp. 20878–20887

A19_04 Integration of Sub-wavelength Structures with Silicon Photonic Devices

Y D'Mello[1], S Bernal[1], DV Plant[1], and N Abadía[2,3] Yannick.DMello@mail.McGill.ca

[1]Department of Electrical and Computer Engineering, McGill University, Montreal, Quebec, H3A 0E9, Canada; [2]School of Physics and Astronomy, Cardiff University, Queen's Building, The Parade, Cardiff, CF24 3AA, United Kingdom; [3]Institute for Compound Semiconductors, Cardiff University, Queen's Building, The Parade, Cardiff, CF24 3AA, United Kingdom.

Micro-opto-electronic integrated circuits are commonly developed using the Silicon-on-Insulator (SOI) platform. Silicon Photonics (SiP) offers a competitive advantage over other platforms by leveraging mature fabrication techniques from Complementary Metal-Oxide-Semiconductor (CMOS) technology in the micro-electronics industry [1]. The advanced lithography enables the production of compact, low cost, and mass manufacturable on-chip systems that are crucial to modern sensing, communications, and signal processing applications. The resulting demand for SiP devices has spurred developments in fabricating feature sizes at the nanometer scale. This lithographic resolution has attracted research into the implementation of photonic band engineered devices that avail of the strong light confinement offered by a high refractive index difference in the SOI platform [2]. Metamaterials such as sub-wavelength gratings (SWG) and photonic crystals (PC) have been integrated into waveguides [3], surface [4] and edge [5] fiber-chip couplers, directional couplers [6], and multimode interferometers (MMI) for polarization splitting [7] or intensity distribution [8].

Through a combination of photonic band structure analysis, simulations, and experimental measurements, we demonstrate a generalized conversion protocol for the integration of periodic structures in conventional device geometries by drawing on our recent developments [4][6][7][8] regarding the utilization of metamaterials in SiP designs. The analysis leads to key observations including: (i) wavelength and polarization filtering via photonic band engineering, (ii) the reduction in effective index caused by incorporating sub-wavelength anisotropy leading to shorter beat lengths in MMI-based devices, and (iii) the relative spectral insensitivity of the effective index that allows for an extremely broadband performance typically larger than 100 nm.

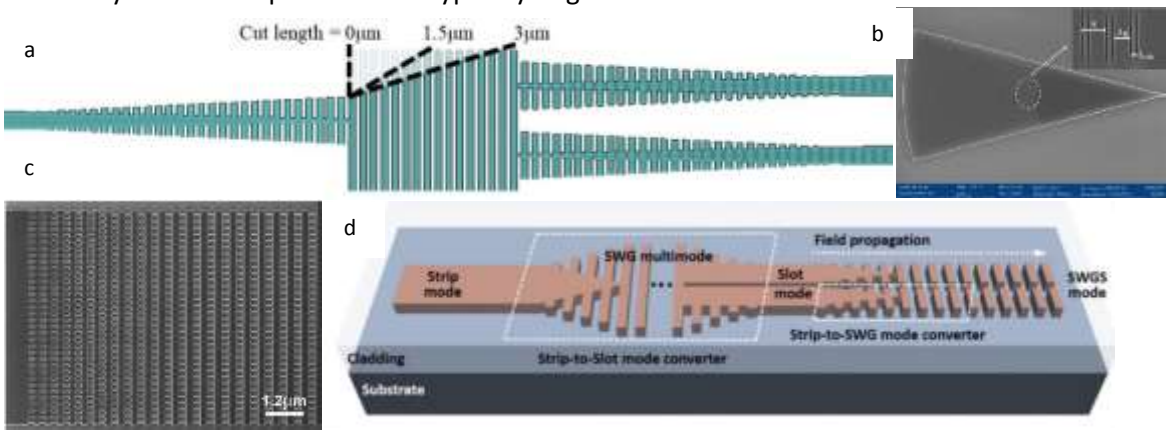

Figure 1: Examples of SWG-based SiP devices: a) 1x2 MMI with variable splitting ratios [8], b) surface grating coupler [4], c) apodized grating coupler [1], d) SWG waveguide design [3].

References

[1] D. Thomson *et al.*, "Roadmap on silicon photonics." Journal of Optics 18, no. 7: 073003 (2016). [2] R. Halir *et al.*, "Waveguide sub-wavelength structures: a review of principles and applications", Laser & Photonics Reviews, 9: 25-49 (2015).[3] Z. Ruan *et* al., "Subwavelength grating slot (SWGS) waveguide on silicon platform," Opt. Express 25, 18250-18264 (2017). [4] Y. Wang *et al.*, "Compact single-etched sub-wavelength grating couplers for O-band application," Opt. Express 25, 30582-30590 (2017). [5] M. Papes *et al.*, "Fiber-chip edge coupler with large mode size for silicon photonic wire waveguides," Opt. Express 24, 5026-5038 (2016). [6] Y. Wang *et al.*, "Compact broadband directional couplers using subwavelength gratings." IEEE Photonics Journal 8.3: 1-8 (2016). [7] L. Xu *et al.*, "Polarization Beam Splitter Based on MMI Coupler With SWG Birefringence Engineering on SOI," IEEE Photonics Technology Letters, vol. 30, no. 4, pp. 403-406 (2018). [8] E. El-Fiky *et al.*, "Ultra-Broadband and Compact Asymmetrical Beam Splitter Enabled by Angled Sub-Wavelength Grating MMI," in Conference on Lasers and Electro-Optics, OSA Technical Digest (online). Optical Society of America, 2018, paper STh4A.7.

A19_18 Raman Scattering Effect on a QKD and High Speed Classical Data Hybrid Link

H Qin[1], A Wonfor[1], S Yang[1], RV Penty[1], IH White[1]
[1]*Electrical Engineering Dept., University of Cambridge, 9 JJ Thomson Ave, Cambridge CB3 0FA*

Quantum Key Distribution (QKD) is currently receiving much attention as it provides a secure source of encryption keys [1]. It is possible for single photon transmission in QKD to co-exist with and encode classical wavelength division multiplexed (WDM) data with appropriate system design. This paper describes both laboratory experiments and field trials of such high-speed hybrid QKD links.

There are a number of factors which can limit the secure key rate in hybrid QKD – WDM systems by introducing unwanted noise photons to the detected signal, such as leakage of the classical channels through the finite isolation wavelength filters isolating the quantum channel, which can be mitigated by additional filtering, but at the expense of increased optical loss in the quantum channel. Other processes contributing to noise on the quantum channel are four wave mixing and more importantly spontaneous Raman scattering from the classical to the quantum wavelength; neither of which can be removed by spectral filtering of the quantum channel as the resultant photons have the same energy as those in the quantum channel.

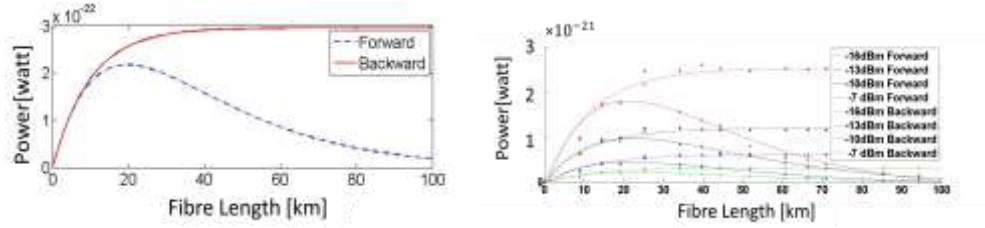

Figure 1. Raman photons (a) theoretical plot and (b) experimental plot

In order to assess the magnitude of this effect, a laboratory scale experiment has been performed comprising multiple classical power levels exploring the corresponding effect on the quantum channel. Figure 1 shows both the experimental and theoretical plots of Raman noise power versus fibre length, and indicates that the forward Raman power starts to decline when the fibre link length is longer than 25km and the backward Raman saturates at lengths longer than 30km.

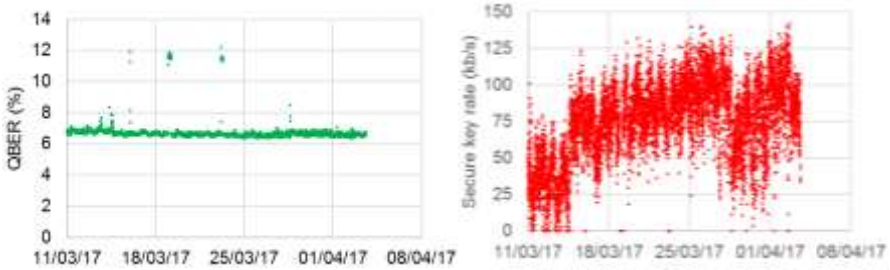

Figure 2. Quantum bit error rate and secure key rate for the loop back field trial coexisting with commercial 100 Gbps system

In order to confirm the significance of Raman scattering, a field trial was also performed using a commercial 100Gb/s and 25GBd polarisation multiplexed QPSK classical data source from ADVA together with a QKD system from Toshiba [2]. A mean QBER of 6.6% with standard deviation of 0.5% and a mean secure key rate of 80.2kb/s with a standard deviation of 28.4kb/s have been achieved for a long-term field trial shown in Figure 2.

In conclusion, we see that Raman scattering can be the dominant source of impairments to secure key rate in long distance hybrid QKD – WDM systems. This can be mitigated by optimisation of the launch power of the classical optical channels, subject to maintaining adequate optical signal to noise ratio. Additional results of classical data transmission secured by QKD in the same fibre in both laboratory experiments and long distance field trials will be presented at the conference.

[1] C. H. Bennett and G. Brassard, in Proceedings of the IEEE International Conference on Computers, Systems and Signal Processing, Bangalore, India, 1984 (IEEE, New York, 1984), pp. 175–179; IBM Tech. Discl. Bull. 28, 3153–3163 (1985) [2] K. A. Patel, J. F. Dynes, I. Choi, A. W. Sharpe, A. R. Dixon, Z. L. Yuan, R. V. Penty, and A. J. Shields, Phys. Rev. X 2, 041010 –20 November 2012

Abstracts

Session 7: Integration Strategies & Approaches II

A19_40 Generating optical frequency combs via nano-scale all-optical modulators

H Francis, S Chen, KJ Che, M Hopkinson and CY Jin.
Department of Electrical and Electronic Engineering, University of Sheffield

Integrated microwave photonics (MWP) is a relevant and timely research field in semiconductor optoelec- tronics. It is bridging the gap between classical analogue electronics and contemporary photonic integrated circuits (PIC)[1]. In any MWP system the need for an integrated multi-wavelength source is paramount, this can be achieved in the form of an optical frequency comb (OFC). In the work presented here, we propose a novel scheme that combines traditional OFC generation with state of the art nano-fabrication. By using photonic crystal (PhC) all-optical intensity and phase modulators, we aim to produce an OFC using small scale devices that have the potential for on-chip integration. Photonic crystal devices are a strong candidate for the universal platform of PICs given the high density integration potential.

The generation of OFCs can be achieved using a variety of different techniques. Most prevalent in today's research is to use high-Q micro-toroidal cavities. Nondegenerate four wave mixing (FWM) is utilised within the micro-resonator to produce a broad range of side bands that are equidistant apart [2]. The free spectral range between the comb lines is directly dependant on the size of the cavity, which can range from hundreds of micrometres to millimetres in size. In the scheme proposed here, outlined in Fig. 1, a di_erent approach is taken and tested by theoretical description of photonic crystal modulators based on the coupled mode theory; this derives itself from more conventional electro-optic modulators [3]. In this method of OFC generation, light from a continuous wave laser is shaped to generate a at topped pulse using an intensity modulator. This is followed by a phase modulator which can compress the signal in the time domain and produce a mirrored image of the time domain signal in the frequency domain. By replacing optoelectronic intensity and phase modulators with all-optical PhC modulators [4], we demonstrate it is possible to generate spectrally at OFCs on a scale smaller than previous approaches.

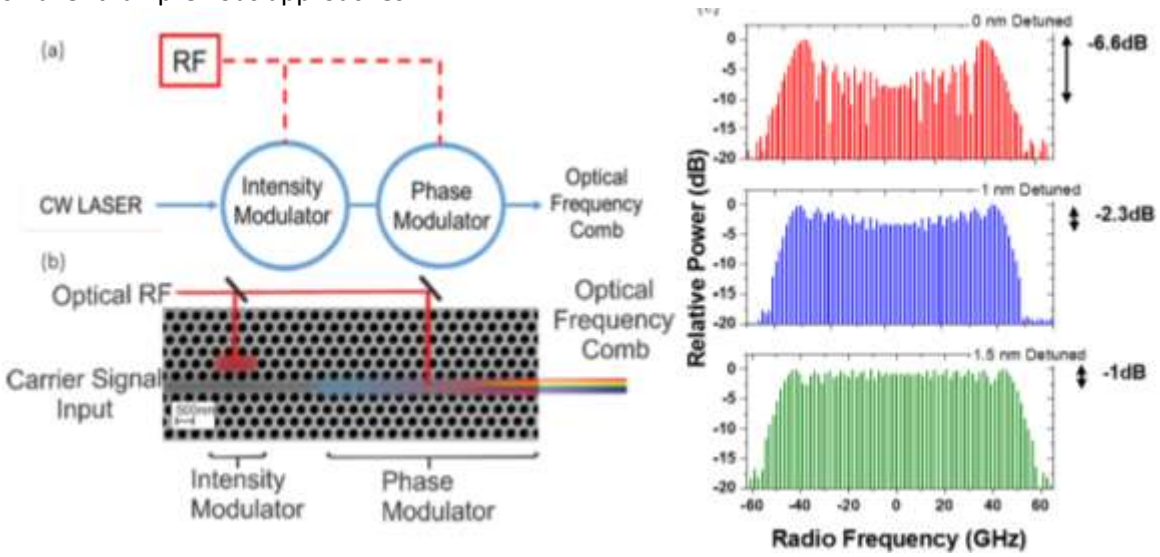

Figure 1: (a) Schematic of OFC generation using cascaded electro-optic modulators (b) An SEM image with the proposed scheme superimposed on top, showing the implementation of (a) using PhC structures. RF-Radio Frequency(c) The generated OFCs from the output of the simulated devices with cavity resonance detuning's

References

[1] D. Marpaung, J. Yao, and J. Capmany, \Integrated microwave photonics," Nature Photonics, vol. 13, no. February, 2019.[2] J. Wu, X. Xu, T. G. Nguyen, S. T. Chu, B. E. Little, R. Morandotti, A. Mitchell, and D. J. Moss, \RF Photonics: An Optical Microcombs' Perspective," IEEE Journal of Selected Topics in Quantum Electronics, vol. 24, no. 4, 2018.[3] V. Torres-Company, J. Lancis, and P. Andres, \Lossless equalization of frequency combs," Optics Letters, vol. 33, no. 16, pp. 1822{1824, 2008. [4] C. Y. Jin and O. Wada, \Photonic switching devices based on semiconductor nano-structures," Journal of Physics D: Applied Physics, vol. 47, no. 13, 2014.

A19_53 Particle Manipulation and Control for Integrated Optoelectronic Microfluidics

D Giliyana*, E Le Boulbar, S Gillgrass and PM Smowton
School of Physics and Astronomy, Cardiff University, The Parade, Cardiff, CF24 3AA

The development of integrated microelectronic microfluidic devices is receiving substantial interest owing to these and other applications in chemistry, medicine and particle science. The isolation and regular flow of microparticles within a single stream are required to perform detection, sorting and manipulation of microparticles or cells according to their size and / or shape for a multi-functional microfluidic platform. In pump driven microfluidics several techniques to physically manipulate microparticles exist such as dielectrophoresis (DEP), which is the induced movement of dielectrically polarised particles subjected to a non-uniform electric field, has been widely used to physically manipulate microparticles. In DEP the particle can be attracted toward or away from the zone of high strength electric field. [1]

In this work a combination of AC-DEP force and laminar flow in a 3D capillary driven of 50 µm wide and 27 µm height is used to position microparticles into the centre of a microchannel within a flowing fluid stream. The particle focusing within a steady velocity over the experiment duration is achieved by designing and fabricating four-triangular shaped microelectrodes at the top and bottom surface of the microchannel (Figure 1). The results when operating the microelectrodes with appropriate voltage (v) and frequency (f), and through observations of frames from a high speed digital camera for 6 µm polystyrene beads and with a code written in MATLAB, are shown in figure 2. In the absence of applied voltage, the microparticles were randomly distributed within the microchannel width while all of the recorded microparticles were pushed to the centre of the channel with the applied voltage (Figure 2a). We observed the distribution velocities of the beads were also narrower with applied field relative to without any applied field (Figure 2b). This example shows one way the DEP microfluidic platform can be integrated on active semiconductor material and could be utilized to support the body of the work in optofluidic diagnosis.

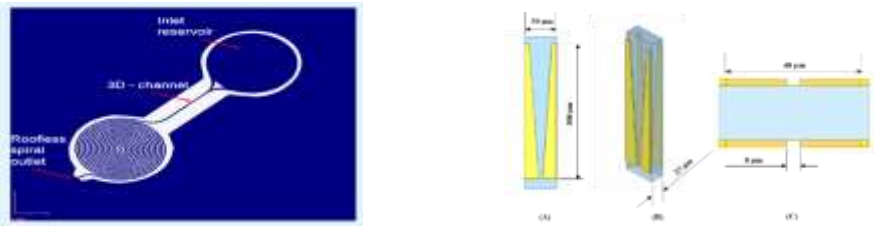

Figure 1) A Schematic design concept of capillary fill and DEP (A) top-view, (B) side-view and (C) cross-sectional view for particle focusing.

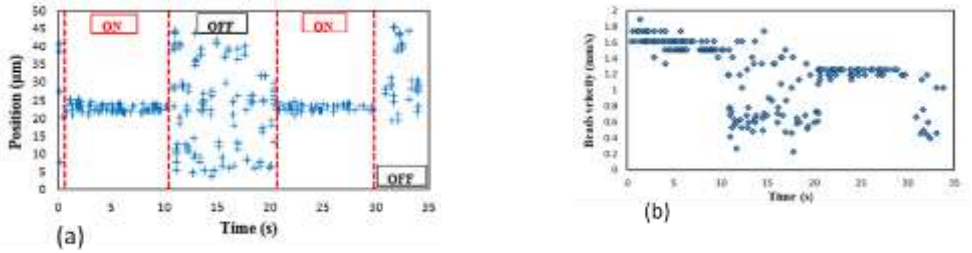

Figure 2) 6 µm PS beads (a) position distribution and (b) velocity measured while toggling the applied AC potential of 30 V_{p-p} at a frequency of 10 MHz.

[1] D. Holmes, H. Morgan, and N. G. Green, "High throughput particle analysis: Combining dielectrophoretic particle focussing with confocal optical detection," Biosens. Bioelectron., vol. 21, no. 8, pp. 1621–1630, 2006.

A19_43 Optically Controlled Millimetre-wave Switches with Coplanar Stepped-Impedance Lines

Y Zhang, AW Pang and MJ Cryan yz15243@bristol.ac.uk, m. cryan@bristol.ac.uk
Department of Electrical and Electronic Engineering, University of Bristol, U.K

Optically controlled attenuation or switching of microwave and millimetre-wave signals has attracted increasing attention partly due to the high linearity and high isolation between signal and control circuitry [1]. Modelling of a photoconductive coplanar waveguide (CPW) millimetre-wave switch controlled by a single infrared light emitting diode (LED) is presented. It will be implemented on a transparent fused silica substrate using optical lithography which is similar to our previous work [2]. However, in this paper we adopt an alternating stepped-impedance line structure [3] instead of a conventional straight CPW transmission line to increase the gap length under illumination for higher signal absorption and attenuation. The transition from a straight CPW line switch to our proposed 13 section stepped-impedance CPW line switch is shown in Fig. 1.

A brass block is placed underneath the substrate to hold the device and connectors. Moreover, a slot is created in the brass block to make the CPW transmission line ungrounded which is important to suppress unwanted spurious modes and to hold the LED which generates plasmas in the silicon superstrate placed upon the substrate. Fig. 2 compares the simulated transmission of the proposed switch with the straight one and fewer stepped-impedance sections cases in different LED states using CST modelling. The plasma conductivity is calculated as 88.7 S/m [4] to correspond with the nominal radiant power of the LED (1.45 W). It can be seen that the illuminated isolation keeps increasing when the number of stepped-impedance line sections increases up to 35 GHz while the dark state insertion loss has not changed too much as the number of sections goes up. This indicates the CPW stepped-impedance line structure can be attractive in photoconductive millimetre-wave switch designs which have many applications in modern microwave and millimetre-wave systems (e.g. switched antenna beamforming systems).

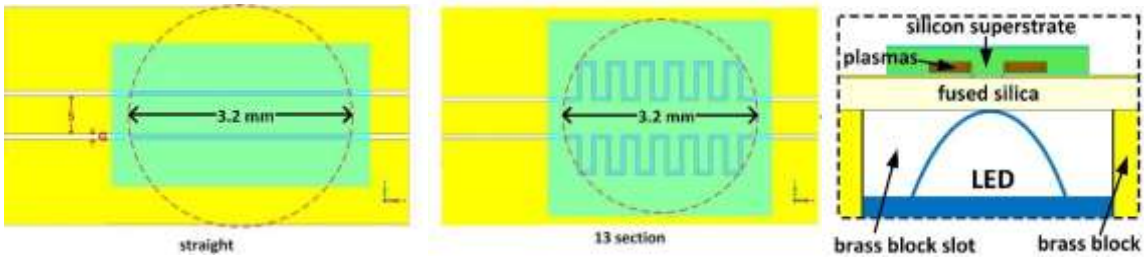

(a) (b) (c)

Figure 1: Transition from (a) straight CPW line switch to (b) proposed 13 section stepped-impedance CPW line switch. S = 500 um, G = 70 um. dashed circle: illuminated area; (c) sideview of the device showing LED position taken from the dashed line in (b).

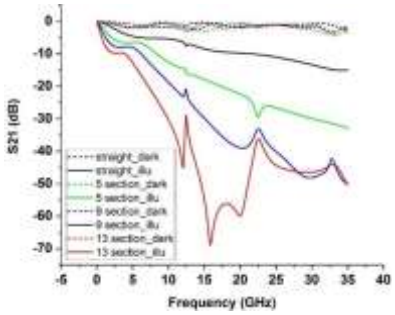

Figure 2: Simulated transmission of photoconductive switches with different numbers of stepped-impedance line

Abstracts

Session 8: Materials Development and Devices I

A19_50 Monolithic Growth of 1.5 µm InAs Quantum Dots Lasers on (001) Si and Material Studies

Z Li[1], S Shutts[1], CP Allford[1], B Shi[2], W Luo[2], KM Lau[2] and PM Smowton[1] LiZ74@cardiff.ac.uk

[1]EPSRC Future Compound Semiconductor Manufacturing Hub, School of Physics and Astronomy, Cardiff University, Queen's Building, The Parade, Cardiff, UK, CF24 3AA; [2]Department of Electronic and Computer Engineering, Hong Kong University of Science and Technology,Clear Water Bay, Kowloon, Hong Kong

III-V Quantum dot (QD) laser structures capable of providing broad optical gain bandwidth, with low sensitivity to material defects and operation temperature, is believed to be a promising candidate to achieve monolithic growth on a silicon platform. Although direct growth on silicon has been successfully demonstrated for 1.3 µm emitting InAs QDs incorporated with GaAs-based alloys, [1] the growth of InAs QDs with InP-based materials, thus extending lasing wavelength to 1.55 µm range, still faces big challenges. Only recently, electrically pumped broad-area 1.55 µm QDs lasers on silicon have been reported [2]. Using the same material published in [2], we fabricated both broad-area stripe lasers and multiple segmented contact devices to extend the study on its optoelectronic and material properties.

Figure 1 (A) gives the epi-structure of 1.55 µm InAs QDs on nano-patterned (001) silicon substrates. The active region was formed by three layers of InAs QDs growth in InGaAs quantum-wells covered with InAlGaAs quantum-barrier layers, and sandwiched by InP cladding layers. Due to the large lattice mismatch between silicon and InP, surface defects can be observed after growth in optical microscope and became even more obvious under the differential intensity contrast (DIC) mode, as shown in Figure 1 (B). These materials were then fabricated into co-planar electrode broad-area devices with 100 µm wide mesas and 50 µm wide p-contact on top. For segmented contact devices, each contact was 292 µm in length with 8 µm gap. Device schematics are shown in Figure 1 (C). The same laser structure grown on an InP substrate was also processed into both device types for comparison. All laser measurements were driven by a pulsed source (5 kHz duty cycle and 1 µs pulse width) at 20°C. Figure 2 gives the Light-Current (L-I) curves of lasers on silicon and InP, with the inserted plots showing the lasing spectrum measured just above threshold, where the current density was 1.63 kA/cm^2 and 1.72 kA/cm^2 for lasers on silicon and on InP respectively, the corresponding cavity length was 2140 µm and 1860 µm. To have a deeper understanding of 1.55 µm QD material, we will present our optical gain and absorption measurement results using multiple segmented contact device by analysing amplified spontaneous emissions (ASE).

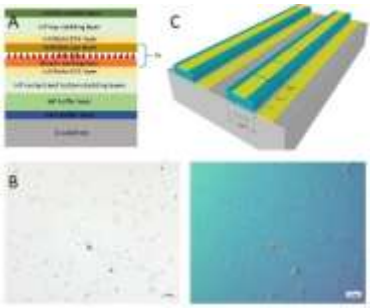

Figure 1, (A) Diagram of 1.55 µm InAs QD laser structure grown on silicon, (B) Images of material's surface captured by normal optical microscope (left) and under differential intensity contract mode (right), (C) Schematic of broad-area stripe laser and multiple segmented contact devices fabricated for the experiments.

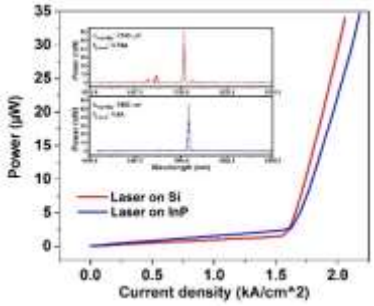

Figure 2, L-I curves of 1.55 µm QDs laser growth on silicon (red) and InP (blue), inserted: the corresponding lasing spectrum measured at ~1.74A pulsed current for silicon and at ~1.6 A pulsed current for InP sample.

[1] S Chen, et al., Electrically pumped continuous-wave III–V quantum dot lasers on silicon, Nature Photonics, 10, 307–311 (2016) [2] Si Zhu, et al., 1.5 lm quantum-dot diode lasers directly grown on CMOS-standard (001) silicon, Applied Physics Letters, 113, 221103 (2018)

A19_05 Sub-mm(>100μm) thick diamond layer on aluminium nitride for thermal management applications.

S Mandal[1]*, JA Cuenca[1], H Bland[1], C Yuan[2], F Massabuau[3], JW Pomeroy[2], D Wallis[3,4], R Oliver[3], M Kuball[2], OA Williams[1] Mandals2@cardiff.ac.uk

[1]School of Physics and Astronomy, Cardiff University, Cardiff, UK, [2]Center for Device Thermography and Reliability, Bristol University, Bristol, UK, [3]Department of Materials Science & Metallurgy, University of Cambridge, Cambridge, UK, [4]School of Engineering, Cardiff University, Cardiff, UK

Inefficient heat extraction in high power and high frequency devices is a major obstacle towards full utilisation of materials like GaN. The current technique of using SiC substrate has allowed good device performances, but it still cannot harness the full potential of high power materials. Replacing SiC(k_{SiC} ~ 360 – 490 W/m K) with diamond($k_{Diamond}$ ~ 2100 W/m K) is a very good option. For diamond to be used for thermal management it is important that the diamond layer is at least 50-100 microns thick[1]. While the growth of thin diamond layer on GaN is possible[2], growing a 100 micron thick layer is non-trivial. This is due to absence of any covalent bond between diamond and the GaN layer. Hence, the growth of a thick diamond layer on GaN can only be achieved by a suitable intermediate layer. In the literature there are studies where SiN_x layers have been used but they have shown high thermal barrier resistance. Alternatively, AlN can be used for such thick diamond growth. AlN is also the seed layer for growth of GaN on silicon. As a result no extra seed layer needs to be deposited after flipping the GaN film onto a suitable carrier.

In this work we demonstrate the growth of >100 micron thick diamond layer on AlN. We have measured the zeta potential of the AlN surface. The zeta potential was found to be negative but still we found that both H-terminated (positively charged) and O-terminated (negatively charged) seeds had resulted in a good diamond layer. For growth of diamond with O-terminated seeds the surface was pre-treated with a H_2/N_2 gas mix plasma. X-ray photo luminescence spectroscopy on the treated substrates revealed an increase in oxygen content on the surface after plasma treatment. This could be due to removal of surface nitrogen from the substrates and oxygenation of the aluminium bonds on subsequent exposure to air and seed solution. Cross-sectional studies of the films showed larger grains at the interface with a small number of voids in the films grown with O-terminated seeds. The voids are likely to relax the stress in the film caused due to unmatched thermal expansion coefficient of AlN and diamond. The growth of diamond on AlN seeded with H-terminated seeds resulted in good quality films as expected. Thermal barrier resistance between the diamond and AlN layer was also studied and low thermal barrier resistance was confirmed for films grown with O-terminated seeds. The study has clearly shown that even though H-terminated seeds are needed for high seed density on AlN surface, O-termiated seeds can be used to grow thick diamond films with large grains at the diamond-AlN interface.

References

[1] Y. Zhou, R. Ramaneti, J. Anaya, S. Korneychuk, J. Derluyn, H. Sun, J. Pomeroy, J. Verbeeck, K. Haenen, and M. Kuball, Appl. Phys. Lett. **111**, (2017).

[2] S. Mandal, E.L.H. Thomas, C. Middleton, L. Gines, J.T. Griffiths, M.J. Kappers, R.A. Oliver, D.J. Wallis, L.E. Goff, S.A. Lynch, M. Kuball, and O.A. Williams, ACS Omega **2**, 7275 (2017).

A19_26 Angled Cage Etching for Integrated Photonics in GaN

GP Gough[1,2], DM Beggs[2], RA Taylor[3], B Humphreys[4], AD Sobiesierski[5], S Shabbir[5], S Thomas[5], K Sun[5], AJ Bennett[5,6]

[1]Quantum Engineering Centre for Doctoral Training, Nanoscience and Quantum Information (NSQI) Building,University of Bristol, Tyndall Avenue, Bristol,BS8 1FD; *[2] School of Physics and Astronomy, Cardiff University, Queen's Buildings, Cardiff, CF24 3AA, UK*; *[3] Department of Physics, University of Oxford, Clarendon Laboratory, Parks Road, Oxford, OX1 3PU, UK*; *[4] Seren Photonics, UK Technology Centre, Pencoed Technology Park, Bridgend, CF35 5HZ, UK*; *[5] Institute for Compound Semiconductors, Cardiff University, Queen's Buildings, Cardiff, CF24 3AA, UK; [6] School of Engineering, Cardiff University, Queen's Buildings, Cardiff, CF24 3AA, UK*

We have developed a single step angled etching technique using a Faraday cage to create free-standing gallium nitride photonic devices. We will present results from our first cantilevers and waveguides.

Silicon has become the default material for integrated photonics due to its excellent passive optical properties and investments in fabrication. However, it is limited by its indirect band-gap, lack of $\chi^{(2)}$ Pockel's electro-optic effect and two photon absorption at 1550nm. Compound semiconductors could be an active alternative to silicon, ideally with a direct band-gap, wide band-gap over 1.6 eV to avoid two photon absorption at 1550nm, and a large Pockel's electro-optic effect while maintaining the advantages of silicon (large refractive index for high contrast, high confinement waveguides and easy and scalable fabrication).

Gallium nitride (GaN) has a wide direct band-gap of 3.4 eV and refractive index of 2.3 at 1550 nm, but fabrication of photonic integrated circuits is not as mature as silicon e.g. high-index contrast of silicon-on-insulator or undercutting of silicon devices. GaN is usually processed by reactive ion etching (RIE) or inductively couple plasma (ICP) etching, producing vertical sidewalls limiting the number of device geometries. For example, GaN photonic devices are usually created in multi-step etch processes [1].

The aim is to eliminate these additional processing steps by the angled etching of the substrate to undercut waveguides and devices. An angled Faraday cage over the sample during ICP etching directs the ions along field lines perpendicular to the cage and towards the substrate at a steep angle (see Fig. 1). The angled etching can create high contrast waveguides without the need for additional undercutting steps, which are difficult to achieve in GaN. This angled etching is similar to that pioneered in diamond [2]; however, we aim to create our waveguides in a single etch step. Other angled etching schemes are found in ref. [3,4].

Optical eigenmodes of equilateral triangular cross-section waveguides with side length *w* and refractive index *n* = 2.30, are calculated (inset of fig. 1(b)). Fig 1(b) shows the effective index of the waveguide mode as a function of the triangle size *w*. A single TE (TM) polarization mode exists for widths between *w* = 500 – 850 nm (*w* = 480 – 710 nm). The modes are highly confined to the waveguide core (Figure 1(c,d)). technology will find applications in nanolasers, active integrated photonic devices and nitride-based single photon sources.

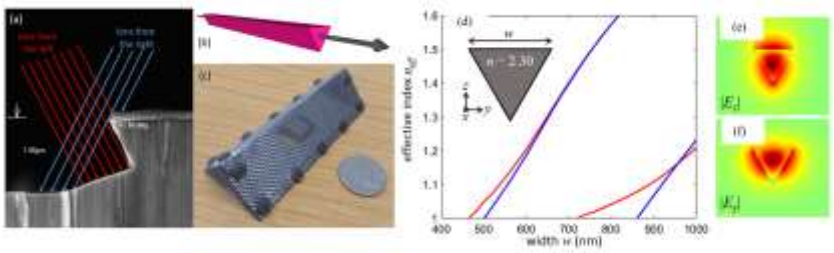

Fig. 1. Illustration of the angled etching. (a) A scanning electron micrograph of a cleaved edge of a GaN waveguide sample etched in the cage. The schematic shows how ions directed at steep angles cause the undercutting of the GaN in a single etch step. (b) Effective index of the waveguide modes (blue: TE, red: TM) as a function of the waveguide size. Inset: schematic of calculation. (c-d) Mode profiles for the fundamental TE mode (c) and TM mode (d) at w=700nm.

We are grateful for support from the Future Compound Semiconductor Manufacturing Hub (CS Hub) funded by EPSRC grant reference EP/P006973/1.

[1] N. Niu, et al., "Ultra-low threshold gallium nitride photonic crystal nanobeam laser," Appl. Phys. Lett. 106, 231104 (2015).[2] P. Latawieca, *et al.* "Faraday cage angled-etching of nanostructures in bulk dielectrics," J. Vacuum Sci. & Technol. B 34, 041801 (2016). [3] T. Takamori, L. A. Coldren, J. L. Merz, "Angled etching of GaAs/AlGaAs by conventional Cl2 reactive ion etching," Appl. Phys. Lett. 53, 2549 (1988). [4] D. M. Beggs, *et al.*, "Compact polarization rotators for integrated polarization diversity in InP-based waveguides," Optics Letters 32 (15), 2176-2178 (2007)

A19_35 Growth, Fabrication and Characterization of Integrated Green HEMT-LED Devices

Y Cai, Y Gong, J Bai, X Yu, C Zhu, V Esendag, KB Lee and T Wang t.wang@sheffield.ac.uk
Department of Electronic and Electrical Engineering, University of Sheffield, Sheffield, S1 3JD

There is an increasing demand for developing a monolithic integration of electronics and photonics featured with multiple functions and enhanced performance. This is becoming particularly important for III-nitride based optoelectronics, for example, digitalised white emitters for simultaneous general illumination and visible light wireless communication (i.e., Li-Fi), where a white light emitting diode (LED) featured with both high efficiency and high data transmission rates is required. So far, current state-of-the-art white LEDs, primarily based on the well-known "blue LED + yellow phosphor" technique, have approached their limits in terms of overall performance. One of the fundamental limitations for the Li-Fi applications is due to the very slow response time of yellow phosphors, typically on the order of microseconds, leading to a very limited bandwidth which is down to the MHz level. It is ideal to fabricate white LEDs by mixing red, green and blue (RGB) LED components in order to not only further improve overall optical efficiency but also completely avoid the fatal limit as a result of utilising yellow phosphors. Furthermore, the electronic parts which are used to control a white LED also require a high response. In this case, high electron mobility transistors (HEMTs) would be an ideal option. Therefore, it is necessary to develop a monolithic integration of III-nitride HEMTs and LEDs. So far, there are no reports on integrating green LEDs and HEMTs, one of the major challenges which we are facing.

In this work, by means of selective overgrowth approach we have successfully demonstrated a monolithic epitaxial integration of AlGaN/GaN HEMTs and green LEDs, where a circular HEMT is surrounded by a ring-shaped LED so that these two devices are seamlessly interconnected electrically by matching the n-GaN layer of the LED and the two-dimensional electron gas (2DEG) channel of the HEMT. The full structure is schematically illustrated as in Figure 1 (a) and (b). A circular HEMT is surrounded by the LED mesa, modulating or controlling injection current to the LED. A finger-shaped circular electrode is used for the green LED in order to facilitate current spreading. Current can be injected from the ring-shaped anode of the LED into the n-GaN layer uniformly through the 2DEG channel of the HEMT and finally reach the source of HEMTs. By adopting such a novel circular layout design, the integrated HEMT-LED has fundamentally eliminated the current crowding issues which occurred to lateral blue HEMT-LED devices reported previously. Therefore, a uniform green light emission at 507 nm has been achieved by simply tuning its gate voltage as shown in Fig. 1 (c) and (d). Our monolithic integration work of HEMT with green LED enables a uniform, controllable green LED light source, serving as an essential element in the red-green-blue (RGB) LED solution for Li-Fi applications with wavelength division multiplexing (WDM) modulation schemes. This will move forwards the Li-Fi technology for practical applications.

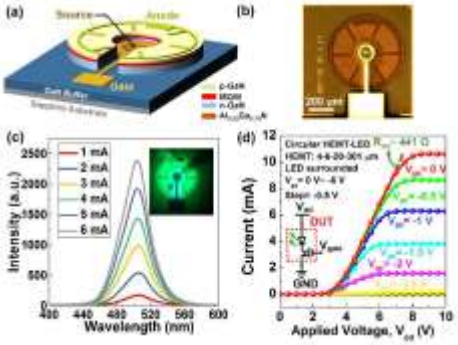

Fig. 1: (a) Schematic illustration of our device in 3 dimension; (b) Optical microscope image of our HEMT-LED devices; (c) EL spectra as a function of injection current and Inset: EL emission image taken at 1 mA; (d) typical I-V characteristics and inset: an equivalent circuit of HEMT-LED)

A**cknowledgment**
This work was supported by the Engineering and Physical Sciences Research Council of United Kingdoms under Grant EP/P006973

A19_37 Nonpolar (11-20) InGaN/GaN light-emitting diodes overgrown on a micro-rod Template

L Jiu, J Bai, N Poyiatzis, P Fletcher and T Wang
Department of Electronic and Electrical Engineering, University of Sheffield, Mappin Street, Sheffield, S1 3JD, United Kingdom

Nonpolar InGaN-based light-emitting diodes (LEDs) are attracting extensive attentions because they are expected to lead to significant improvement in internal quantum efficiency due to the elimination of piezoelectric and spontaneous polarization induced electric fields. In addition, non-polar InGaN-based LEDs has the advantage of generating a polarized light source due to that its valence band splitting can be caused by anisotropic biaxial stress, which is important in the backlighting applications for a liquid crystal display by reducing power consumption and compactness.1 Up to date, non-polar III-nitride devices with high performance have to be grown on extremely expensive GaN substrates, where the size of GaN substrates is typically limited to 10×10 mm2. Conventional epitaxial lateral overgrowth techniques employed for the growth of nonpolar GaN on either sapphire or sapphire are based on a selective area overgrowth approach on normally stripe-patterned templates. However, it is difficult achieve quick coalescence and an atomically flat surface as a result of intrinsically anisotropic in-plane growth rate by using such a stripe-patterned template

Recently, our group has achieved high quality *a*-plane (11-20) GaN overgrown on regularly arrayed *a*-plane GaN micro-rods.2 Non-polar *a*-plane GaN is first grown on *r*-plane sapphire by a standard metal organic chemical vapour deposition using our high temperature AlN buffer technology. Subsequently, the as-grown template is fabricated into a regularly arrayed micro-rod template by means of a standard photolithography technique and then dry-etching processes. The micro-rod templates are fabricated with a mushroom configuration on *r*-plane sapphire, using a dry-etching technique and subsequent ultra-violet assisted photo-enhanced chemical etching processes. An overgrowth on such a template allows us to obtain quick coalescence and an atomically flat surface as a result of our designed patterning which can compensate for the intrinsically anisotropic in-plane growth rate of non-polar GaN. High quality *a*-plane (11-20) GaN with a layer thickness of 3 µm has been achieved, with the X-ray rocking curve line widths of 270 arcsec along the [0001] direction and 380 arcsec along the [1-100] direction, which is the best report so far. The LED structure is grown on such high quality *a*-plane GaN templates, which consists of a 1 ?m Si-doped *n*-type GaN layer, three pairs of InGaN/GaN QWs, and finally a 150 nm Mg-doped *p*-type GaN layer.

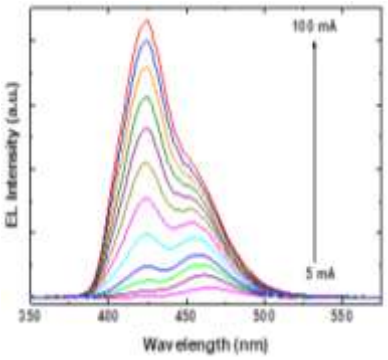

Figure 1 shows the electroluminescence (EL) spectra measured at different injection currents. At low currents, only one emission with peak wavelength at 450 nm is observed. With increasing the current, an emission with a shorter wavelength (~ 420 nm) appears, and the intensity increases with the current. At high currents, the 420 nm emission becomes the main emission. Through wavelength mapping of Confocal PL measurements, the double emission can be ascribed to different indium composition in different areas in connection with the underlying micro-rod pattern of templates. It is important to note, with the current increasing from 10 mA to 100 mA, the wavelength of the main emission (~ 420 nm) shifts only about 1.6 nm. It means the piezoelectric field induced quantum confined Stark effect (QCSE) in the nonpolar InGaN/GaN MQWs is nearly eliminated.

In order to investigate the polarization properties of the *a*-plane LED, polarized EL spectra are obtained from the top surface of the LED using on-wafer measurements, by rotating a polarizer positioned between the device and a spectrometer. Figure 2 shows the spectra along *c*-polarization and *m*-polarization measured at different injection currents of 5 mA, 30 mA, and 100 mA. Generally, the EL intensities with *m*-polarization are larger than those with *c*-polarization. For the spectra at 30 mA with two emission peaks observed clearly, the intensity difference between the *m*-polarized light and the *c*-polarized light is larger for the low-energy peak in comparison with the high-energy peak. At 30 mA current, the polarization degree □ is 0.34 and 0.49 for the high-energy peak and the low-energy peak, respectively, which confirms that higher indium composition leads to a larger polarization degree. It is also noted that the polarization ratios for both emissions are nearly independent of injection current. Furthermore, the photon-energy difference □*E* between the emission spectra associated with the two polarizations increases with the injection current for both emissions, which can be explained by the anti-crossing of □*Z*> and □*Y*> subbands, or crystal momentum conservation.

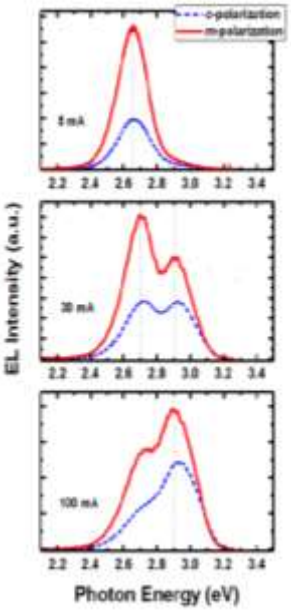

In summary, nonpolar *a*-plane (11-20) InGaN MQW LEDs have been achieved on high quality *a*-plane GaN grown on micro-rod templates. The effect of piezoelectric field on optical properties is not observed in power-dependent EL measurements. The polarization ratios for both emissions are nearly independent of the driving current, with a larger polarization degree for the emission with a higher indium composition. The energy separation between the *c*- and *m*- polarizations increases with the current.

Acknowledgment
This work was supported by the Engineering and Physical Sciences Research Council of United Kingdoms under Grant EP/P006973/1

References:

1. H. Masui, A. Chakraborty, B. A. Haskell, U. K. Mishra, J. S. Speck, S. Nakamura, and S. P. DenBaars, Jpn. J. Appl. Phys., Part 2 44, L1329 (2005).
2. L. Jiu, Y. Gong, and T. Wang, Scientific Reports **8**, 9898 (2018).

A19_13 Optimization of thin Ge buffer layers on Silicon for integration of III-V on silicon Substrates

J Yang[1], P Jurczak[1*], F Cui[1], K Li[1], M Tang[1], L Billiald[2] , R Beanland[2], AM Sanchez[2], and H Liu[1]
[1] Department of Electronic and Electrical Engineering, University College London, Torrington Place, WC1E 7JE London, United Kingdom, [2] Department of Physics, University of Warwick, CV4 7AL, Coventry, United Kingdom

Realising a highly-efficient Si based laser source is the key to Silicon photonic integrated circuits. Monolithic integration of III-V semiconductor components on Silicon has been considered as one of the most promising solutions to achieve a reliable, electrically pumped, silicon-based laser source. Due to a large lattice mismatch between III-V and Si, thick GaAs buffer layers are adopted, leading to high cost and dense thermal cracks. This paper reports on optimization of thin Ge buffer layers, which are used to replace a large part of the thick GaAs buffer layer and reduce the overall thickness. Finally, a high quality multi-layer InAs/GaAs QDs laser structure grown on a 270-nm-thick Ge buffer has been demonstrated, which further supports the feasibility of this method.
Keywords: Ge buffer layer, III-V on Silicon integration
Two-step Ge buffer layers were grown on N-type (100) silicon substrates using a solid-source MBE system. Four 270-nm-thick Ge buffer layer have been grown and annealed continuously at 750, 800, 850 and 900°C. Based on threading dislocation density (TDD) and the surface roughness, 850°C is suggested as the optimal annealing temperature for thin Ge buffer layers. In addition, it has been observed that cyclic annealing and N-type doping have positive impact on the TDD reduction and the TDD is inversely proportional to the buffer layer thickness.
For a typical GaAs buffer layer with DFLs from [3], the TDD of 1.4µm GaAs with one DFL is comparable with 270nm Ge buffer layer. In order to demonstrate the possibility of replacing 1.4µm GaAs with a 270-nm-thick Ge buffer layer, multi-layer InAs QDs were grown. The 270-nm-thick Ge buffer layer used in this case was cyclically annealed at 850°C/450°C. The peak of room temperature PL is at 1297nm with a full width at half maximum (FWHM) equal to 35.7meV. The QD density of about $3.5\times10^{10}/cm^2$ was observed

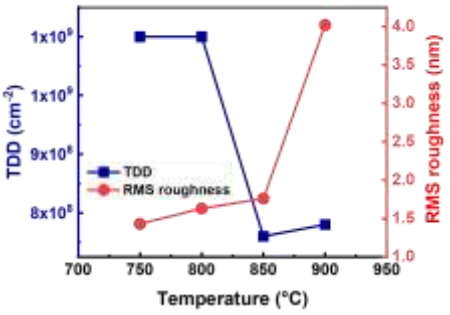

Fig. 1. Summary of TDD and RMS roughness for buffer layers (270nm) annealed continuously for 30 minutes at 750, 800, 850 and 900°C

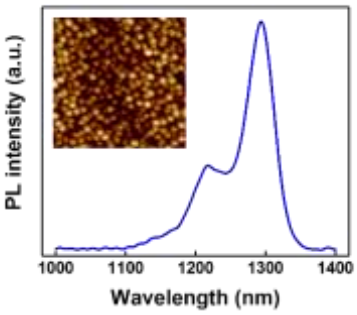

Fig. 2. Room-temperature PL results for the multi-layer InAs/GaAs QDs structure. Inset: 1μm×1μm AFM image of InAs QDs

[1] M. Tang, S. Chen, J. Wu et al., "1.3-µm InAs/GaAs quantum-dot lasers monolithically grown on Si substrates using InAlAs/GaAs dislocation filter layers," Optics Express, vol. 22, no. 10, pp. 11528-11535, 2014.[2] T. Wang, H. Liu, A. Lee et al., "1.3-µm InAs/GaAs quantum-dot lasers monolithically grown on Si substrates," Optics express, vol. 19, no. 12, pp. 11381-11386, 2011.[3]S. Chen, W. Li, J. Wu et al., "Electrically pumped continuous-wave III–V quantum dot lasers on silicon," Nature Photonics, vol. 10, no. 5, pp. 307-311, 2016

A19_34 Hybrid III–V/IV Nanowires: High-Quality Ge Shell Epitaxy on GaAs Cores

H Zeng,[†,‖] X Yu,[*,†,‖] H Fonseka,[‡] JA Gott,[‡] M Tang,[†] Y Zhang,[†] AM Sanchez, [‡] and H Liu

haotian.zeng.13@ucl.ac.uk

[†]*Department of Electronic and Electrical Engineering, University College London, London WC1E 7JE, United Kingdom;* [‡]*Department of Physics, University of Warwick, Coventry CV4 7AL, United Kingdom*

To meet the enormously growing requirements for data transfer and processing, the higher density and thus the reduced size for the integrated circuit are mandatory. As a representative member of the big family of nanoscale structures, semiconductor nanowires have been extensively investigated as potential building blocks for the evolution of the modern CMOS and other technologies. Among them, III-V semiconductor nanowires have attracted plenty of interests due to their superb optical properties while IV semiconductors Si and Ge nanowires, with excellent thermal stability and relatively cheaper cost, have also been intensively studied due to the compatibility of Si and Ge bulk materials with the mainstream CMOS technologies.

Here, we demonstrate the growth of GaAs/Ge core-shell nanowires with smooth shell surface, a sharp and dislocation-free interface, and almost defect-free nanowire body by systematic transmission electron spectroscopy characterization. X-ray diffraction and Raman spectroscopy measurements on ensemble nanowires have revealed consistent results that negligible strain was residing in GaAs/Ge nanowires, further confirming dislocation-free features of the NWs. In addition, the photoluminescence measurements show that GaAs/Ge nanowires are optical-active, and Ge shell is acting like a surface passivation coating. It is promising that GaAs/Ge NWs as a combination of both III-V and group IV materials in a single nanowire would further promote the level of integration of circuits on Si chip.

A19_16 Novel Hydrogen Silsesquioxane Planarization for Electronic-Photonic Integrated Circuit Applications

A Al-Moathin, L Hou, S Thoms, JH Marsh
School of Engineering, University of Glasgow, Glasgow G12 8QQ, U.K

The performance of advanced Electronic-Photonic Integrated Circuits (EPICs) is increasingly limited by the efficiency of the interconnect Electrical-Optical (E-O) interface. In the case of EPIC technology for Radio Frequency (RF) applications, an additional consideration is the need to minimise the parasitic capacitance of passive components such as tracks and bond pads, which in turn makes low permittivity insulators highly desirable. Surface planarization of low permittivity insulators such as Benzocyclobutene (BCB) is difficult to apply in EPIC technology due to the complexity of the fabrication process, and the relatively low accuracy of photolithography (~1 µm).

Hydrogen Silsesquioxane (HSQ) is a spin-on dielectric designed for low-k applications, which has been identified as a promising material for forming planarized dielectric films [1]. HSQ-based films have a lower permittivity than SiO2, which can reduce electrical signal delays [2, 3]. In standard Integrated Circuits (ICs), HSQ-based films are formed over the entire substrate by spinning; good planarity can be achieved with a single spin coating providing a film thickness up to 800 nm, depending on spin speed. Thicker planarized films can be realized with a multi-spin process, however thermal curing is required to prevent the previously deposited HSQ from dissolving [4, 5].

In this work, for the first time, a new method is presented to implement a thick dielectric structure using HSQ planarization. The structure was created using a multi-spin process, and, instead of thermal curing, e-beam exposure was used to define a selected pattern, then a thin film of Plasma-Enhanced Chemical Vapor Deposition (PECVD) SiO2 was deposited. This sufficiently protects the HSQ from dissolving and adds the flexibility of defining the planarization shape. Various structures with thicknesses up to 10 µm were fabricated on selected areas of the substrate surface. The new process has the advantages of minimizing the need for etch-back, simple fabrication steps and avoiding high-temperature thermal curing.

In conclusion, our new approach to HSQ planarization has proved to be a promising method for fabricating a low-k structure with thickness of up to 10 µm. The method has been applied successfully for different purposes such as building thick, low-permittivity, insulator layers or forming a dielectric substrate for Transmission Lines (TLs). Compared with conventional BCB or polyimide-based planarization, both of which require many steps and high curing temperatures, this process using spin-coatable HSQ planarization is easy and quick to apply. Furthermore, the shapes of the planarized structures are defined as an integral part of the fabrication process.

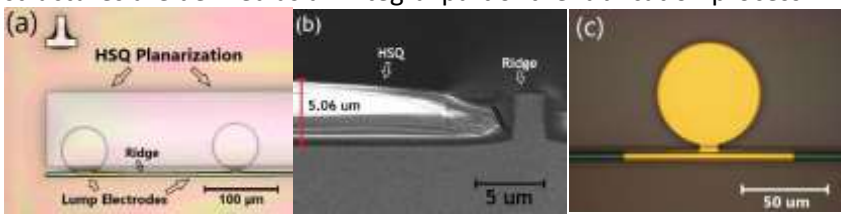

Figure 1: HSQ planarization structure with thickness 5 µm. (a) HSQ structure planarized on InP substrate, (b) cross-section SEM image for the planarized HSQ, and (c) the electrode pad after metal deposition over the HSQ planarized structure.

This work was supported by the EPSRC Centre for Doctoral Training in Photonic Integration and Advanced Data Storage (EP/L015323/1).

References

[1] C. W. Holzwarth, T. Barwicz, and H. I. Smith, "Optimization of hydrogen silsesquioxane for photonic applications," *J. Vac. Sci. Technol. B Microelectron. Nanom. Struct.*, vol. 25, no. 6, p. 2658, 2007. 2] M. J. Loboda, C. M. Grove, and R. F. Schneider, "Properties of a-SiOx:H Thin Films Deposited from Hydrogen silsesquioxane resins," *J. Electrochem. Soc.*, vol. 145, no. 8, pp. 2861–2866, 1998. [3] M. Olewine, R. Wall, and G. Colovos, "Integration of Hydrogen Silsesquioxane into an advanced BiCMOS process," vol. 3508, no. 505, pp. 42–50, 2017. [4] Y. K. Siew, G. Sarkar, X. Hu, J. Hui, A. See, and C. T. Chua, "Thermal Curing of Hydrogen Silsesquioxane," *J. Electrochem. Soc.*, vol. 147, no. 1, p. 335, 2000. [5] C. C. Yang and W. C. Chen, "The structures and properties of hydrogen silsesquioxane (hsq) films produced by thermal curing," *J. Mater. Chem.*, vol. 12, no. 4, pp. 1138–1141, 2002.

Abstracts

Session 8: Materials Development and Devices II

A19_39 AlInAs Gettering Layer for Resonant Tunnelling Diode Barrier Symmetry

R Baba[1], BA Harrison[2], BJ Stevens[3], R Beanland[4], T Mukai[5], RA Hogg[1]
[1]The University of Glasgow, Glasgow, G12 8LT UK; [2]EPSRC National Epitaxy Facility, Sheffield, S3 7HQ UK; [3]IQE Europe Ltd., Cardiff CF3 0LW UK; [4]Integrity Scientific Ltd., Warwick, CV34 4JP UK; [5]ROHM Semiconductor Co. Ltd., Kyoto, 615-8585 Japan

We investigate the cause of unwanted asymmetry of the AlAs barriers in partially strain balanced [1] AlAs/InGaAs/AlAs double barrier QW based devices grown by MOVPE on InP. This asymmetry occurs as [Al]3+ ions are highly reactive, combining with [O]2- contaminants present in the reactor chamber, resulting in reagents for the first barrier being depleted due to gettering of oxygen. This process is dependent on the susceptor plate temperature, prime chemical purity, and overall reactor cleanliness status. High temperatures prevent oxygen adsorption but are sub-optimal in terms of InGaAs layer uniformity. In this study we discuss the role of an added lattice matched AlInAs buffer expected to getter atomic impurities prior to the deposition of the AlAs/InGaAs QW.
Experimental and theoretical effects of barrier asymmetry are discussed. We then proceed with a comparative TEM study is presented between two nominally identical samples, with, and without this buffer. It is found that on average, the AlInAs containing sample produces barriers with a symmetric thickness ratio of top/bottom barrier of ~1 vs. 0.9 in the case of the InGaAs-only sample. An alternative structure employing superlattices is discussed. We then discuss the implications of this additional layer in terms of complications requiring an additional growth calibration step, and in terms of the required non-destructive wafer characterization scheme [2] involving X-ray and low temperature photoluminescence spectroscopy. Together, these two techniques provide accurate information on the structural double-barrier QW heterostructure using advanced mesoscopic modelling.
This information is fed back into the growth process for ultimate control of epitaxial thickness and mole fractions.

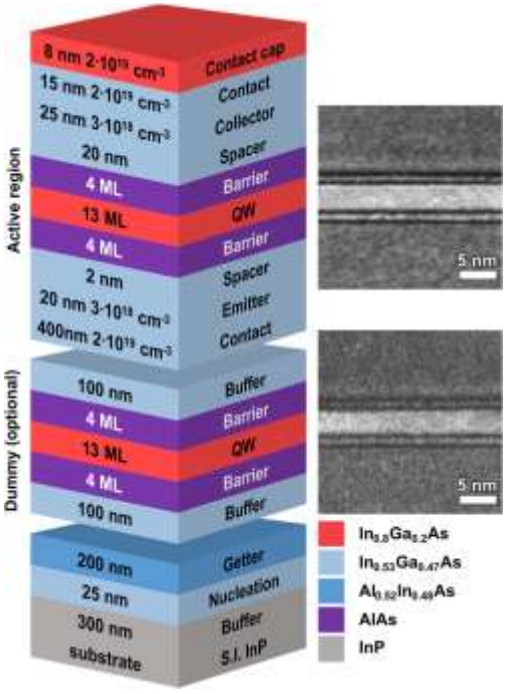

Fig. 1. Epitaxial layer structure of the finalised resonant tunnelling diode presented with dark field [002] chemically sensitive TEM images

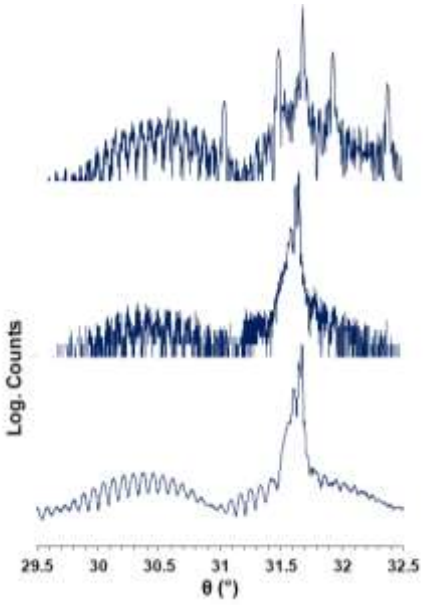

Fig. 2. Modelled **(top)** HR-XRD ω-2θ diffraction curves of a 20-layer AlAs/InGaAs superlattice alternative. Measured **(middle)** structure in Fig. 1 and its fit **(bottom)**.

REFERENCES [1] R. Baba, B.J. Stevens, T. Mukai, R.A. Hogg, IEEE J. Quantum.Electron. **54**, 1 (2018). [2] R. Baba, O. Kojima, K.J.P. Jacobs, B.A. Harrison, B.J. Stevens, T. Mukai, and R.A. Hogg, in Proc. SPIE, Quantum Dots Nanostructures Growth, Charact. Model. XVI (6 Febr. 2019).

A19_36 A two-step method of growing (11-22) semi-polar GaN on (113) silicon

Y Cai, S Shen, X Yu, X Zhao, L Jiu, C Zhu, J Bai and T Wang t.wang@sheffield.ac.uk
Department of Electronic and Electrical Engineering, University of Sheffield, Sheffield, S1 3JD

Compared with semi-polar GaN grown on a sapphire substrate, the growth of semi-polar GaN on silicon substrates offers extra benefits in spite of a number of extra challenges. Silicon substrates provide an excellent platform for semiconductor industry as a result of technology maturity, low-cost, up-scalability, devices integration and good thermal conductivity. However, the growth of semi-polar GaN on silicon substrates tends to be very challenging. The greatest challenge for the growth of semi-polar (11-22) GaN on patterned (113) silicon is due to the Ga melt-back etching. The melt-back etching not only degrades crystal quality significantly but also destroys growth. Currently, one method is to use mixed N2 and H2 as a carrier gas instead of pure H2 carrier gas, which is not ideal due to N2 impurity. Another alternative method to reducing the Ga melt-back etching is to reduce GaN growth temperature down to below 900˚C, which is far from the optimised temperature for GaN growth and thus is clearly not ideal, either. This situation becomes even worse for the growth of AlxGa1-xN based structures such as high electron mobility field effect transistors (HEMTs), as a higher growth temperature for AlxGa1-xN is required compared with GaN growth.

In this paper, we have developed a two-step approach for the growth of semi-polar (11-22) GaN on patterned (113) silicon substrates, which effectively eliminates Ga melt-back etching at a high temperature, one of the most challenging issues. A (113) Si substrate is patterned into groove trenches by means of using a standard photolithography technique and then anisotropic chemical etching, forming (111) facets with an inclination angel of 58˚ with respect to c-axis in addition to the un-etched (113) facets. After this, a thick layer AlN layer is first epitaxially grown to fully cover all the facets of patterned (113) silicon and then selective overgrowth of (11-22) GaN only on the desired (111) inclined facets, which can be achieved by selectively depositing SiO2 masks in order to cover the top (113) facets only by using an electron-beam sputtering technique. Further GaN growth at a high temperature normally required leads to the achieved (11-22) GaN with high crystal quality and optical performance while remaining large windows for optimising both the fabrication of the patterned (113) silicon (such as large trenches) and the subsequent GaN growth (a high growth temperature will never be within our concerns). After growth, stimulated emission at room temperature has been observed with a low threshold. Low-temperature photoluminescence measurements confirm a significant reduction in basal stacking faults (BSFs) density.

Our method provides a promising approach to effectively suppress the Ga melt-back etching issue, which is particularly important for Al(Ga)N growth on semi-polar GaN that requires a high growth temperature. The presented results are crucially important for the developing a monolithic on-chip integration of electronics and photonics on silicon.

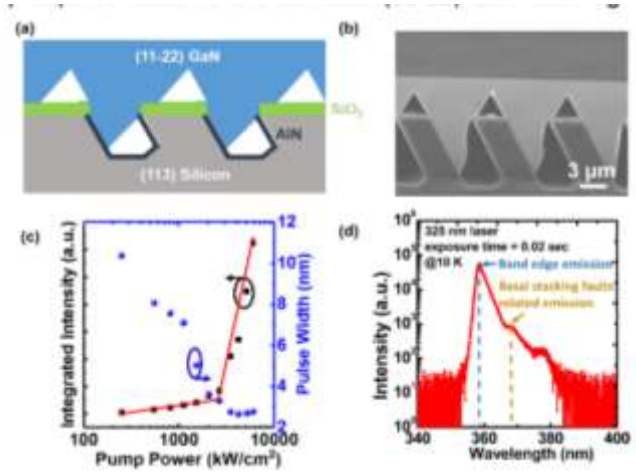

Fig. 1: (a) Schematic illustration of growing (11-22) GaN on silicon; (b) Cross-sectional SEM image of the (11-22) GaN; (c) Stimulated emission at 375 nm; (d) Low-temperature photoluminescence at 10 K.

Acknowledgment
This work was supported by the Engineering and Physical Sciences Research Council of United Kingdoms under Grant EP/P006973/

A19_17 Engineering the optical transitions in InAs/GaAsSb QDs using thin InAlAs layers

A Salhi[1, 2], S Alshaibani[2], Y Alaskar[2], A Albadri[2], A Alyamani[2] and M Missous[1]
abdelmajid.salhi@manchester.ac.uk
[1]School of Electrical and Electronic Engineering. The University of Manchester, Sackville Street, Manchester M13 9PL, United Kingdom; [2]National center for Nanotechnology and advanced materials, KACST, 11442 Riyadh, Saudi Arabia

Over the last 20 years, self-organized InAs quantum dots (QDs) have attracted a great deal of interest. They have been investigated intensively owing to their attractive optical and electronic properties. Strain reducing layers (SRLs) are used routinely to extend the emission wavelength to cover the optical communication wavelength bands. GaAsSb SRL has received attention as the band alignment can be adjusted to type I or type II by the Sb content in the ternary alloy. The insertion of thin InAlAs layers prior to GaAsSb SRL may be of interest to engineering the type of radiative recombination. Moreover, it is expected to decrease In segregation and suppress In and Ga atoms intermixing between the InAs QDs and the GaAsSb SRL.

In this work, the optical transitions of InAs quantum dots QDs capped with GaAsSb SRL is engineered by the insertion of thin InAlAs layers. Thin InAlAs layers with thickness t = 1nm, 2nm, and 3nm were inserted between the InAs QDs and a 6nm-thick GaAsSb SRL. The PL emission of the reference sample made of a single InAs/GaAsSb QD layer is characterized by the coexistence of type I and type II emissions as demonstrated by the power dependent PL measurement shown in Fig. 1(a). The effect of inserting thin InAlAs interlayers is depicted in Fig. 1(b). The insertion of 1nm-thick InAlAs layer maintains the 2 types of emissions with a reduction and an increase of PL intensity for the type II and type I emission, respectively. Increasing the InAlAs interlayer to 2nm reduces significantly the intensity of the type II transition as a result of a reduction of the electron-hole wave functions overlap. The type II emission was suppressed completely for a 3nm-thick InAlAs interlayer favoring the type I emission centered at 1.27µm. The present study shows that the type of emission from InAs/GaAsSb QDs can be tailored to the type of optoelectronic application requiring either a short or long carrier lifetime by means of thin InAlAs interlayer.

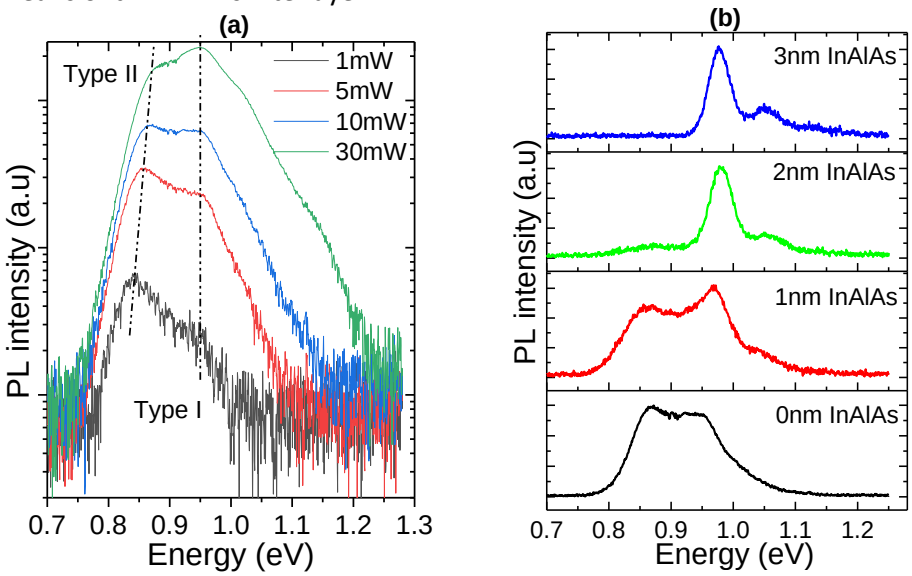

Fig.1 (a) Power dependent PL at room temperature showing the coexistence of type II and type I emissions from the InAs/GaAsSb reference sample. (b) PL emission at room temperature for the samples including 0, 1, 2 and 3nm-thick InAlAs interlayer for an excitation power of 10mW.

A19_25 Analytical model of optical amplification in strained Ge

EE Orlova and RW Kelsall
Pollard Institute, School of Electronic and Electrical Engineering, University of Leeds, Leeds LS2 9JT, UK

Strained germanium is attracting a great deal of attention as a potential gain medium for monolithically integrated laser sources compatible with Si technology. The first observation of lasing in strained germanium was reported almost a decade ago [1]. However, the mechanism of lasing was not clear. Indeed, the measured amplification on inter-band transitions in Ge with strain level corresponding to that of [1] was found to be more than an order of magnitude smaller than pump-induced absorption for injected carrier densities about 10^{20} cm^{-3} [2]. Rigorous numerical calculations [3] have shown the possibility of positive gain in germanium with donor concentration of 10^{20} cm^{-3} and tensile strain above 1.4 % at a pumping level of 10^{19} cm^{-3}. However, the gain calculated for the same material at the level of pumping of 10^{20} cm^{-3} appeared to be negative [3]. This means that the dependence of net amplification on the pumping level in strained germanium can be non-monotonous even when pumping does not cause heating of the sample. Clearly, this fact is of crucial importance for determination of lasing conditions. However, numerical calculations do not answer the questions: (i) what are the parameters that determine the optimum level of pumping and (ii) what is the condition of positive gain in strained Ge. The non-monotonous dependence of the net gain on the pump power cannot be explained within a model using pump power independent cross sections of intra-valence band optical transitions [2,4]. In this paper we build an analytical model of amplification in strained germanium. Within this model, the dependences of the maximum interband gain and of the intra-valence band absorption on temperature and Fermi levels of electrons and holes are described by analytical functions with a small number of numerically calculated parameters. We show that the change of energy distribution of charge carriers leads to a strong non-linear dependence of cross sections of optical transitions on pumping power. At high pumping powers, the cross section of intervalence band transitions grows exponentially, while the cross section of inteband transitions exhibits a sublinear growth. This explains a decrease of the net optical gain at high pumping powers. We formulate lasing conditions in strained germanium in terms of Fermi levels of electrons and holes and temperature, determine the minimum doping level required for lasing as a function of strain, and the optimum pump power as a function of strain and doping level.

[1] J. Liu, X. Sun, R. Camacho-Aguilera, L. C. Kimerling, and J. Michel, Opt. Lett. 35, 679 (2010).
[2] L. Carroll, P. Friedli, S. Neuenschwander, H. Sigg, S. Cecchi, F. Isa, D. Chrastina, G. Isella, Yu. Fedoryshin, J. Faist, Phys. Rev. Lett. 109, 057402 (2012).
[3] H. Wen and E. Belotti, Phys. Rev. B 91, 035307 (2015).
[4] J. Liu, X. Sun, D. Pan, X. Wang, L. C. Kimerling, T. L. Koch, and J. Michel, Opt. Express 15, 11 272 (2007).

A19_38 Electroluminescence from GaAsBi/GaAs multiple quantum well devices – potential for broadband light source applications

TBO Rockett[1], RD Richards[1]*, Y Liu[1], F Harun[1], Z Zhou[1], Y Gu[2], JR Willmott[1], and JPR David[1]
R.Richards@Sheffield.ac.uk
[1]University of Sheffield, Sheffield, South Yorkshire, S1 3JD, U, K[2]Shanghai Institute of Microsystem and Information Technology, Chinese Academy of Sciences, China

GaAsBi has demonstrated significant band engineering capabilities, with the incorporation of Bi reducing the band gap of GaAs by ~620 meV per percent strain, which is much larger than that of In at ~240 meV per percent strain. There are several applications for which this band engineering is potentially useful, such as telecommunications [1], or photovoltaics [2]. However, GaAsBi exhibits a pronounced tail of radiative localized states that extends into the band gap [3] and has, to date, hindered the development of dilute bismide devices. While research is underway to mitigate this effect (e.g. [4]), this tail of states and the broad luminescence that it produces may be useful for certain applications.

In this work, a series of GaAsBi/GaAs multiple quantum well (MQW) pin diodes is characterised by electroluminescence (EL). The EL spectra are very broad (~ 80 meV) due to the localised states associated with the presence of Bi. However, the broad EL is a reasonable approximation to a Gaussian lineshape and its integrated intensity is comparable with the integrated intensity of a very well optimised InGaAs/GaAsP MQW device with a similar structure. These properties make GaAsBi a strong candidate as a broadband light source in the near infrared. One technology that requires such a light source is optical coherence tomography (OCT). The EL spectra from the GaAsBi/GaAs MQW devices are compared with other recently published candidate light sources for OCT.

1. Sweeney, S.J. and S.R. Jin, Bismide-nitride alloys: Promising for efficient light emitting devices in the near- and mid-infrared. Journal of Applied Physics, 2013. 113(4): p. 043110.
2. Richards, R.D., et al., Photovoltaic characterisation of GaAsBi/GaAs multiple quantum well devices. Solar Energy Materials and Solar Cells, 2017. 172: p. 238-243.
3. Wilson, T., et al., Assessing the Nature of the Distribution of Localised States in Bulk GaAsBi. Scientific Reports, 2018. 8: p. 6457.
4. Mooney, P.M., et al., Deep level defects in dilute GaAsBi alloys grown under intense UV illumination. Semiconductor Science and Technology, 2016. 31(8): p. 085014.

A19_27 Dilute Magnetic Contact for a Spin GaN HEMT

JE Evans[1], G Burwell[2], FC Langbein[3], SG Shermer[2], and K Kalna[4] J.E.Evans@Swansea.ac.uk
[1]Centre for NanoHealth & [2]College of Science, Physics, Swansea University, SA1 8EN, Wales, UK; [3]School of Computer Science and Informatics, Cardiff University, Cardiff CF24 3AA, Wales, UK; [4]Nanoelectronic Devices Computational Group, Swansea University, Swansea, SA1 8EN, Wales, UK

Semiconductor CMOS nano-electronics is intensively seeking solutions for future digital applications. One of the most promising solutions to deliver a technological breakthrough is exploring electron spin in metals and semiconductors with applications from spin transistors to quantum sensors, and quantum computing [1]. Spintronic applications rely on magnetic semiconductor materials with suitable properties [2]. In particular, dilute magnetic semiconductors (DMS), such as Mn doped GaN, show the great promise of a high Curie temperature (220K–370K), exceeding room temperature, and a large concentration of holes. These are all the essential pre-requisites for operation of spin transistors (see Fig. 1) in circuits. In this work, we dope an AlGaN/GaN heterostructure consisting of a GaN (2 nm) cap layer, an Al0:25Ga0:75N (25 nm) barrier, and a GaN (2 _m) substrate grown on a 6 00 Si wafer with Mn by sputtering deposition and thermal annealing to create a dilute magnetic semiconductor material following the process flow depicted in Fig. 3. While initial attempts resulted in the formation of a MnO surface layer [3], the SEM/XDS and XPS data in Figs. 4 and 5, respectively, suggest a diffusion of Mn into the GaN layer using thermal annealing at 900_C for 7h with a concentration of 4.5% which is very close to the desired concentration of 5% needed for a DMS. The annealing temperature has to be below 1000_C since temperatures around 1000_C result in significant damage to the 2DEG and diffusion of Al from the AlGaN layer.

References:[1] J. Fabian et al., Acta Phys. Slovaca 57, 565-907 (2007). [2] T. Dietl and H. Ohno, Rev. Mod. Phys. 86, 187-251 (2014). [3] F. C. Langbein et al., Cardiff Materials Net. Conf., Chepstow, UK, 17-18 Jan (2019).